AD-A084 687 WATKINS-JOHNSON CO SCOTTS VALLEY CA F/6 9/1
HIGH CONTRAST CRT.(U)
FEB 80 N H LEHRER, G A HOLMQUIST DAAB07-77-C-2639
UNCLASSIFIED DELET-TR-77-2639-F NL

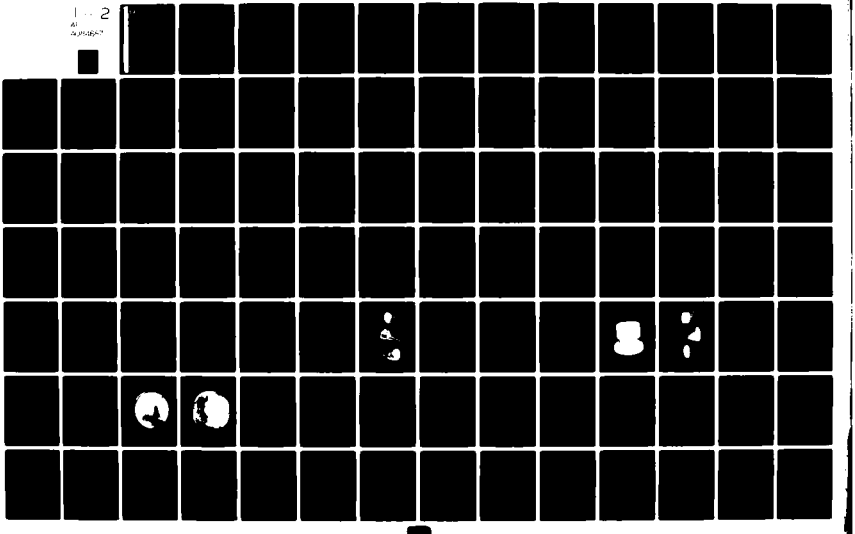

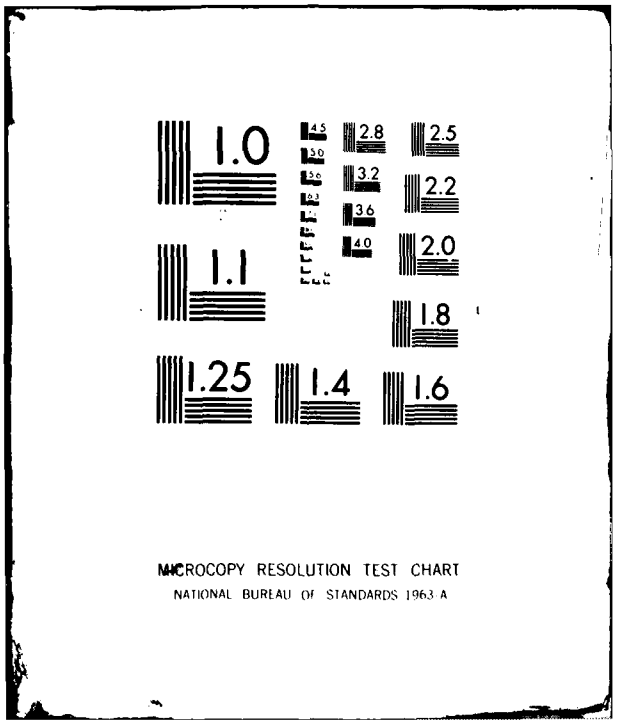
1.0
1.1
1.25
1.4
1.6
1.8
2.0
2.2
2.5
2.8
3.2
3.6
4.0
4.5
5.0
5.6
6.3
7.1
8.0
9.0
MICROCOPY RESOLUTION TEST CHART
NATIONAL BUREAU OF STANDARDS 1963 A

Research and Development Technical Report

DELET-TR-77-2639-F

HIGH CONTRAST CRT

Norman H. Lehrer
Glenn A. Holmquist
Watkins-Johnson Company
440 Mt. Hermon Road
Scotts Valley, CA 95066

February 1980

Final Report

Distribution Statement:
Approved for public release; distribution unlimited

Prepared for:

ELECTRONICS TECHNOLOGY and DEVICES LABORATORY

ERADCOM
US ARMY ELECTRONICS RESEARCH AND DEVELOPMENT COMMAND
FORT MONMOUTH, NEW JERSEY 07703

NOTICES

Disclaimers

The citation of trade names and names of manufacturers in this report is not to be construed as official Government indorsement or approval of commercial products or services referenced herein.

Disposition

Destroy this report when it is no longer needed. Do not return it to the originator.

SECURITY CLASSIFICATION OF THIS PAGE (When Data Entered)

REPORT DOCUMENTATION PAGE

READ INSTRUCTIONS BEFORE COMPLETING FORM

1. REPORT NUMBER: DELET-TR-77-2639-F	2. GOVT ACCESSION NO.: AD-A084687
3. RECIPIENT'S CATALOG NUMBER:	
4. TITLE (and Subtitle): HIGH CONTRAST CRT.	5. TYPE OF REPORT & PERIOD COVERED: Final Technical Report, 1 Jan 1977 — 30 Jun 1979,
	6. PERFORMING ORG. REPORT NUMBER:
7. AUTHOR(s): Norman H. Lehrer, Glenn A. Holmquist	8. CONTRACT OR GRANT NUMBER(s): DAAB07-77-C-2639
9. PERFORMING ORGANIZATION NAME AND ADDRESS: Watkins-Johnson Company, 440 Mt. Hermon Road, Scotts Valley, CA 95066	10. PROGRAM ELEMENT, PROJECT, TASK AREA & WORK UNIT NUMBERS: 1L1 62705 AH94 D1 08
11. CONTROLLING OFFICE NAME AND ADDRESS: US Army Electronics Research and Development Command, Fort Monmouth, NJ 07703 ATTN: DELET-BD	12. REPORT DATE: Feb 1980 13. NUMBER OF PAGES: 91
14. MONITORING AGENCY NAME & ADDRESS (if different from Controlling Office)	15. SECURITY CLASS. (of this report): UNCLASSIFIED 15a. DECLASSIFICATION/DOWNGRADING SCHEDULE

16. DISTRIBUTION STATEMENT (of this Report)

Approved for public release;
Distribution unlimited

17. DISTRIBUTION STATEMENT (of the abstract entered in Block 20, if different from Report)

18. SUPPLEMENTARY NOTES

19. KEY WORDS (Continue on reverse side if necessary and identify by block number)

3-Inch CRT
Two-Color CRT
Thin Film Phosphor
Color Penetration Tube
High Contrast Displays
Laminar Flow Electron Gun

20. ABSTRACT (Continue on reverse side if necessary and identify by block number)

This program developed a CRT fabrication technology incorporating La_2O_2S:Tb and La_2O_2S:Eu thin film phosphor coated faceplates backed with a nonreflecting coating. The resulting color CRT is superior to existing monochromatic CRT's in high ambient light conditions.

410583

DD FORM 1 JAN 73 1473 EDITION OF 1 NOV 65 IS OBSOLETE

SECURITY CLASSIFICATION OF THIS PAGE (When Data Entered)

PREFACE

This report was prepared by the Cathode-Ray Tube Department, Stewart Division, Watkins-Johnson Company, Scotts Valley, California on contract number DAAB07-77-2639 High Contrast CRT for the period January 1977 through June 1979.

This report was submitted in December 1979.

This research and development effort was sponsored by the U.S. Army Electronics Research and Development Command, Ft. Monmouth, New Jersey. The work was administered under the direction of Phil Krzyzkowski, Project Engineer; Dr. Elliot Schlam, Team Leader; and Mr. Irving Reingold, Director, Beam, Plasma and Display Division.

Mr. Norman H. Lehrer was Project Engineer for the Watkins-Johnson Company and Glenn A. Holmquist played the major role in the preparation of the reports and performance of the work on the program. The high contrast two color screens were fabricated by the Lockheed Palo Alto Research Laboratories. Dr. R. A. Buchanan was Department Manager of the Lockheed Non-Destructive Testing Technology Laboratory and Dr. T. G. Maple, Staff Scientist was directly responsible for the fabrication of the screens.

This is the final report and concludes the work on the contract.

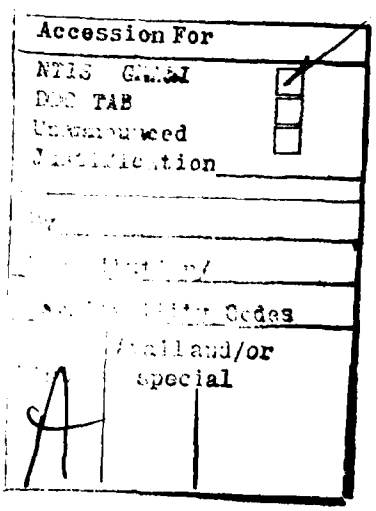

TABLE OF CONTENTS

Section		Page
1.0	INTRODUCTION	1
	1.1 Program Objective and Goals	2
	1.1.1 Detailed Program Objectives	2
	1.2 Subcontract Identification	5
2.0	THIN FILM PHOSPHOR FACEPLATE	7
	2.1 Description of the High Contrast Two-Color Faceplate	7
	2.2 Faceplate Fabrication	7
	2.2.1 Sputtering System	7
	2.2.2 Sample Fixturing	9
	2.2.3 Controlled Atmosphere Heat Treatment	12
	2.2.4 Thickness Monitor	12
	2.3 Aluminosilicate Glass Faceplates	14
	2.3.1 Cleaning Faceplates	18
	2.3.2 Sputtering Procedures	19
	2.4 Nonreflecting (NR) Film	20
	2.5 Faceplate Structural Integrity - Heat Treatment	21
	2.5.1 Surface Distortion	21
	2.5.2 Bulk Distortion	26
	2.5.3 Slumping During Heat Treatment	26
	2.6 Reflectance and Brightness Measurements	26
	2.6.1 Specular Reflectance	26
	2.6.2 Diffuse Reflectance	27
	2.6.3 Cathodoluminance Brightness	31
	2.7 NR Film Reaction Study	41
	2.7.1 Preparation and Test Condition	41
	2.7.2 Reflectivity Measurements	42
	2.7.3 Cathodoluminescent Brightness Measurements	44
	2.8 CRT Contrast Study	44

TABLE OF CONTENTS (Continued)

Section		Page
3.0	CRT FABRICATION	49
	3.1 Faceplate Fabrication	49
	3.2 Frit Seal	55
	3.2.1 SG-7 Frit Versus 7593 Frit	60
	3.2.2 Problems - Engineering Design	60
	3.2.3 Frit Seal Thickness	60
	3.2.4 Frit Porosity	61
	3.2.5 Subassembly Thermal Shock Resistance and Frit Patching	62
	3.2.6 Controlled Atmosphere Frit Firing	66
	3.3 Neck Extension	66
	3.4 Electron Gun Stem	66
	3.5 Electron Gun	66
	3.5.1 Bipotential Versus Einzel	67
	3.5.2 Cathode Poisoning	67
	3.6 Exerciser	69
	3.7 CRT Data	69
	3.7.1 Discussion - Line Width	78
	3.7.2 Discussion - Brightness	78
	3.7.3 50,000 Inches/Second Data	78
	3.7.4 Einzel Gun Versus Bipotential Gun	79
	3.7.5 Line Width - Focus Voltage Dependence	79
	3.7.6 Discussion - Saturation	82
	3.7.7 Discussion - CRT (Faceplate 19)	83
	3.8 Individual CRT Fabrication History	84
4.0	SUMMARY OF RESULTS	87
5.0	CONCLUSIONS	89
	5.1 Further Development	89
	REFERENCE	91
	Appendix A - U.S. PATENT 4,132,919	
	Appendix B - CRT OPTICS CALCULATIONS	

LIST OF ILLUSTRATIONS

Figure		Page
1	Schematic of High Contrast Two-Color Screen	8
2	Thickness Variation Without Supplementary Ring	10
3	Effect of Supplementary Shield Rings	11
4	Laser Interferometer for Film Thickness Measurement During Deposition	13
5	Thicknesses Using the Laser Interferometer Versus Thicknesses Using the Angstrometer	15
6	Cross-Section of Thickness Variation After Polishing	24
7	Diffuse Reflectance Geometry	30
8	Reflected Beam Profiles for a Specular Reference Mirror and Two Faceplate Samples, for an Angle of Incidence Setting of $\theta = 20°$	32
9	Reflected Beam Profiles for a Specular Reference Mirror and Two Faceplate Samples, for an Angle of Incidence Setting of $\theta = 40°$	33
10	Reflected Beam Profiles for a Specular Reference Mirror and Two Faceplate Samples, for an Angle of Incidence Setting of $\theta = 60°$	34
11	Demountable Brightness Data FP 11 - FP 17	36
12	Demountable Brightness Data FP 18 - FP 21	37
13	Demountable Brightness Data FP 22 - FP 25 and FP 27	38
14	Demountable Brightness Data FP 28 - FP 32	39
15	Demountable Brightness Data FP 33 - FP 37	40
16	Cathodoluminescent Brightness Before Treatment	46
17	Contrast Versus CRT Brightness in Bright Sunlight	47
18	CRT Fabrication Flow Diagram	50
19	Cathode Ray Tube WJ-3414-11	51
20	Cathode Ray Tube Outline WJ-3414-11	52
21	Funnel	53
22	CRT Photographs	54
23	Frit Sealing Fixture Assembly	56

ILLUSTRATIONS (Continued)

Figure		Page
24	Organic Binder	57
25	Frit Sealing Fixture Assembly	58
26	Frit Sealing Fixture Disassembly	59
27	Maximum Stress Location in Cross Section View of Faceplate	63
28	Al-V Alloying After Two Frit Patch Attempts	64
29	Al-V Alloying After Four Frit Patch Attempts	65
30	CRT Brightness Versus Grid Drive Data 10 kV Anode Potential	71
31	CRT Brightness Versus Grid Drive Data 15 kV Anode Potential	72
32	CRT Brightness Versus Grid Drive Data 18 kV Anode Potential	73
33	CRT Brightness Versus Grid Drive Data 20 kV Anode Potential	74
34	CRT (FP 19) Brightness Versus Grid Drive Data	77
35	Cathode Current As a Function of Grid Drive	80
36	Brightness Versus Grid Drive, FP 32 at 50,000 Inch/Sec Writing Speed	81
B1	Cross-Section of CRT Faceplate Showing Interfaces for Reflection of Ambient Light	B-2
B2	Contrast Ratio for Various Values of L	B-11
B3	Reflectivity Versus Angle of Incidence	B-20

LIST OF TABLES

Table		Page
1	Corning Aluminosilicate Glasses	17
2	Viscosity - Temperature Data 1720 Glass	22
3	Results of Reflectance Measurements	28
4	Results of Reflectance Measurements	29
5	Measured Cathololuminescence Brightness, fL	35
6	NR Film Reaction Study	43
7	Cathodoluminescent Brightness	45
8	Glass TCE Data	49
9	WJ-3414-11 Electrical Requirements	68
10	Operating Parameters	69
11	Testing Parameters	69
12	Einzel Gun Configuration CRT Data	75
13	Bipotential Gun Configuration CRT Data	76
14	Brightness (fL)	78
15	50,000 Inches/Second Data	79
16	Einzel Gun CRT Data at Constant Focus Voltage	82
17	CRT Fabrication History	85
B1	No AR-1720-La_2O_2S - Ideal NR	B-10
B2	$C = 2.362 \times 10^{-3} L + 1$, AR-1720-$La_2O_2S$ - Ideal NR	B-10
B3	Glass Plate	B-16
B4	Glass Plate Over La_2O_2S Film	B-17
B5	Glass Plate Over La_2O_2S Film	B-18
B6	Glass Plate Over La_2O_2S Film Over Ideal NR Film	B-19

1.0 INTRODUCTION

Existing displays limit the performance of most systems. On one hand the human observer has the ability to not only see images in color but with resolution of photographic quality. On the other hand existing radar, electronic warfare, forward looking IR, camera and computer systems can generate vast amounts of information. Obviously, the optimum display is one which provides the widest communication channel between the electronics and the human eye permitting full use of the color and resolution capability of the eye. For example, in the case of an airborne EW direction finding (threat) display, color coding the threats in terms of priority or type would reduce the reaction time of the observer, which is critical to his survival. The brightness of such a display can be low for use at night but very high contrast is essential if the display is not to be washed-out by daylight.

Existing color tubes do not have the brightness or resolution required for advantageous use in the above example or for that matter in most military applications. Color tubes employing masks have low brightness because the mask absorbs 80% of the beam current and cannot be used in airborne applications as the colors change with orientation to the earth's magnetic field. The use of color penetration phosphors is attractive in that the color purity is not affected by changes in the tube orientation and the resolution is higher than that which can be achieved with a mask-type tube. Conventional color penetration tubes which employ powdered-phosphors cannot be used for daylight (high brightness) viewing because of their high reflectivity which produces a washed-out low contrast display. This problem is overcome by the fabrication of a high contrast color penetration CRT. The screen phosphors of the CRT are of the transparent film type backed by a black, light asborbing coating. The phosphor screen incorporates a two layer penetration type multicolor structure.

The use of such a high contrast transparent thin-film color penetration phosphor will overcome the contrast limitation of the powdered phosphor because the reflectance of the transparent screen is only about 1% to 2% compared to 80% for the powdered screen. Thus, even though the luminous efficiency of the transparent screen is in the order of 10% of the powders, under high brightness conditions the information will be seen on the transparent screen because the contrast will be maintained while the information will be washed-out on the powdered-phosphor screen due to the high reflectivity of the phosphor.

1.1 Program Objective and Goals

A prime objective of this program is the incorporation of a phosphor-faceplate technology that results in transparent film phosphors deposited on a substrate which is an integral part of the CRT envelope. The phosphored faceplate incorporates a two layer penetration type multicolor structure. This faceplate is attached to available tube envelopes in a manner consistent with economical CRT manufacturing methods. The goal of the program is a CRT that is electrically and physically replaceable with the KC-3055 CRT presently used in AN/APR-39. Moreover, the CRT is to operate under ambient illumination from 10^4 to 10^{-3} fc. The display shall be legible under direct sunlight under its normal mode of operation without the use of added contrast enhancement devices.

The program shall include but not be limited to the following:

a. Study and identification of the optimum tube design to replace the present tube in the AN/APR-39.

b. Fabrication, optimization and measurement of two color bilayer transparent black backed phosphor film.

c. Optimization of the technique for fabricating low reflectance black films.

d. Measurements of tube performance with regard to brightness, contrast and resolution.

e. Development of specific quantitive criteria to satisfy the requirement for legibility in direct sunlight. Such criteria shall be used to establish optical instrumentation tests which can be used for its verification.

1.1.1 Detailed Program Objectives

For clarity, the program goals are spelled out very accurately as detailed program objectives.

1.1.1.1 Phosphor Screen Characteristics

a. Luminescent Material - The luminescent material shall be one that has a demonstrated high cathodoluminescent efficiency in transparent form. Since it is intended that bilayer films be used, the demonstrated efficiency should be with various colors, particularly red and green. It is not intended that phosphor development work per se, be part of this program.

b. Phosphor Persistence - The transparent phosphors used in the CRT screen should have persistence in the range of JEDEC designations "medium short" to "medium."

c. Physical Characteristics - It is intended that a bilayer type of phosphor screen shall be used in the CRT. In that event, each phosphor layer shall be transparent and may or may not be separated by a transparent dielectric layer.

d. Light Absorbing Layer - A requirement of this program is that the phosphor screens be backed, on the electron gun side, with a uniform light absorbing coating that can be effectively penetrated by the electron beam. Specular reflection from this coating, on the phosphor side, should be no greater than 1 percent. Diffuse reflectance shall be no greater than 0.25 percent. This coating shall not cause any substantial reduction in electron-current or electron-energy into the phosphor screen.

e. Phosphor Electrode - The phosphor electrode shall be a thin aluminum film, behind the black coating of 1.1.1.1-4, and electrically insulated from all other tube electrodes by means sufficient to withstand the operating levels within the tube without electrical breakdown or appreciable leakage current.

f. Phosphor-Screen Substrate - The phosphor screen substrate shall be capable of withstanding all necessary fabrication techniques of the transparent film screen without change of shape or curvature that would degrade the end result of a completed CRT.

1.1.1.2 CRT Characteristics

As stated, the goal of this program is a CRT that is physically and electrically replaceable with a currently existing CRT. To this effect, the envelope, deflection angle and means, focusing means, and basing should duplicate a Dumont KC3055 (formerly KC2626) CRT used in the AN/APR-39. It is accepted that an improved electron gun may be used with this phosphor screen. To this effect, it is desirable that the final CRT be electrically interchangeable with the KC3055, as closely as possible, so that power supplies driving the KC3055 need not be replaced.

1.1.1.2.1 CRT Contrast

It is necessary that the CRT be legible in direct sunlight under its normal mode of operation, without the use of added contrast enchancement devices. Specific quantitative criteria to satisfy this requirement should be developed so that optical instrumentation tests may be used for its verification.

1.1.1.2.2 Faceplate Characteristics

The faceplate size should be directed to the above CRT. The faceplates shall be bonded to the tube envelope by conventional means or use of graded seals. Glass-to-metal seals are undesirable. This program is not intended to support special envelope development.

1.1.1.2.3 Phosphor Voltage Range

The CRT should operate within conventional limits of anode potential. In no case should this potential exceed 20 kV. In the penetration screen configuration, anode potential shifts to achieve color changes should be minimized.

1.1.1.2.4 Resolution

A line width, taken at the half amplitude point of the spot distribution, of 0.012 inches or better is desirable. The line width should not exceed 0.016 inches.

1.1.1.2.5 Display Luminance

The CRT is to operate under ambient illumination from 10^4 to 10^{-3} fc. The CRT luminance is to be uniformly adjustable to provide satisfactory legibility under these conditions.

1.1.1.2.6 Writing Speed

A minimum writing rate of 50,000 in/sec for a single trace for all color fields is desirable.

1.1.1.2.7 Phosphor Maintenance

The transparent phosphors shall have high maintenance under normal modes of operation consistent with paragraph 1.1.1.2.1, and burn se· sitivity tests shall be conducted on the screens incorporated into the CRT.

1.1.1.2.8 Reliability Consideration

Since the CRT's developed under this program are intended for tactical and airborne applications, adequate consideration must be given throughout the development program to the reliability of this tube for such environments. As an objective, the CRT should be able to pass the physical tests for CRT's specified in MIL-E-1.

1.1.1.2.9 Environmental Testing

Environmental testing of the CRT's will not be part of this program.

1.1.1.2.10 Program Emphasis

The program emphasizes the investigative areas outlined in paragraph 1.1.1.1-1), 1.1.1.1-4), 1.1.1.2), 1.1.1.2.1), and 1.1.1.2.5). These emphasized objectives are specifically reviewed in the Summary of Results of this report.

1.2 Subcontract Identification

Lockheed Palo Alto Research Laboratory, of the Lockheed Missiles and Space Company, Incorporated, Palo Alto, California was subcontracted to fabricate the thin film phosphor faceplates. The Watkins-Johnson Company then incorporated the faceplates into CRTs.

2.0 THIN FILM PHOSPHOR FACEPLATE

2.1 Description of the High Contrast Two-Color Faceplate

Figure 1 is a schematic representation of the two-color high contrast film employed in this program. As shown in the illustration, the two-color phosphor is supported on a transparent substrate which forms the faceplate of the CRT.

The green-luminescent film is immediately adjacent to the substrate. The red-luminescent film resides on top of the green one. The opaque layer is deposited on the other face of the red phosphor film. Finally, a thin conducting aluminum layer covers the opaque layer. In operation, the red phosphor layer absorbs most or all of the electron beam energy at potentials below 10 kV. At high potentials, for example, at 20 kV, most of the electron beam is absorbed in the green phosphor. At intermediate potentials, some electrons are absorbed by both layers, generating the additive color yellow. Therefore, at low beam energies, only the red phosphor is excited and the display appears red. At high beam energies, the green-luminescent material is more excited and the display appears green. Various mixtures of the two colors are obtained at intermediate values of the potential. Note that since the luminous efficiency of the red is much lower than that of the green, it is important that the red be placed closest to the electron gun to prevent color contamination of the red by the green. If the green film were closest to the gun, it would not be possible to excite the red without getting some color contamination from the green phosphor.

The optimum film thicknesses were determined to be:
red phosphor - 4000Å, green phosphor - 7000A, NR coating - 3400Å, and aluminum - 600Å.

2.2 Faceplate Fabrication

2.2.1 Sputtering System

The RF sputtering system consists of an MRC Model SM-8500 RF downward sputtering module mounted on an NBC 6-in. diffusion pumped vacuum system, plus a Lepel 5 kW sputtering power supply and auxiliary impedance matching network. The system is capable of attaining bell jar pressures at the low end of the 10^{-7} Torr range within a reasonable evacuation period. Manual valves permit throttling the pump to obtain sputtering pressures of the ordering 5μ. The pressures is established using an Alphatron vacuum gauge and subsequently monitored during sputtering with an MRC shielded Pirani gauge.

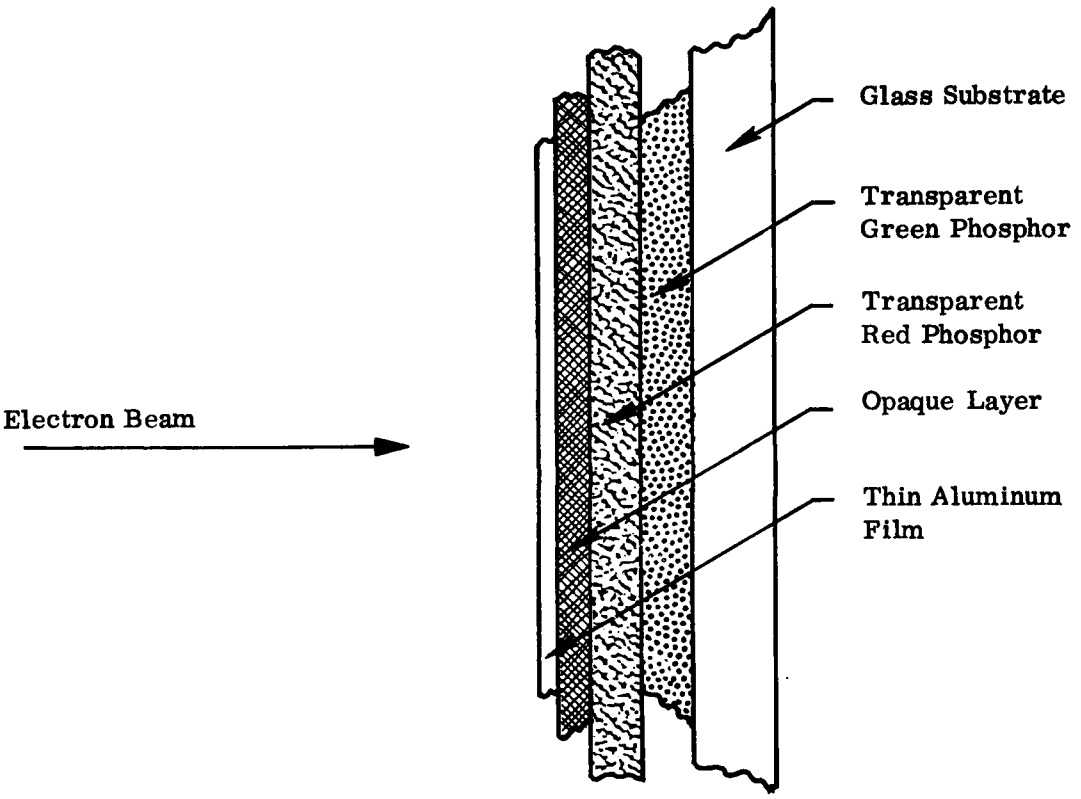

Figure 1. Schematic of High Contrast Two-Color Screen

Matheson Ultrapure Agon is used as the primary sputtering medium. A small amount of hydrogen sulfide, 4.0×10^{-5} Torr, is added to the argon. Nupro bellows sealed micrometer valves are used to regulate gas flow.

Terbium doped and europium doped lanthanum oxysulfide powers prepared in the Lockheed Missile and Space Company (LMSC) lab were used to make the sputtering targets. The targets, in the form of sintered discs, 5-in. in diameter and 0.25-in. thick, were pressed from the powder in a graphite die under an argon atmosphere at a pressure of 1920 psi and temperature of 1410°C, and allowed to sinter under these conditions for somewhat longer than 1 hours. As a precaution, the discs were subsequently dry lapped on 120 grit carbide cloth to remove the surface layer which may have reacted with the graphite, although there was no visual evidence of any reaction having occurred. The targets were then mounted on the target backing plates, using a silver-filled epoxy adhesive. Composition of the targets to be used for this program are La_2O_2S:0.2% Tb for the green and La_2O_2S:6.5% Eu for the red.

2.2.2 Sample Fixturing

Thickness measurements of a La_2O_2S:Eu film with a Varian Angstrometer on preliminary films deposited on glass microscope slides indicated a variation in thickness from the center of the substrate to the periphery as shown by Figure 2. The thickness at the center was 2900Å and at the 1/2-inch radius it measured 2090Å. To eliminate the thickness variation, it was originally thought it would be necessary to construct a special fixture that would rotate and oscillate the substrate. It was known that the shield which surrounds the sputtering target produces a concentration of equipotential lines near the periphery of the target; this has a focusing effect on the argon ions. It was believed that increasing the length of the shield be addition of supplementary rings might intensify the focusing effect, increase the sputtering rate near the target edge, and possibly reduce the thickness variation to acceptable limits.

Rings having thicknesses of 1/16 inch to 1/8 inch, and 3/16 inch were fabricated from aluminum sheet stock. Two screws served to attach the rings to the shield. Measurements were made on a series of films, each deposited using one of the supplementary rings. The results are indicated by the curves of Figure 3. It was found that the 1/16-inch ring improved the distribution over the central 3-inch diameter area to within ±2-1/2% of the center thickness. The center thickness was 3,007Å and the thickness at the 1-1/2-inch radius was 29,320Å. This is considered sufficiently uniform for the program requirements, obviating the need for the more elaborate fixture.

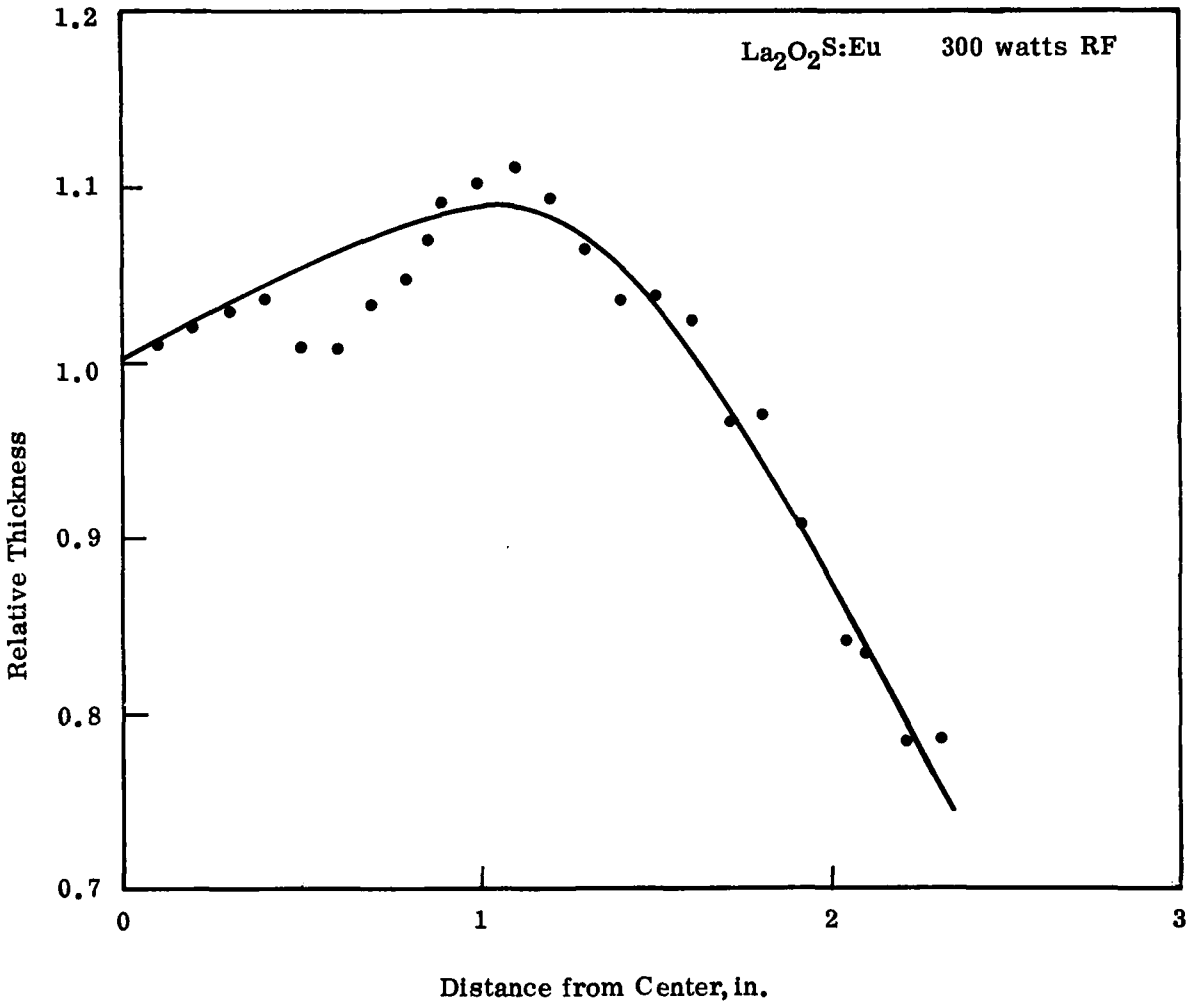

Figure 2. Thickness Variation Without Supplementary Ring

aa41534

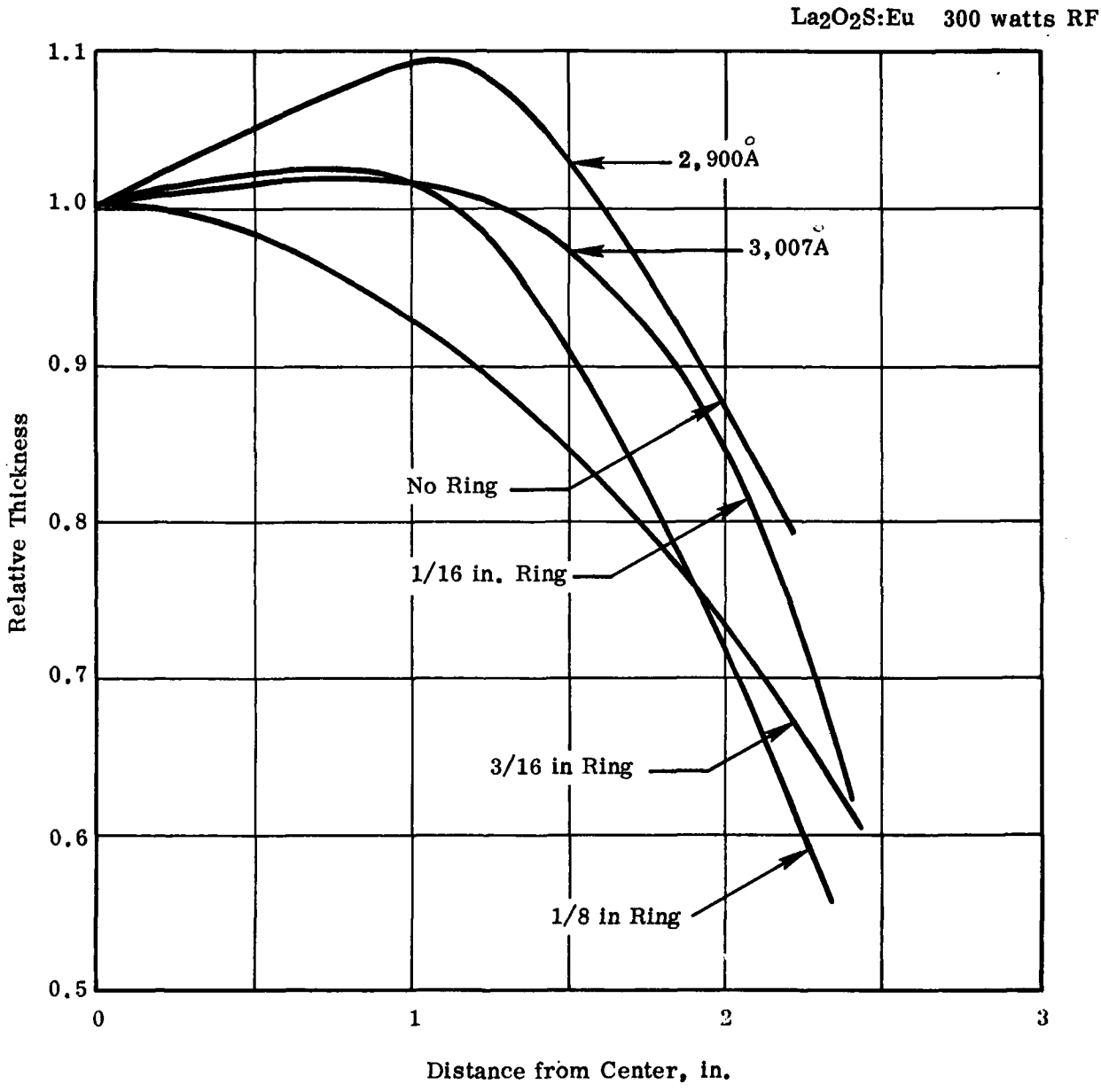

Figure 3. Effect of Supplementary Shield Rings

aa41535

2.2.3 Controlled Atmosphere Heat Treatment

The results of previous studies have shown that it is desirable to subject the films deposited by RF sputtering to a post-deposition heat treatment which significantly increases the luminescent brightness of the oxysulfide films. Optimum results have been obtained by treating in an $H_2 + SO_2$ mixture at 1050°C. At elevated temperature this atmosphere is composed of H_2, SO_2, H_2S and H_2O. This heat treatment promotes atomic mass transport for atomic ordering of the lanthanum oxysulfide and to reach a stoichiometry in equilibrium with the atmosphere at the heat treatment temperature.

2.2.4 Thickness Monitor

The thickness monitoring system consists of a Spectra Physics Model 132 He-Ne laser, a motor-driven beam chopper, a UDT PIN-5 Schottky barrier diode to detect the beam reflected from the sample, a 741-type operational amplifier, a Varian 100 mV strip-chart recorder, and a Tektronix oscilloscope. The monitoring set-up is sketched in Figure 4. A second, identical diode placed in a light-tight housing adjacent to the beam detector diode provides an opposite polarity input to the 741 amplifier, to cancel noise pick-up in the coaxial cables.

The reflected beam consists of light reflected from the film surface plus light reflected from the film-substrate interface. The strip chart recorder provides a continuous record of interference peaks and nulls during growth of the film. The oscilloscope provides a visual indication of the operational amplifier output and is a convenience in aligning the detector.

The most precise thickness control is achieved by terminating deposition exactly at a null; termination between nulls results in somewhat less precision.

From the geometry and Snell's law, it can be shown that interference nulls will occur at thickness given by the equation:

$$t = \frac{m\gamma}{4(n^2 - \cos^2 \alpha)^{1/2}}$$

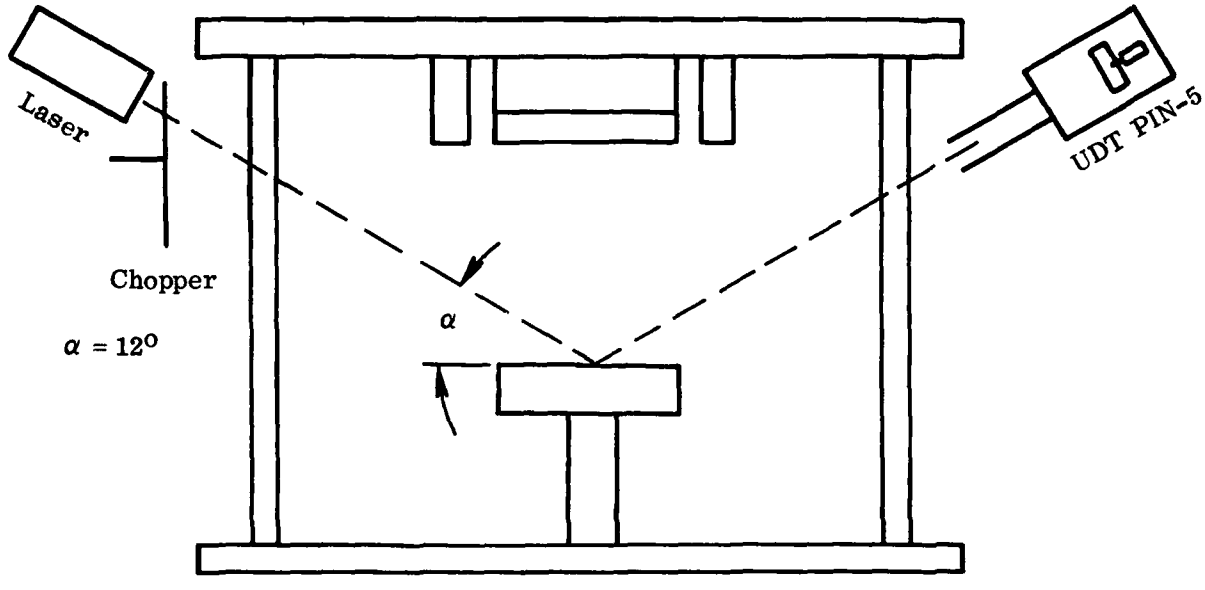

Figure 4. Laser Interferometer for Film Thickness Measurement During Deposition

aa41537

where m is an odd interger, γ the wavelength of the laser light, n the refractive index of the film, and α the angle between the beam and the plane of the substrate. For this situation, $\alpha = 12°$, n = 2.196 for La_2O_2S at 6328 Angstroms. With these conditions, the equation simplifies to

$$t + 804.63\ m \text{ Angstroms.}$$

A more accurate determination of thickness can be made by multiple-beam interferometric measurements on the completed film, using a Varian Model 980-4000 Angstrometer. This requires removal of a part of the film from the substrate by etching or masking part of the substrate during deposition. A thin film of aluminum must then be evaporated over the step at the film edge to provide a reflecting surface. Thickness measurements with the Varian Angstrometer are considered to be accurate to ±40 A. The Angstrometer measurements are also useful in determining deposition rate at constant RF power. Using care to duplicate deposition conditions, thickness may also be controlled by deposition time, probably at some loss in precision.

Figure 5 shows thicknesses determined using the laser interferometer versus thicknesses measured on the same samples using the Angstrometer. The values agree within 6%. The difference is probably due to a difference between the refractive index of the film and that of stoichiometric bulk La_2O_2S.

2.3 Aluminosilicate Glass Faceplates

It was proposed to use Corning No. 1720 aluminosilicate glass for the faceplates. This was based on previous studies at the LMSC Palo Alto Laboratory which had shown that rare earth osysulfide films on No. 1720 glass could be treated at 900°C to give 85% of the luminescent brightness of similar films on sapphire treated at 1050°C. However, 1720 glass was unavailable from Corning. A quotation was requested on faceplates of Corning No. 1723 aluminosilicate glass which had a softening point only 7°C lower than that of No. 1720 glass, according to Corning data sheets.

Other producers of aluminosilicate glass were also contacted but none would quote on the 1720 faceplate requirements.

A quotation on faceplates of No. 1723 glass was obtained from Applied Precision Optics, Inc. of Monrovia, California. This firm had successfully located a distributor with a supply of Corning No. 1723 glass in stock. An order was placed.

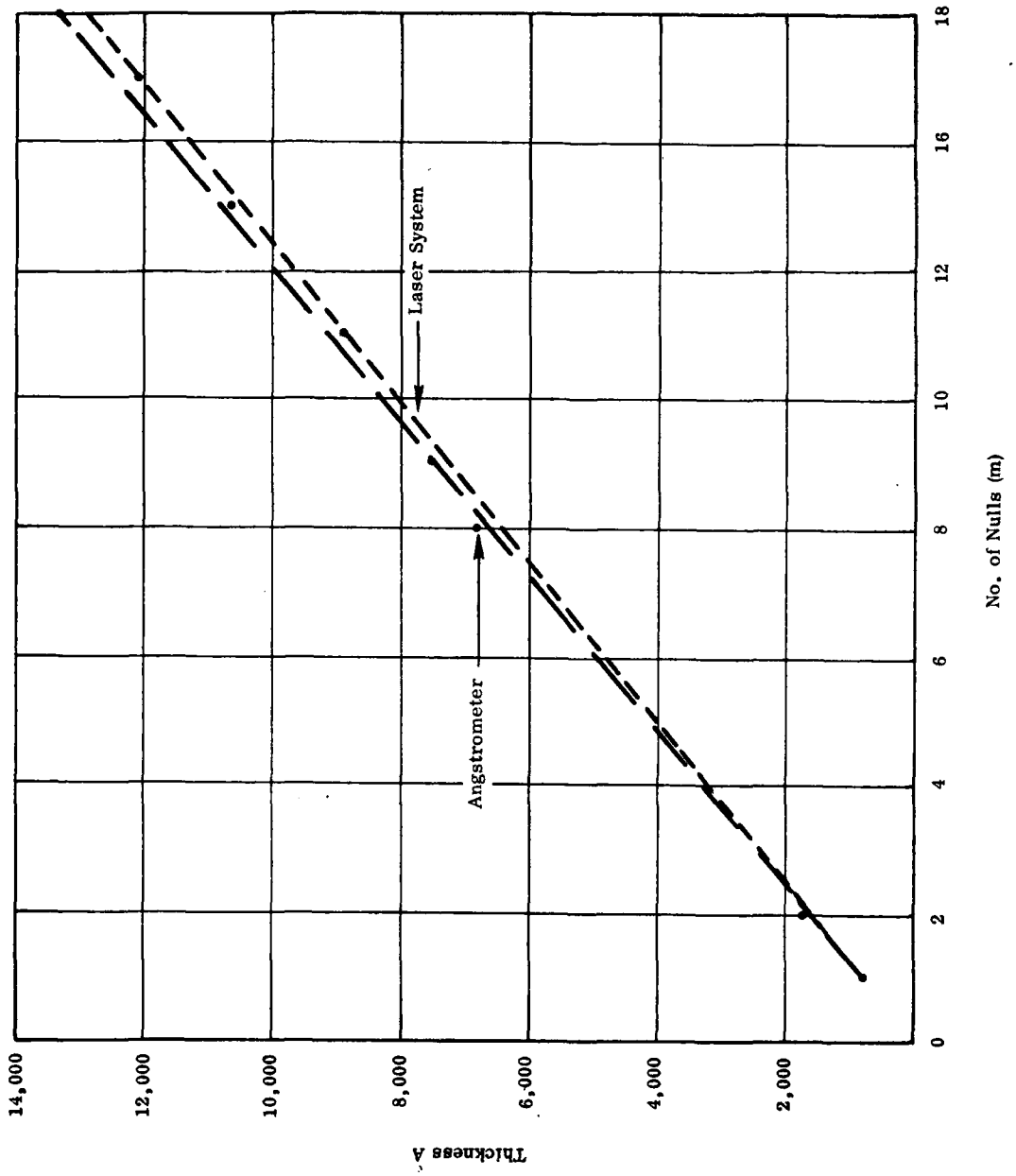

Figure 5. Thicknesses Using the Laser Interferometer Versus Thicknesses Using the Angstometer

The 20 faceplates were received from Applied Precision Optics, Inc. Measurements showed the diameters to be near, but not within, the upper limit specified. Thicknesses ranged from 0.002 to 0.012 greater than specified, but were judged satisfactory for the program. It was observed when viewing the discs edge-on, that some appeared green while others were water-white. The green discs were returned to Applied Precision Optics, Inc. as it was thought a mix-up in glass may have occurred during grinding and polishing. Applied Precision Optics, Inc. contacted their supplier who guaranteed that all the glass supplied was No. 1723 glass. No explanation, other than possible lot-to-lot variation, was given for the green coloration. Presumably, it is due to an impurity, possibly traces of iron, associated with one of the glass constituents.

Applied Precision Optics also supplied some scrap pieces of No. 1723, at LMSC's request. These will be used for practical tests at the 900°C temperature in the reaction tube.

Glass manufacturers do not ordinarily reveal the composition of their glasses. The information available in the literature has usually been obtained by chemical analysis. Variations in results have been noted between investigators for the same glass. This may be due to poor homogeneity of the glass manufacturer's melt or to differences in the analytical procedures used. The reported compositions, however, probably approximate the manufacturer's proprietary "recipe" within a few tenths of a percent for the major components.

The approximate compositions of Corning Numbers 1710, 1720, 1723, and 7059 glasses have been collected in Table 1 from different literature sources.

It appears that the chief difference between the 1720 and 1723 glasses is the presence of 6% BaO in 1723 glass and its absence in 1720 glass. Considerably more BaO is present in the sodium-free 7059 glass. An earlier study in the LMSC Laboratory had shown that 7059 glass was not well suited as a substrate for rare earth oxysulfide films. The low softening point precluded treatment at a high enough temperature to obtain a practical level of luminescent brightness. The maximum temperature to which 7059 glass could be subjected was found to be about 700°C. Extending the time of treatment in $H_2 + SO_2$ increased the brightness but the glass acquired a brown coloration. After ten hours at 700°C, the coloration became sufficiently intense so that brightness measurements became meaningless.

Table 1

CORNING ALUMINOSILICATE GLASSES

(Approximate Percentage by Weight)

	No. 1710 (Ref. 1)	No. 1720 (Ref. 2)	No. 1723 (Ref. 2)	No. 7059 (Ref. 3)
SiO_2	57.0	62.0	57.0	50.2
Na_2O	1.0	1.0	--	--
MgO	12.0	7.0	7.0	--
CaO	5.5	8.0	10.0	--
BaO	--	--	6.0	25.1
B_2O_3	4.0	5.0	5.0	13.0
Al_2O_z	20.5	17.0	15.0	10.7
As_2O_3	--	--	--	0.4

---

[1] E. B. Shand, Glass Engineering Handbook, McGraw-Hill, 1058, p. 4.

[2] J. R. Hutchins III and R. V. Harrington, "Glass" in Kirk-Othmer Encyclopedia of Chemical Technology, Vol. 10, p. 542, John Wiley and Sons.

[3] L. I. Maissel and R. Glang, Handbook of Thin Film Technology, McGraw-Hill, 1970, p. 6-8.

The reason for the brown coloration of 7059 glass is not known. None of the components form brown sulfides or sulfates. By contrast, No. 1720 glass does not acquire a brown coloration. However, preliminary tests with 1723 glass show some brown coloration similar to but less intense than that of 7059 glass. The discoloration of 1723 does not occur when heated in air, even at 900°C, but occurs in the H_2 + SO atmosphere at temperatures above 825°C. It is believed the coloration results from the presence of BaO because both 1723 and 7059 contain BaO, whereas 1720 does not. This presumably would be some impurity normally associated with BaO which reacts to give a colored product. Examination of reagent chemical suppliers' catalogs indicate that traces of iron are a common impurity in barium compounds.

Reagent grade barium dioxide contains about 0.02% iron. For economical reasons, glass manufacturer's probably use materials of lesser purity than reagent grade. Ferrous sulfide is known to be black-brown and is a likely result of sulfurization of traces of iron oxide.

A second problem was also observed in the preliminary tests of 1723 glass. A piece of 1723 glass placed across a quartz boat and inserted into the tube furnace at 900°C for 30 minutes was found to have sagged into complete conformance with the inside walls of the quartz boat. This means that the H_2 + SO_2 treatment of films on 1723 faceplates must be carried out at some temperature lower than 900°C. Some reduction in luminescent brightness is therefore to be expected.

At this time Corning found some 1720 glass they had overlooked and a sufficient supply was purchased to complete the program.

2.3.1 Cleaning Faceplates

To insure good adhesion of the deposited oxysulfide film to the glass faceplate, the latter must be thoroughly cleaned prior to depositing the film. The following procedure has been found to give good results in the LMSC Laboratory.

The faceplates, in lots of six, are loaded into a specially fabricated glass carrier. The faceplate discs are stood on edge, with adequate drainage space between faces of adjacent discs. The carrier is placed in a glass beaker, a few milliliters of an Alconox detergent solution is introduced into the beaker, and the beaker is then filled with deionized water. The beaker is then placed on a hot plate and heated to the boiling point. If the parts to be cleaned have dirt which is stubborn to remove, the beaker may be transferred to an

ultrasonic bath, but this is not ordinarily necessary. In some cases, a preliminary degreasing in 40°C trichloroethylene may also be advisable.

The beaker with the hot detergent solution is usually maintained at the boiling point for 30 minutes, after which the detergent solution is poured off and the beaker refilled with deionized water. This rinsing is repeated for a total of five changes of water, care being taken to rinse down the walls of the beaker each time. The carrier is provided with a handle so that it may be lifted out of the beaker before discarding the liquid contents.

After the fifth water rinse, the carrier is placed in a beaker of cold chronic acid cleaning solution, then placed on a hot plate to heat to 100°C. After 30 minutes at temperature, the carrier is removed and placed in a clean beaker to cool. Cooling avoids cracking of the faceplates due to thermal shock. After cooling, the faceplates are given five rinses with deionized water, as before. Finally, the parts are covered with transistor-grade isoprophyl alcohol, the carrier agitated somewhat by hand, then removed and the alcohol discarded. The carrier is then replaced in the beaker and the latter transferred to a drying oven. When dry, the beaker is removed from the oven and allowed to cool, then covered with a piece of aluminum foil.

For deposition, the discs are removed individually from the carrier, using flat-faced tweezers; the surface is blown free of any possible dust with a freon jet, and the disc is placed in the sputtering chamber. The edge-mask is then placed over the disc and the chamber closed, after which the chamber is evacuated to less than 1×10^{-6} Torr.

2.3.2 Sputtering Procedures

After evacuation of the sputtering chamber to less than 1×10^{-6} Torr (typically $6 - 8 \times 10^{-7}$ Torr), the high vacuum valve is partially closed to serve as a dynamic pumping throttle. Hydrogen sulfide gas is then admitted through a bellows-sealed valve in series with a micrometer valve and the chamber pressure adjusted to 4.0×10^{-5} Torr. Argon is next admitted to bring the total chamber pressure to 5μ.

A pre-shutter RF discharge at 300 watts is then initiated to clean the target surface of any absorbed material and also the inside surfaces of the chamber. Hydrocarbons normally present in air are known to be absorbed when vacuum chambers are open to air; it has been found in the LMSC Laboratory that unless removed by presputtering, these hydrocarbons will contaminate the oxysulfide films and produce

a degree of optical absorption in the films. During the presputtering period, the substrate discs are protected by a shutter from receiving sputtered target material. The presputter period is ordinarily 45 minutes. At the end of this period, the shutter is rotated aside to expose the substrate to the sputtered material.

A deposition period of 120 minutes is required at 300 watts RF power in order to deposit 7000 A of La_2O_2S:Tb. At the end of the deposition period, the RF discharge is extinguished and the work allowed to cool for 30 minutes. The sputtering gases are then shut off and the chamber brought to atmospheric pressure with nitrogen gas, after which it may be opened and the faceplate discs removed to a dust-free enclosure. If another workpiece is not to be immediately placed in the chamber, the chamber should be closed promptly and evacuated, to minimize absorption of atmospheric contaminants.

The second phosphor layer is applied after replacing the La_2O_2S:Tb target with the La_2O_2S:Eu target. The deposition period is 70 minutes, otherwise the same procedure is followed.

2.4 Nonreflecting (NR) Film

The NR film is a light abosrbing inhomogeneous film utilized to achieve a high contrast ratio with a minimum halation effect. Specifically this inhomogeneous film has a composition varying continuously from vanadium pentoxide to vanadium metal. A complete description of this film, and the method of making same is described in U.S. Patent 4,132,919 (Appendix A). This thin film technique was invented by T. Grant Maple of the Lockheed Missiles and Space Company, Inc., Sunnyvale, California and filed December 12, 1977.

The continuous composition gradient of vanadium and oxygen in the NR film imparts the desired optical properties. Diffusion of the vanadium and/or oxygen will degrade the optical properties. At temperatures high enough for atomic transport, the composition gradient is the primary thermodynamic driving force for diffusion. Note, subsequent firing cycles are necessary for CRT fabrication. The NR film oxide lattice (defect oxide lattice) is identified by X-ray diffraction as vanadium pentoxide. Atomic transport just begins at approximately half the absolute melting temperature [(963°K/2) = 209°C]. This is disquieting as 209°C is exceeded in CRT fabrication, especially the frit sealing firing cycle.

The NR film surface exposed to the frit sealing furnace atmosphere is the metallic vanadium end of the vanadium pentoxide-vanadium composition gradient. If a trace of O_2 or H_2O is present in the furnace atmosphere the vanadium will oxidize. The resulting film would be V_2O_5 - oxygen deficient V_2O_5 - VO_x (x can vary from 0 to 5/2). A little diffusion and the film would have no composition gradient. Degradation of the NR film by the diffusion - oxidation mechanism imposes a limitation on subsequent time-temperature treatments. The location and configuration of the film is essential to CRT operation. It has been observed that the frit sealing firing cycle does not seriously effect the NR film if and only if the furnace atmosphere is free of oxygen and water vapor (high purity gas 5 nines or better). The degradation due to diffusion alone is almost negligible. To minimize the risk of degradation, the subsequent firing cycles (frit seal patching) must be minimized.

2.5 Faceplate Structural Integrity - Heat Treatment

The structural integrity of the coated 1720 glass faceplate was lost during necessary post heat treatments. Surface distortion and bulk warpage were observed. The cathodoluminescent properties of the deposited phosphor thin film are improved by a heat treatment in a $H_2 + SO_2$ atmosphere. Maximum improvement occurs with heat treatment at 1050°C. The 1720 glass faceplate can not withstand this treatment without deforming. The heat treatment temperature must be much less than the softening point of 915°C with the corresponding diminished cathodoluminescent improvement (85% of maximum).

The temperature - mechanical strength properties of 1720 glass are revealed in Table 2. At 667°C, the glass just begins to deform under load. Increasing the temperature to 915°C, the glass deforms under its own weight. Between these temperatures the glass may deform if subjected to stress (load).

2.5.1 Surface Distortion

A number of possible causes of the surface distortion were considered. Among these was the possibility that the lot of Corning 1720 glass discs had in some manner been mislabeled and that the discs were in reality 1723 glass, which has a lower softening point than that of 1720 glass. Another possibility was that some manufacturing mistake had resulted in a composition different from either 1720 or 1723 glass.

2.5.1.1 Composition Analysis of Glass

As one of the discs in this lot had been cut into a number of pieces to serve as specimens for the NB film reaction study, a sample was

Table 2

VISCOSITY - TEMPERATURE DATA 1720 GLASS

1720 Glass Temp (°C)	Viscosity (Point)		
1200	10^4	Working Point	Plastic liquid
915	$10^{7.6}$	Softening Point	Deforms under its own weight
712	$10^{13.4}$	Annealing Point	Strain free in 15 minutes
667	10^{14}	Strain Point	No longer rigid under load

readily available for submission to the electron microprobe facility of the LMSC Palo Alto Laboratory. Samples definitely known to be 1720 and 1723 glasses were submitted at the same time to serve as standards for direct comparison. The request for analysis was accompanied by a table of approximate compositions of the various Corning aluminosilicate glasses which had been gleaned from various literature sources (Table 1). The table indicated that a principal difference between 1720 and 1723 was the absence of barium in 1720 and its presence in 1723 glass.

The electron microprobe analysis results definitely established that the test (potash feldspar) as a standard, the microprobe facility was able to estimate the compositions of 1720 and 1723 glasses with reasonable precision. The estimates compare very closely with the values tabulated from the literature. Prior to the electron micriprobe analysis, we had some doubts about the purported compositions because the literature gave no indication as how the compositions were determined. It is well known that Corning considers the compositions of their glasses as proprietary and does not disclose this information.

2.5.1.2 Definitive Definition of the Problem and Solution

It was found that no surface distortion of an uncoated 1720 glass disc occurred at 844°C for one hour in argon, while a disc coated with La_2O_2S phosphor films showed surface distortion after treatment at the same temperature in the $H_2 + SO_2$.

The surface distortion was in the form of a somewhat complex pattern in that the uncoated surface of the 1720 glass had frosty areas together with clear areas which appeared to have melted. These clear areas looked somewhat like spokes of a wheel, and were generally concave. In all cases, the distortion was confined to regions of the front (uncoated) surface opposite the film-coated area of the back surface (Figure 6). There was no surface distortion in the border region opposite the 1/4-inch wide uncoated border area on the film side.

A further test was made by treating an uncoated 1720 disc in the $H_2 + SO_2$ atmosphere at 870°C for one hour. No surface distortion of the disc occurred, thus ruling out any reaction between the carbon support plate and the glass disc that might have been promoted by the active gaseous ambient.

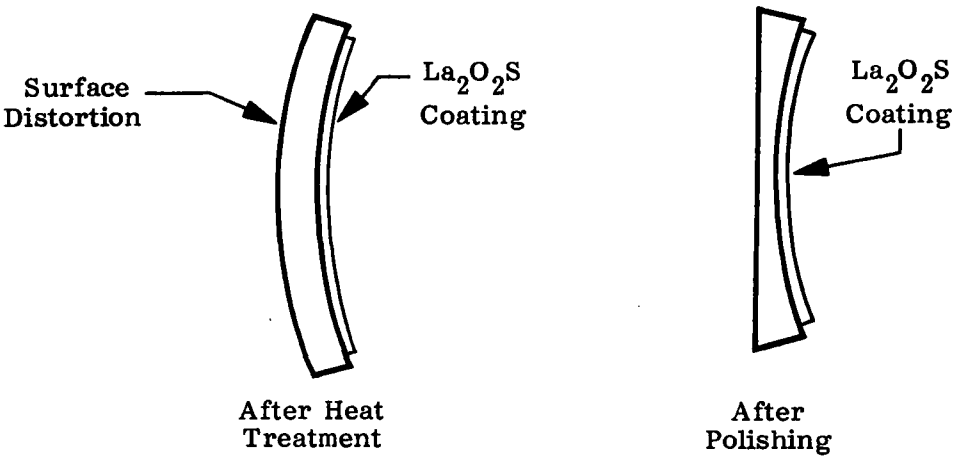

Figure 6. Cross-Section of Thickness Variation After Polishing. Warpage Is Exaggerated.

It is concluded that the very unusual surface distortion observed on treating coated discs is the result of stress arising from the difference in thermal expansion coefficients between the phosphor film and the glass. The linear coefficients for La_2O_2S and 1720 glass are 6×10^{-6} per °C (300-500°K) and 4.2×10^{-6} per °C (273-573°K), respectively. A comparable difference probably exists at 870°C (1143°K), although no literature values are available for either material at this higher temperature. At the treatment temperature, the mismatch of expansion coefficients between film and glass produces a tensile stress upon the coated surface of the glass. As the temperature exceeds the strain point, the stress is relieved by viscous flow of the glass. Holding at the maximum temperature (870°C) for one hour, the glass has time to equilibrate to a strain free condition. On subsequent cooling from 870°C the coated surface would be constrained to contract faster than the uncoated surface. Cooling below 667°C the then rigid glass would be placed under compressive stress beneath the coated surface with a possibility of tensile stress at the uncoated surface.

The surface distortion appears to be greatly accentuated when there is intimate contact between the glass disc and the carbon support, which is the case when the support has been lapped flat. Very little distortion was previously observed using the bowed vitreous carbon or graphite plates, although the discs slumped into the bow (bulk distortion).

An attempt was made to eliminate or at least minimize the distortion by introducing and removing the faceplates from the furnace more slowly than previous practice. A rate of 2 inches per minute, about one-third the former rate, was used. Although some improvement was noted, it was much less than hoped for.

2.5.1.3 Interim Solution

As an interim solution, the possibility of removing the distortion by optical polishing was investigated. One treated faceplate was submitted to Diffraction Optics, Inc., for trial polishing, with the request that their usual method of mounting the discs with optical pitch and subsequent removal by chilling in the freezer by modified. A laboratory test had shown two small slivers of film had spalled when a treated disc was placed in a freezer for 24 hours, then warmed to room temperature. The slivers were only about 1/32 in. x 1/4 in., but this was considered unacceptable.

A second faceplate was sent to Phil Krzyzkowski at ERADCOM for trial polishing on a Mazur machine which does not employ optical pitch mounting.

The faceplate submitted to Diffraction Optics, Inc., was successfully polished without damage to the phosphor film. The remaining faceplates with phosphor films were then submitted to Diffraction Optics, Inc., for polishing. Upon return of the polished faceplates, NR films were deposited. Optical reflectivity and brightness measurements were then made.

2.5.2 Bulk Distortion

The faceplates would warp (bulk distortion) to varying degrees during heat treatment. The thermal expansion coefficient mismatch discussed in the previous paragraph results in the La_2O_2S coating applying a stress to the glass substrate at elevated temperature. Reiterating, for clarity, during heat treatment the glass is under stress while heating until temperatures above 667°C when the glass flows to relieve this stress. Holding at the maximum temperature (870°C) for one hour, the glass has time to equilibrate to a strain free condition. When cooling to 667°C, stress is relieved by viscous flow. However, the La_2O_2S coated surface is contrained to contract more than the other side and this strained (Figure 6) or warped condition is "frozen in" as the faceplate cools below 667°C to room temperature. The distortion results in a thickness variation of the polished faceplate. This condition does not manifest itself as a problem. A grinding step during the frit sealing operation accommodates the distortion.

2.5.3 Slumping During Heat Treatment

It was noted (2.5.1.2) that the glass faceplate slumped to conform to the supporting substrate during the 870°C heat treatment. Moreover the problem was solved by polishing the substrate flat. The verb slump is not entirely accurate. Slumping is glass deforming under its own weight (softening point of 1720 glass is 915°C). Slumping will not occur unless the temperature is increased 45° to 915°C. However, the concave substrate would accommodate stress induced concave warpage just discussed (2.5.2) as the faceplate was placed on the substrate coated side up. The differential thermal expansion plus the unsupported weight of the faceplate combined to make the glass "slump." It was observed the flat substrate reduced this deformation appreciably.

2.6 Reflectance and Brightness Measurements

2.6.1 Specular Reflectance

The specular reflectance for faceplates 22-27 were initially measured on the distorted faceplates at selected positions that were visually

frost-free. In general, these areas were concave, and it is probable that some of the incident light escaped detection by the photmeter by reason of reflection at an angle other than the apparent incident angle.

The faceplates were measured again after optical polishing to remove the distortion. The average of the measurements was 0.3% higher than that for the previous measurements (faceplate 26 was sent to P. Krzyzkowski for polishing on the Mazur machine at ERADCOM and was thus not available for the after-polish measurements).

Specular reflections were again measured for this group of faceplates eight days later, at the time the diffuse reflectance measurements were made. The values were lower than the second measurements, and higher than the initial measurements. There was also a somewhat smaller spread of the individual faceplate values. This may be the result of improved operator skill or perhaps due to aging of the polished surfaces; it is well known that a reduction of reflectance is associated with again of polished surfaces.

The results of the reflectance measurements for faceplates 22-27 are summarized in the accompanying Table 3.

Reflectance measurements for faceplates 29-37 were made only after polishing and are summarized in Table 4.

2.6.2 Diffuse Reflectance

Two methods were used for the diffuse reflectance measurements. In the first method the sample was rotated 16 degrees from the specular measurement position. This produced an angle of incidence of 10° and a measuring angle for the scattered or diffusely reflected light of 16°, (Figure 7). The signal measured in the diffuse position was referenced to the signal obtained in the specular position.

In the second method, the physical arrangement was identical, but the sensitivity of the Pritchard Spot Brightness meter was increased by a factor of 10 and the measured signal referenced to that obtained from a diffuse source (513 Glo Paint on Dow 17 substrate) for which a reflectance of 0.89 had been previously determined for visible light.

For the first method, all samples gave a value of 0 ±0.008; for the second method, all samples gave a value of 0.007 ±0.001. In the second method, it is suspected that the measured signal is due to stray light in the measurement room.

Table 3

RESULTS OF REFLECTANCE MEASUREMENTS

Faceplate Number	Specular Before Polish, 1-12-79	Specular After Polish, 2-12-79	Specular After Polish, 2-20-79	Diffuse After Polish, 2-20-79
22	0.054 = 5.4%	0.051	0.050	<0.010
23	0.056	0.058	0.055	<0.010
24	0.047	0.054	0.053	<0.010
25	0.052	0.058	0.055	<0.010
26	0.046	--	--	--
27	0.053	0.057	0.055	<0.010
28	0.054	0.053	0.053	<0.010

Note: Faceplate 26 was sent to P. Krzyzkowski at ERADCOM for polishing.

Table 4

RESULTS OF REFLECTANCE MEASUREMENTS

Faceplate Number	Specular After Polish, 2-21-79	Diffuse After Polish, 2-21-79
29	0.061 = 6.1%	0.007
30	0.059	0.006
31	0.055	0.006
32	0.064	0.007
33	0.060	0.007
34	0.055	0.007
35	0.058	0.009
36	0.060	0.009
37	0.057	0.006
Average	0.059	0.007

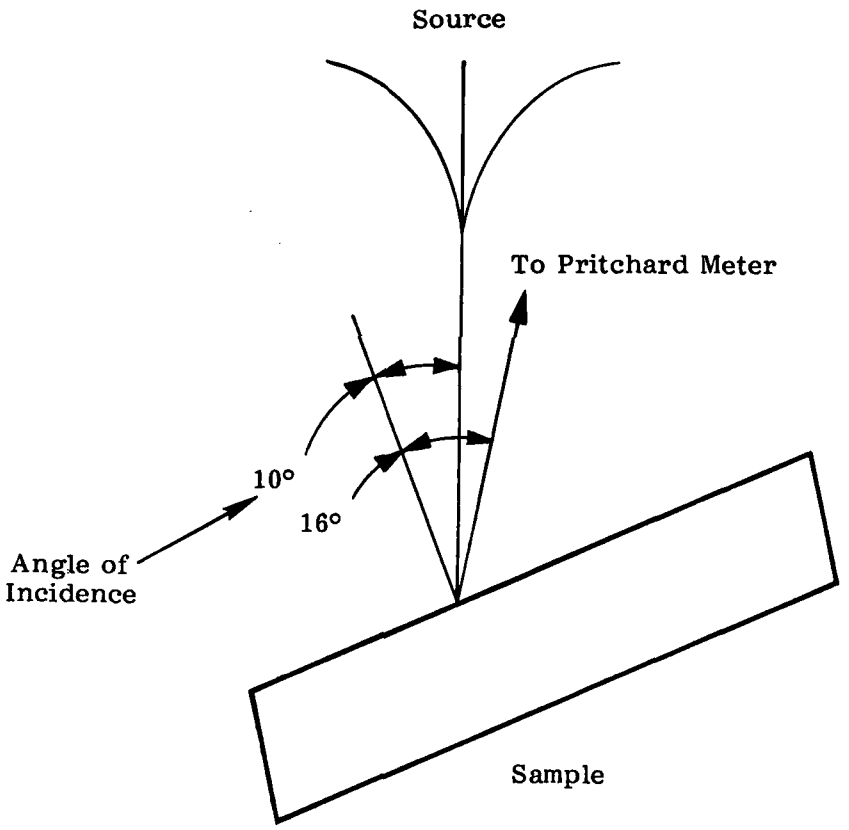

Figure 7. Diffuse Reflectance Geometry

Measurements were also made on two faceplates (6 and 22) by a third method, believed to have greater precision than the preceding two months. Faceplate 22 was selected as typical of the faceplates fabricated under the present contract. Faceplate 6 was an early faceplate, rejected because of its very grainy appearance which was expected to have a large diffuse scattering. In this third method, the faceplate was mounted on a spectrometer table and light from a diffuse source collimated by a slit, was made incident on the faceplate at one of three selected angles (20°, 40°, and 60°). A photomultiplier was mounted on a second arm of the spectrometer table. With the faceplate illumination arm kept fixed at the given angle of incidence, the detector arm was rotated to permit measurements at a number of positions on each side of the specular reflectance angle. The measured values were then referenced to the value at the specular reflectance position. The results were compared to those for a specular front surface aluminum mirror. The results are plotted in Figures 8 through 10. The results for Faceplate 22 fall on the same curve as for the specular mirror, indicating that the diffuse reflectance of this faceplate was negligibly small, and validating the data as absolute. For Faceplate 6 however, the results differ considerably, as expected, from those for the specular mirror.

2.6.3 Cathodoluminance Brightness

Cathodoluminescent brightness of each faceplate was measured at LMSC using the demountable measuring system. The results, normalized with respect to an La_2O_2S:Tb film on sapphire processed at 1050°C, are summarized in Table 5 for Faceplates 22 to 37. The light output (raster brightness) is measured as a function of electron beam energy (anode potential), other parameters being constant. The electron beam current was 5 microamperes producing, at 80% duty cycle, a current density of 170 $\mu a/cm^2$ for the 0.0238 square centimeter bombarded region. This data is plotted and shown in Figures 11 through 15. At higher anode potentials, the luminance is proportional to the electron energy as the electron-electron collision probability is independent of electron energy (anode potential). At lower energies absorption mechanisms contribute nonlinearities. Using the demountable test system, the electron gun and drive parameters are common to all brightness data and would necessarily contribute the same error (if any) to all measurements. Accordingly this data indicates variations of the cathodoluminenscent properties of each faceplate relative to the others. The similar theshold voltage for cathodoluminescence (6 kV) for Faceplates 22 through 37 indicates very uniform film thickness. The scatter at higher potentials is not unexpected because of the limitation in heat treatment temperature imposed by the low softening temperature of the 1720 glass. This results in a discrete amount of reordering (incomplete reordering).

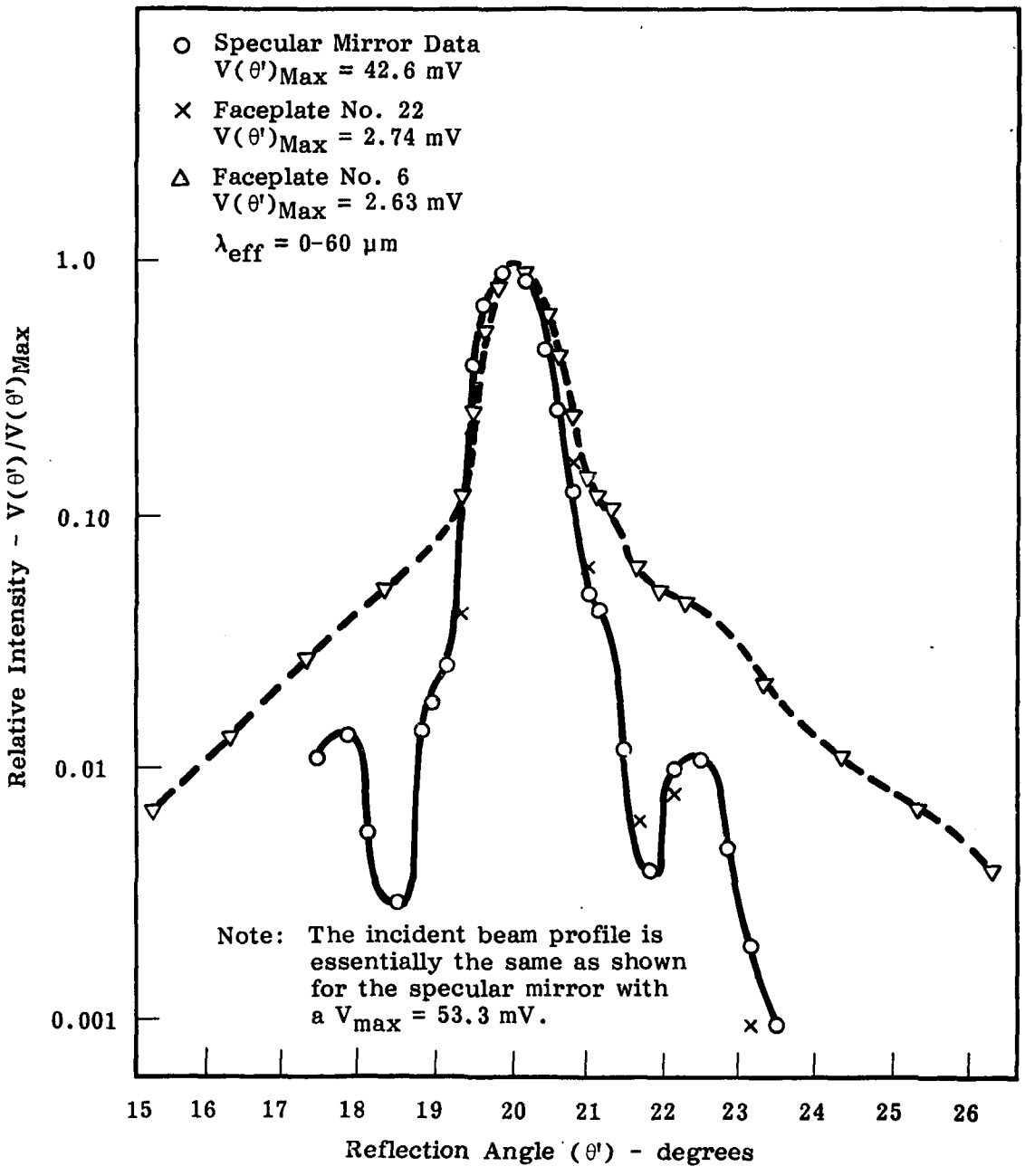

Figure 8. Reflected Beam Profiles for a Specular Reference Mirror and Two Faceplate Samples, for an Angle of Incidence Setting of $\theta = 20°$

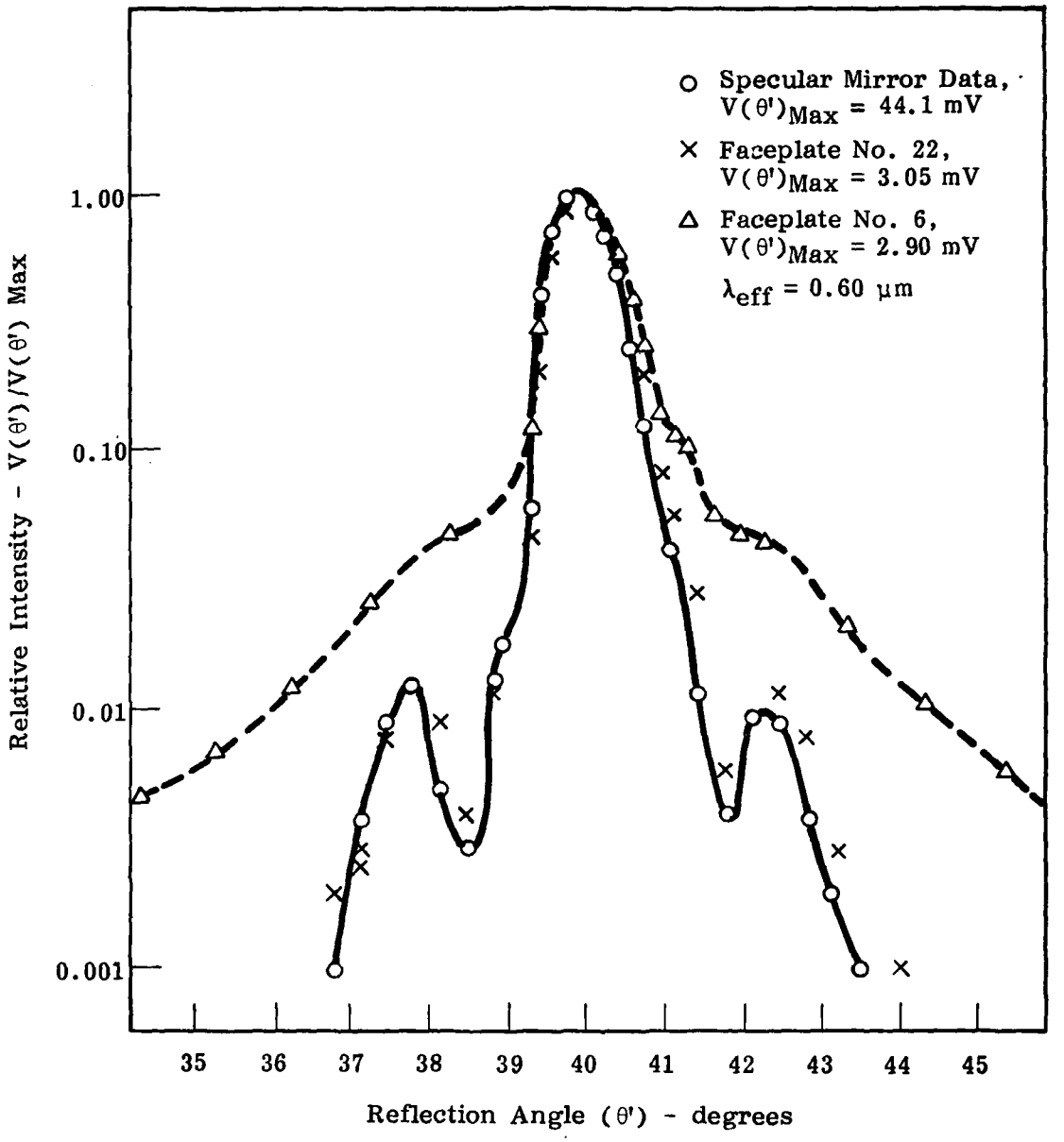

Figure 9. Reflected Beam Profiles for a Specular Reference Mirror and Two Faceplate Samples, for an Angle of Incidence Setting of $\theta = 40°$

aa43945

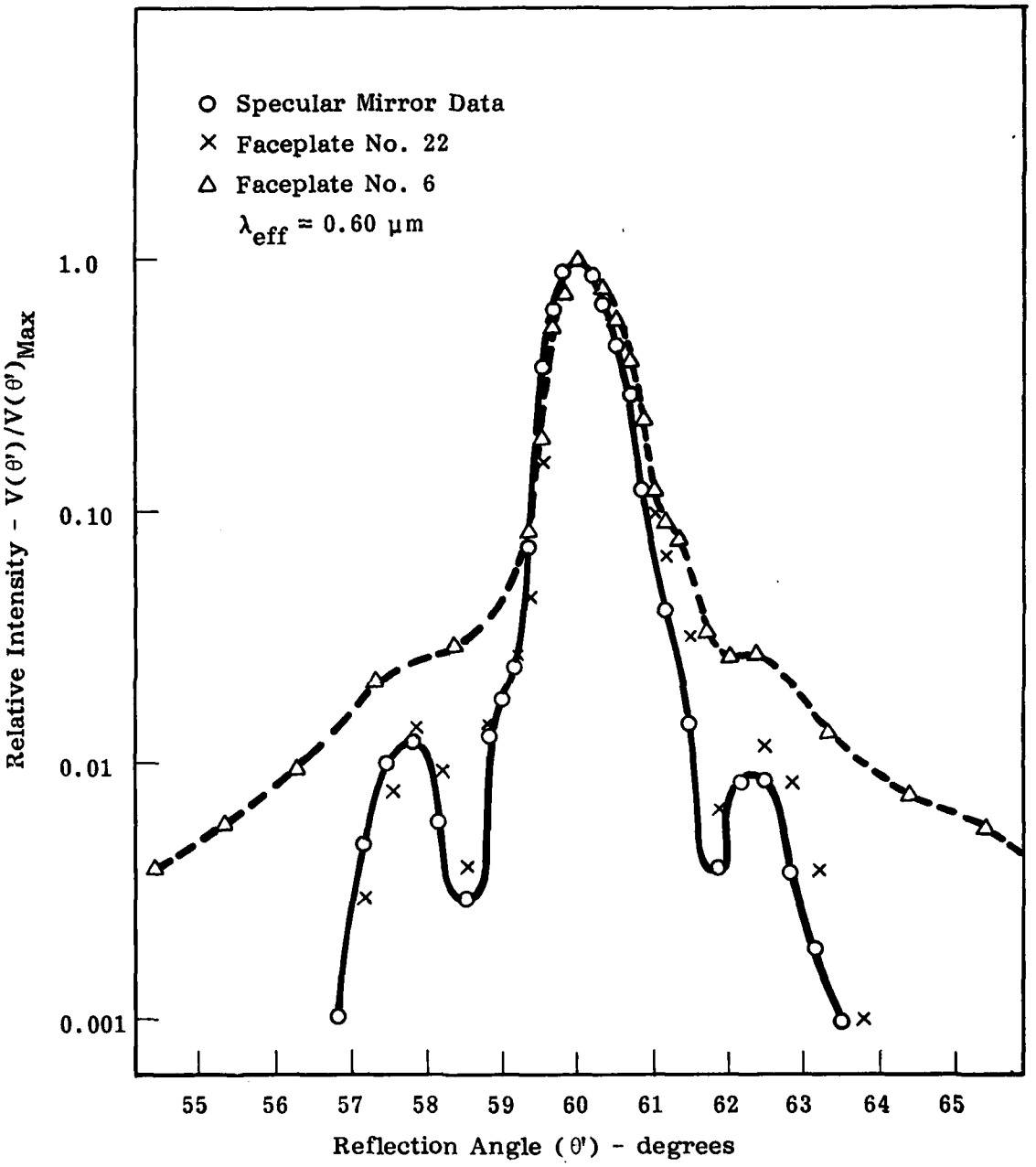

Figure 10. Reflected Beam Profiles for a Specular Reference Mirror and Two Faceplate Samples, for an Angle of Incidence Setting of $\theta = 60°$

Table 5

MEASURED CATHOLOLUMINESCENCE BRIGHTNESS, fL

Electron Energy keV	22	23	24	25	26	27	28	29	30	31	32	33	34	35	36	37
6	0.8	0.4	0.7	0.9	*	0.6	0.7	1.0	0.2	0.2	0.7	0.3	0.7	1.3	0.9	0.4
8	11.0	13	10	16.2	–	19.6	15.5	17.5	6.3	5.2	11.7	8.0	11.8	23.0	16	10.4
10	55	51	52	61	–	76	58	60	32	32	43	29	48	75	54	39
12	130	114	126	136	–	170	131	133	80	94	97	91	106	163	126	95
14	243	224	235	239	–	318	240	249	178	186	192	175	205	286	240	177
15	310	276	293	291	–	388	294	305	224	233	227	240	273	333	308	229

aa43536A

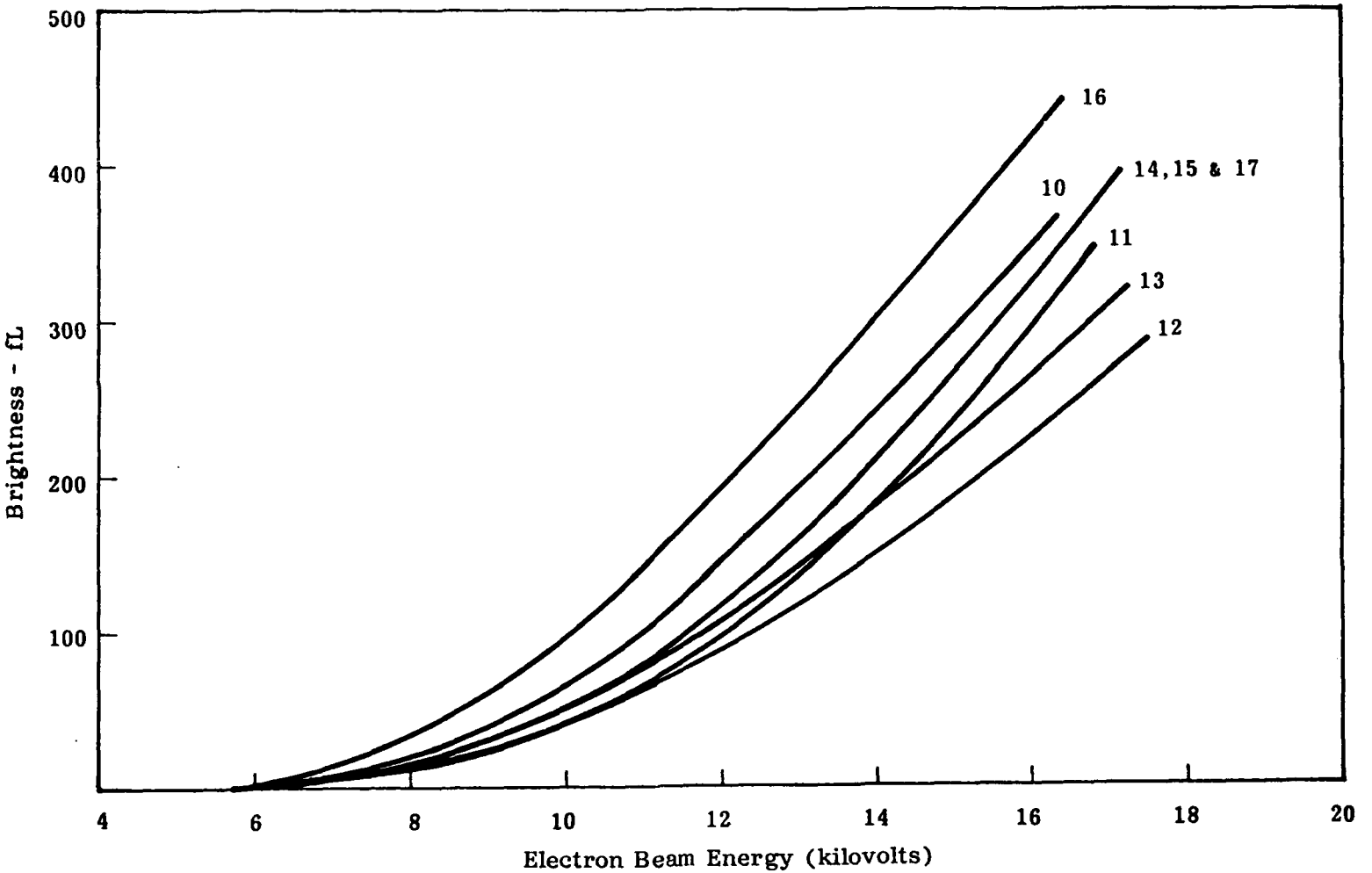

Figure 11. Demountable Brightness Data FP 11 - FP 17

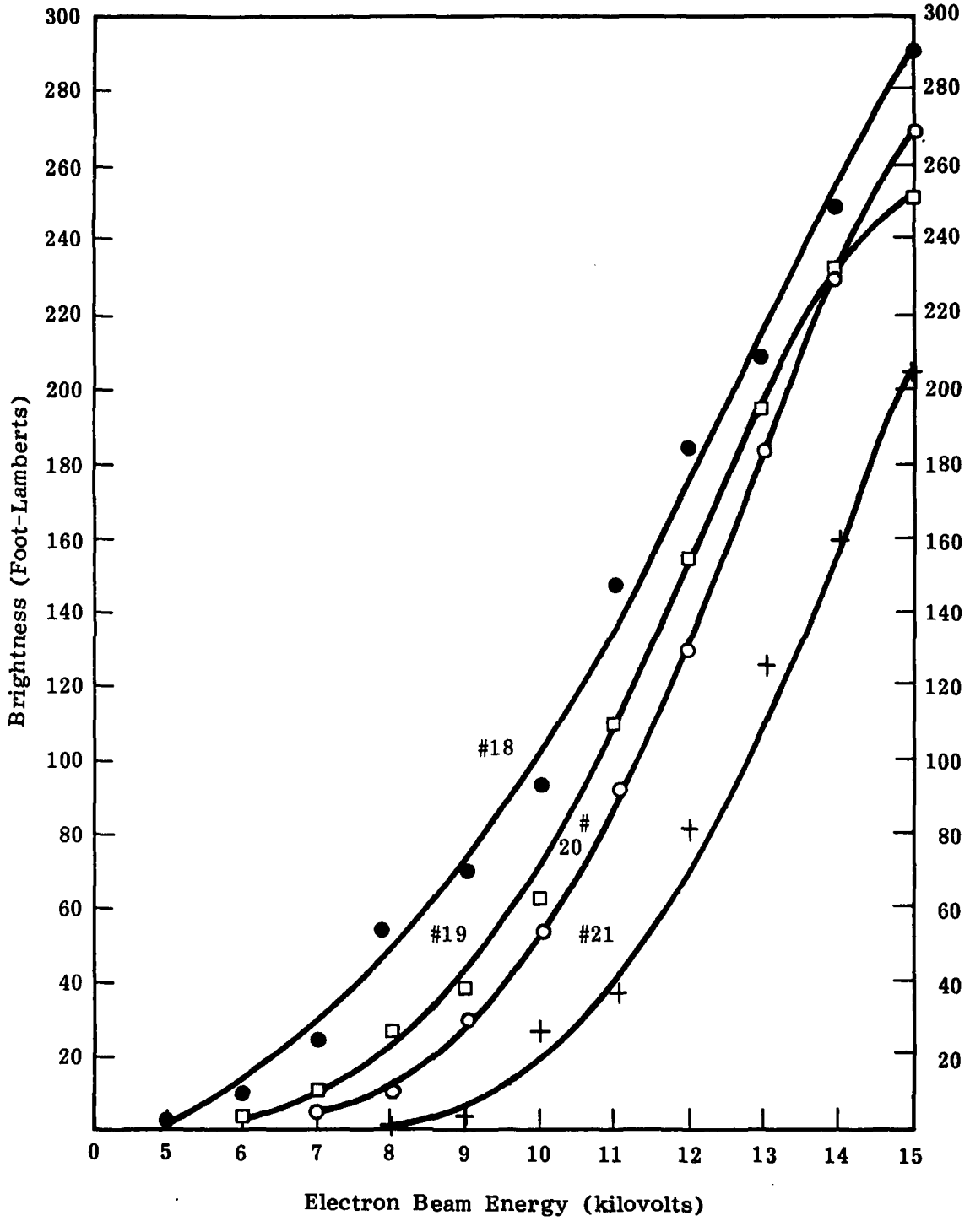

Figure 12. Demountable Brightness Data FP 18 - FP 21

aa43524A

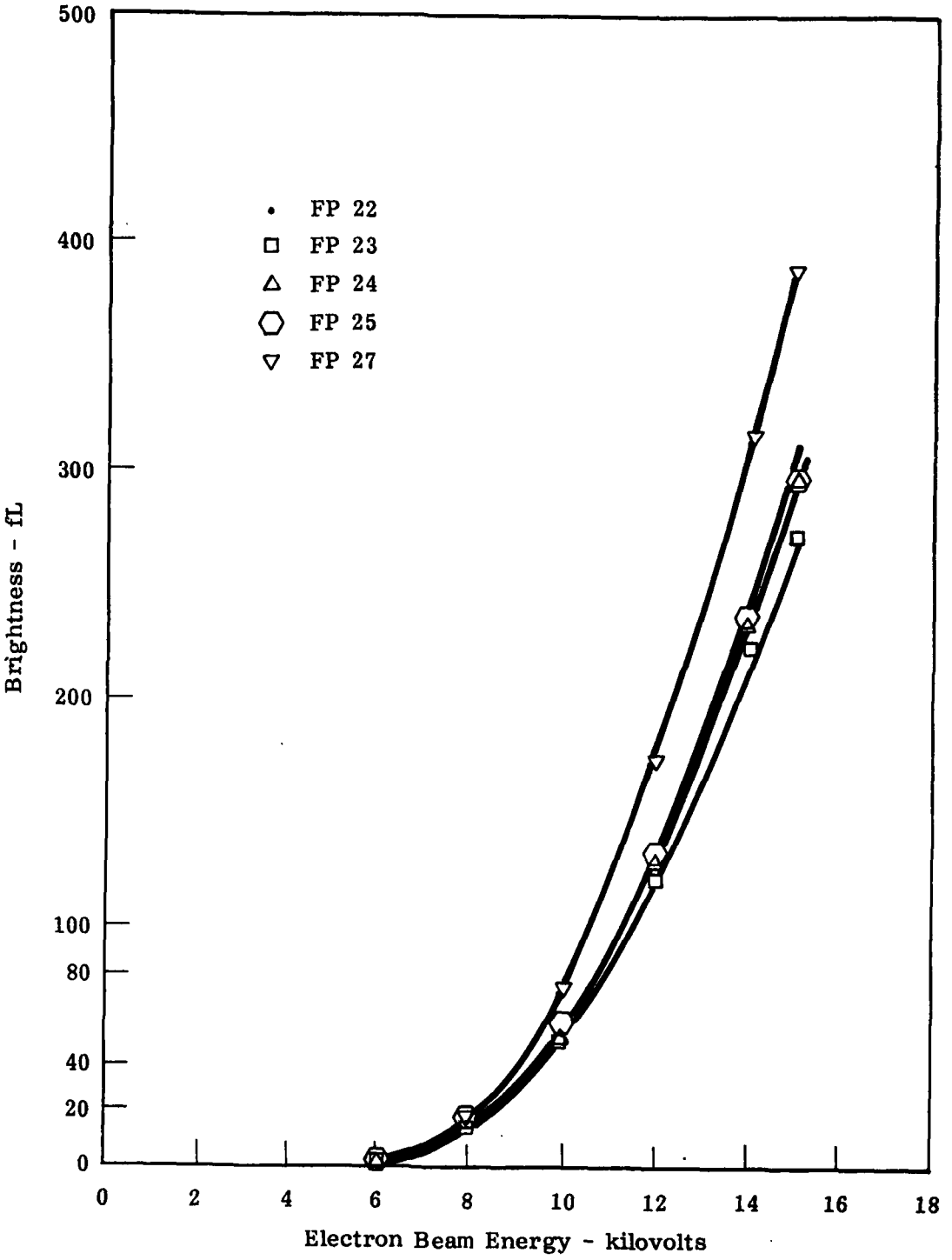

Figure 13. Demountable Brightness Data FP 22 – FP 25 and FP 27

aa43947

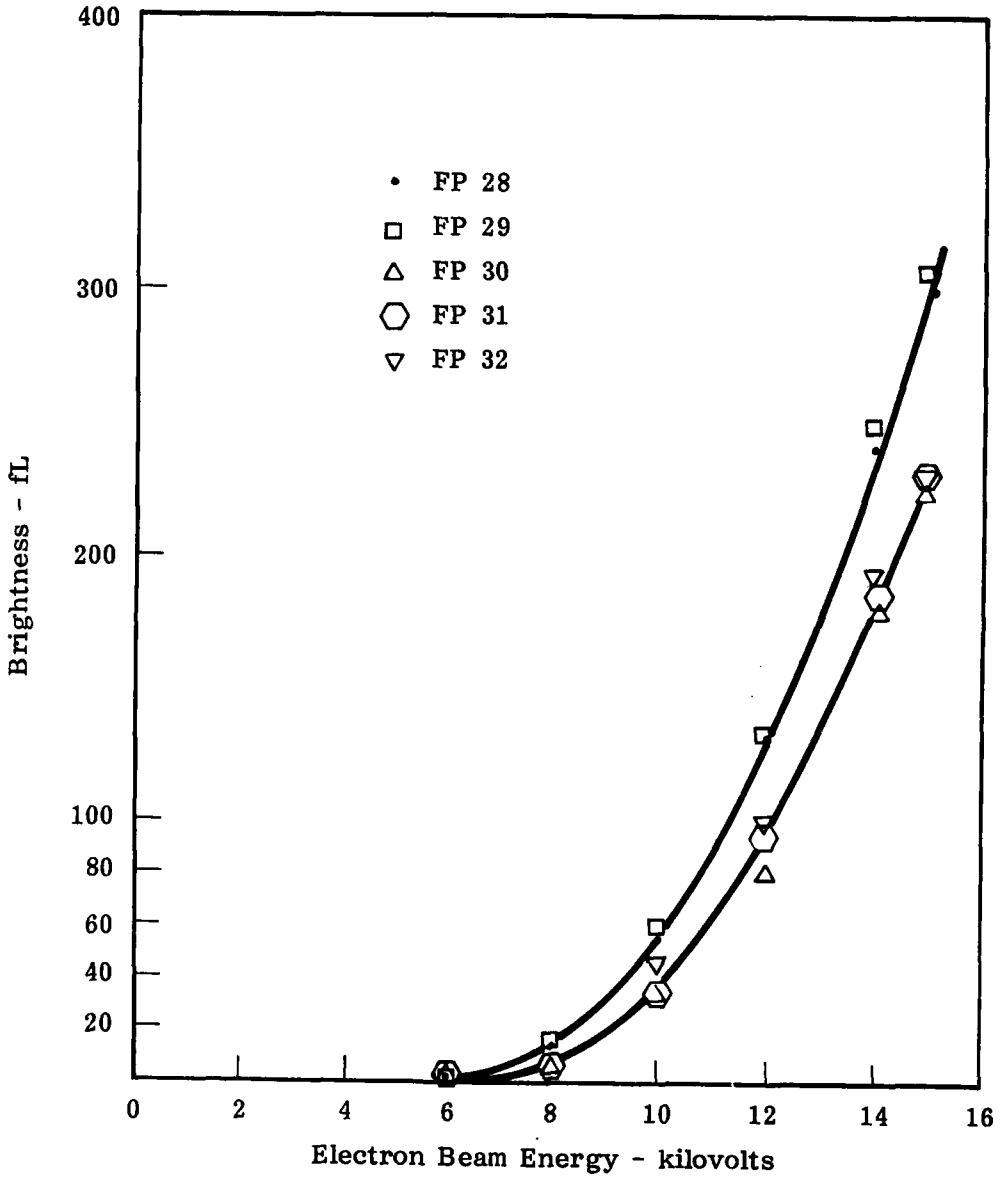

Figure 14. Demountable Brightness Data FP 28 – FP 32

aa43948

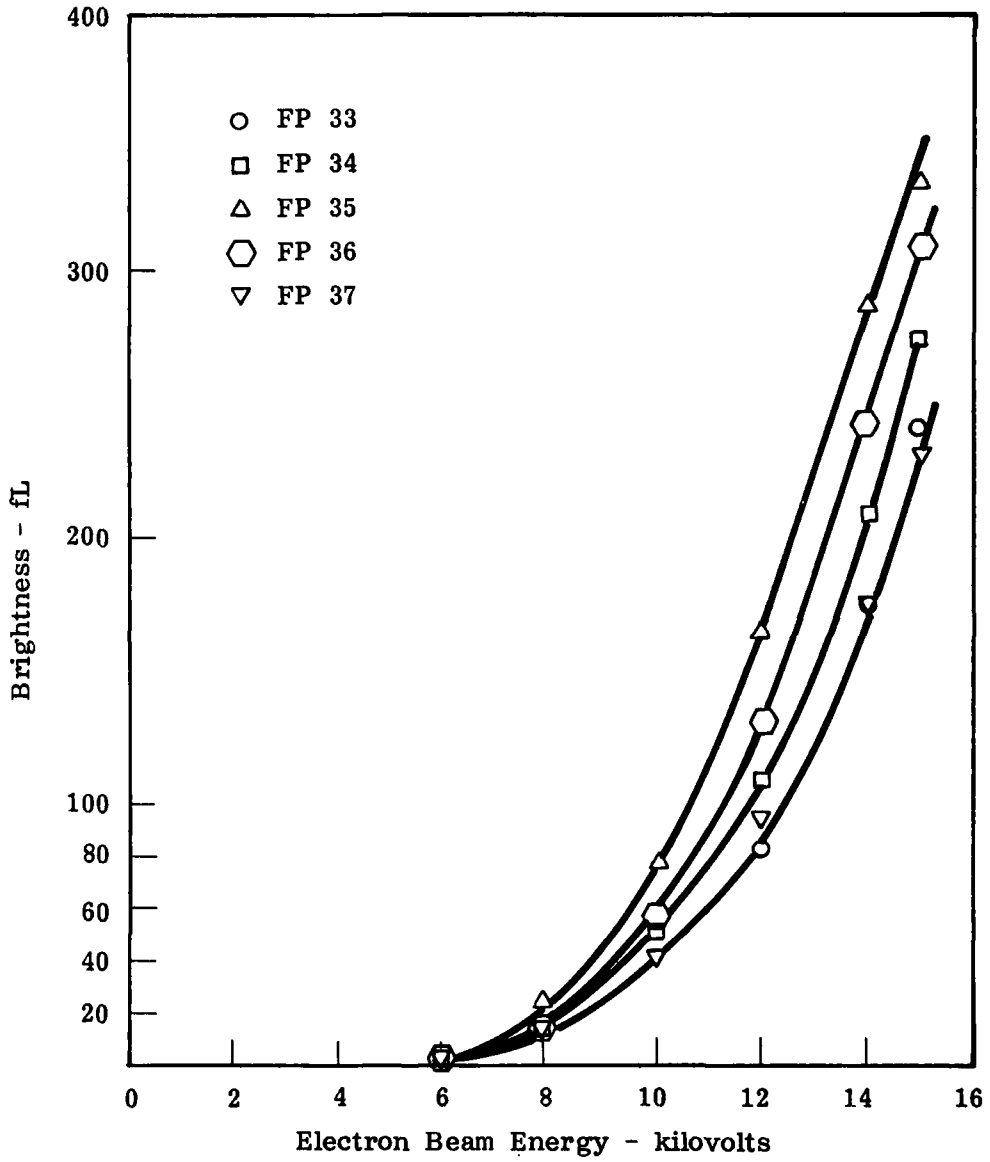

Figure 15. Demountable Brightness Data FP 33 – FP 37

aa43949

It is apparent the amount of disorder originally present can vary. After similar heat treatment, there is a similar variance in the degree of order even though the lattice is more ordered. To reduce this variation to a minimum the faceplate material must be able to withstand 1050°C heat treatment without deformation.

In one instance, Faceplate 19 (Figure 12), the at high potentials indicates cathodoluminescent saturation. The rate of increase of brightness with increasing electron beam energy decreases. All other faceplates show linear relationships at higher potentials. However, the brightness data for the completed CRT (Figures 37 and 38) shows the Faceplate 19 brightness to be in the middle of the scatter of data for all the CRT's for the higher anode potentials of 15 and 18 kV. Furthermore, the demountable data is of average brightness. It is concluded: the saturation indication in the demountable data alone is not valid.

2.7 NR Film Reaction Study

2.7.1 Preparation and Test Condition

During the assembly of a high contrast cathode ray tube, the faceplate is sealed at elevated temperature to the funnel-shaped glass tube envelope by means of a glass frit. The temperature must be sufficiently high to fuse the glass frit and effect a vacuum-tight bond between the faceplate and envelope. The aluminum film used to prevent charge accumulation on the phosphor during tube operation is ordinarily applied by vacuum evaportation only after the seal has been made. The NR film is thus exposed to the ambient atmosphere during sealing; the ambient should therefore be inert towards the NR film. Due to the elevated sealing temperature, there is a possibility of degradation of the NR film, which would be made evident as an increase in the reflectivity of the NR film. There is also the possibility of a reaction between the NR film and the phosphor film, which would become evident as a decrease in the cathodoluminescent brightness of the phosphor film.

A study was made to determine the effect of exposure of the phosphor film - NR film combination to elevated temperature for a period of time in an inert atmosphere. Conditions were chosen to simulate those of sealing the cathode ray tube faceplates to the tube envelope during assembly which is typically 640°C in a nitrogen atmosphere for one hour.

An 8000 Å film of La_2O_2S:Tb phosphor was deposited on a 3-inch diameter disc of 1720 glass identical to those used for the faceplates.

A non-reflective vanadium-based fiom was next deposited over the phosphor. One-half of the disc was masked and 800 A of aluminum deposited on the unmaked NR film area. Specular reflectivities were measured for the aluminum-coated and uncoated areas from the faceplate viewing side.

The disc was then divided into a number of pieces using a diamond saw. After thorough rinsing to remove sawing debris, the pieces were dried. Pairs of aluminum-coated and uncoated pieces were subjected to temperatures of 652°, 627°, and 605°C in an argon atmosphere of a tube furnace for 1 hour. Argon was selected as the ambient atmosphere to insure complete inertness toward the NR film. Nitrogen, however, is presently used as the actual sealing ambient and there is some possibility of an effect on the NR film by reaction of vanadium with nitrogen. The literature (Reference 1) suggests such reaction would be minimal below 700°C.

2.7.2 Reflectivity Measurements

Specular reflectivities were subsequently measured on the individual test pieces. The measured results are shown in Table 6. The reflectivities of all test pieces is seen to have increased. The averaging increase was 20%. The increase for the aluminum-coated samples was about half that of the non-aluminum coated samples at 605° and 627°, but practically identical at 652°C. A more extensive study would be required to draw valid conclusions as to any real difference between aluminum-coated and uncoated faceplates.

Before treatment the samples without aluminum had the normal metallic vanadium appearance of their back sides and had low light transmission as viewed against the laboratory fluorescent lamps from their front side after treatment. All three samples without aluminum lost their metallic appearance and had increased transmission.

The samples with aluminum were opaque due to the aluminum both before and after treatment. The aluminum of the sample treated at 605°C exhibited the usual bright metallic appearance after treatment. The aluminum of those treated at 637° and 652°C had a yellow tone after treatment. The yellow tone is probably due to diffusion of vanadium metal into the aluminum. This alloying is discussed again in Section 3.2.

The increase of transparency (and consequently, reflectivity) is probably due to a diffusion of oxygen or vanadium through the graded vanadium NR film, the initial composition of which is believed to be V_2O_5 at the La_2O_2S-NR film interface and metallic vanadium on

Table 6

NR FILM REACTION STUDY

(MEASURED SPECULAR REFLECTIVITIES)

Sample	Glass	Phosphor	NR Film	Aℓ Film	Temp (°C)	Time (Min)	R_{meas}	ΔR	$\frac{\Delta R}{R}$, %
5	1720	La_2O_2S:Tb	V	No	652	60	0.066	+0.013	+24.5
4	1720	La_2O_2S:Tb	V	No	627	60	0.062	+0.009	+17.0
2	1720	La_2O_2S:Tb	V	No	605	60	0.069	+0.016	+30.2
Untreated	1720	La_2O_2S:Tb	V	No	--	--	0.053	--	--
9	1720	La_2O_2S:Tb	V	Yes	652	60	0.073	+0.015	+25.9
8	1720	La_2O_2S:Tb	V	Yes	627	60	0.064	+0.006	+10.3
13	1720	La_2O_2S:Tb	V	Yes	605	60	0.064	+0.006	+10.3
Untreated	1720	La_2O_2S:Tb	V	Yes	--	--	0.058	--	--

the outside. An interdiffusion would decrease the oxygen gradient through the film, producing a leveling effect with all portions of the NR film tending toward a uniform lower oxide of vanadium.

2.7.3 Cathodoluminescent Brightness Measurements

To assess the possibility of a reaction between the La_2O_2S phosphor film and the NR film, cathodoluminescent brightness measurements were made on the treated samples and compared with the measured brightness before treatment. Any reaction would be expected to result in a reduced brightness. On the other hand, no change of brightness would indicate the absence of reaction.

Results of the brightness measurements are summarized in Table 7. The brightness of the untreated test specimens as a function of the electron beam energy at 5 μA beam current is shown in Figure 16. Comparison of the aluminized part with the unaluminized part shows that at 14 keV, approximately 2 keV is absorbed in the aluminum, with 12 keV remaining for exciting the phosphor. Therefore Table 7 compares the results for the unaluminized samples at 12 keV with those for the aluminized samples at 14 keV. The standard was a La_2O_2S:Tb film on a sapphire substrate which has been treated in an $H_2 + SO_2$ atmospher at 1050°C.

It is seen that there is no significant difference between the normalized results for the treated and untreated samples, so that it may be concluded that there is no reaction between the phosphor film and the NR film.

2.8 CRT Contrast Study

Contrast measurements were not performed. A rigorous and precise analysis of the CRT optics is presented in Appendix B. The results of this analysis are a sound basis to evaluate the results of this program.

Figure 17 shows the functional dependence of contrast CRT luminescence (footlamberts) for worst case conditions, direct bright sunlight.

The luminescence (290 fL) of the green display (20 kV) affords a worst case contrast ratio of 1.28.

Table 7

CATHODOLUMINESCENT BRIGHTNESS

Sample Number	Glass	Phosphor	NR Film	Temp (°C)	Time (Min)	Measured Brightness (fL)	Measured Standard (fL)	Measured Brightness (fL)
Samples Without Aℓ (12 kV)								
5	1720	La_2O_2S:Tb	V	652	60	280	1720	318
4	1720	La_2O_2S:Tb	V	627	60	320	2050	312
2	1720	La_2O_2S:Tb	V	605	60	310	2000	310
Untreated	1720	La_2O_2S:Tb	V	--	--	360	2200	327
Samples With Aℓ (14 kV)								
9	1720	La_2O_2S:Tb	V	652	60	285	1760	324
8	1720	La_2O_2S:Tb	V	627	60	322	2050	314
13	1720	La_2O_2S:Tb	V	605	60	300	2000	300
Untreated	1720	La_2O_2S:Tb	V	--	--	360	2200	327

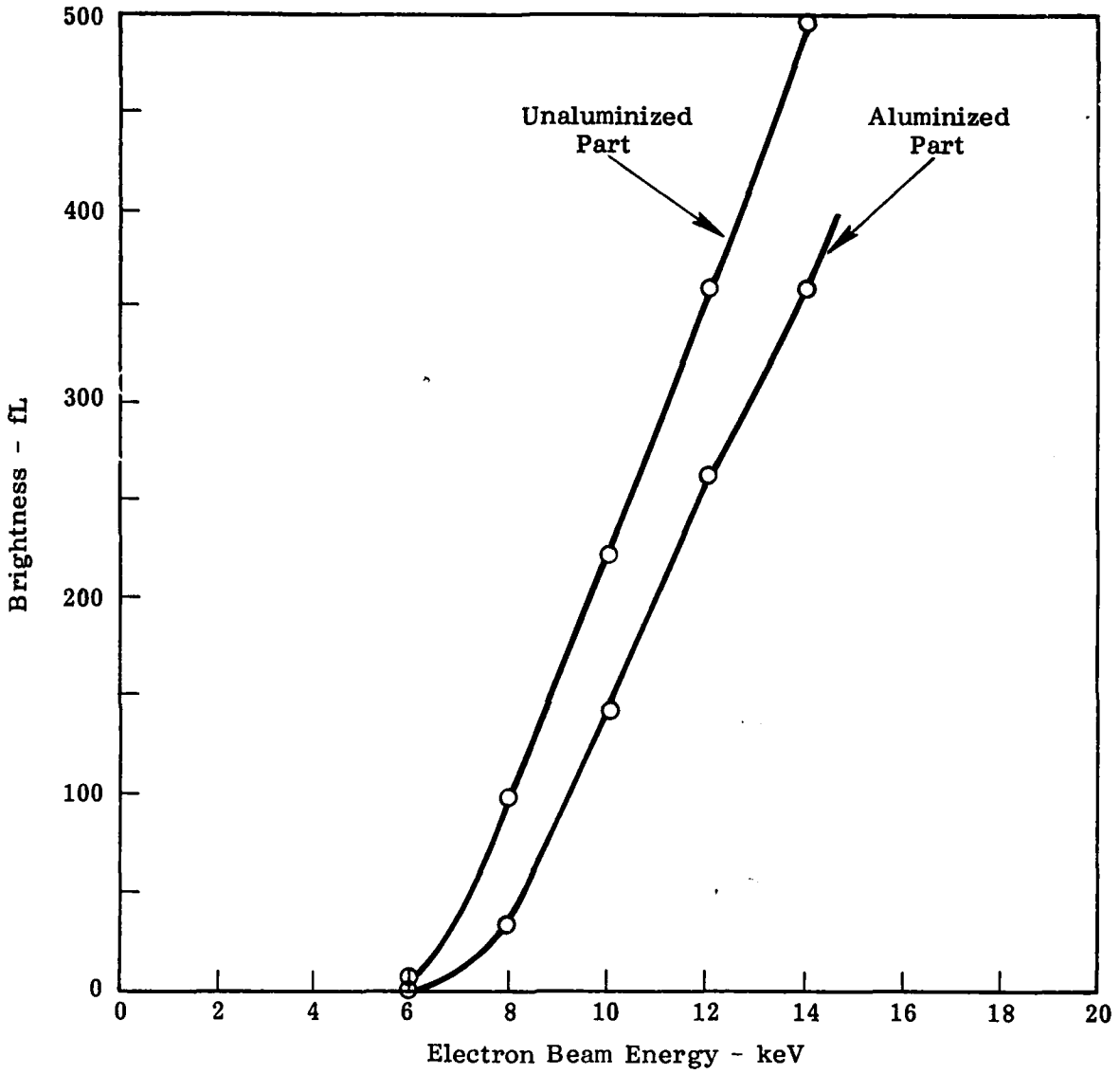

Figure 16. Cathodoluminescent Brightness Before Treatment

aa43950

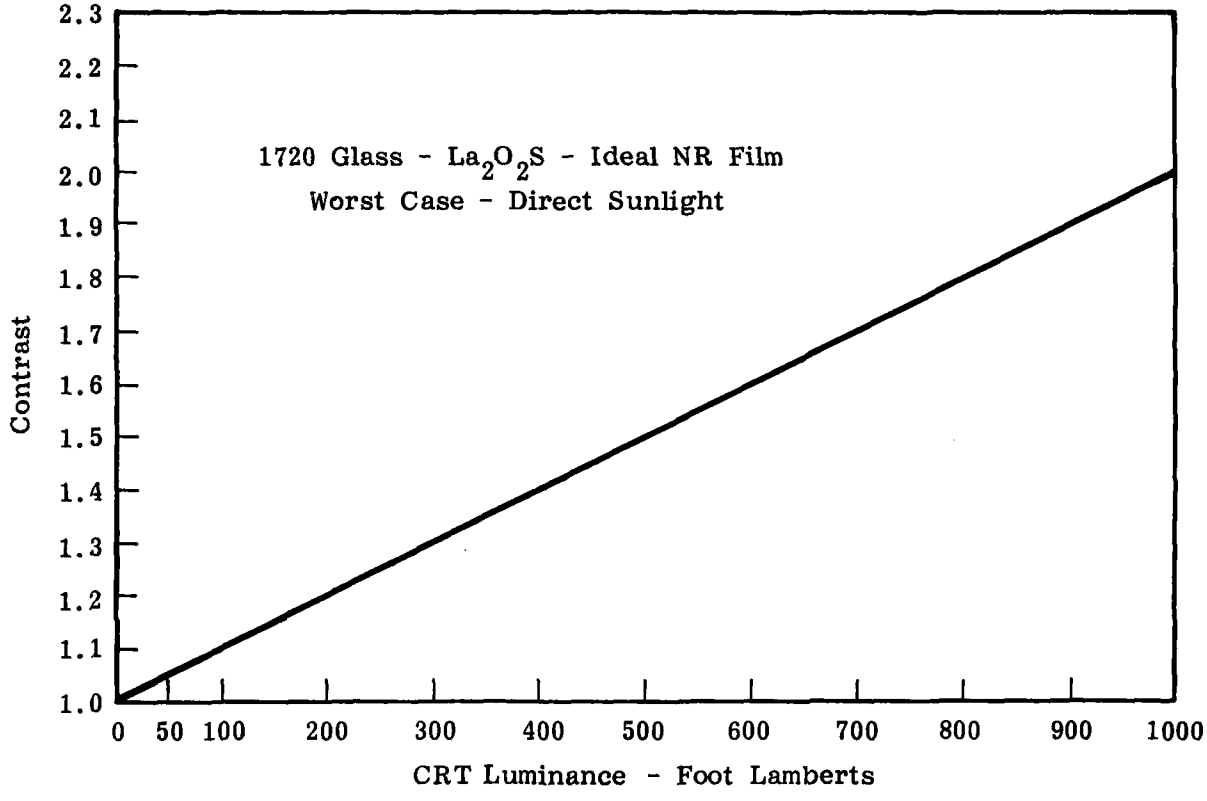

Figure 17. Contrast Versus CRT Brightness in Bright Sunlight

aa43951

3.0 CRT FABRICATION

The CRT fabrication sequence is shown in the assembly flow diagram in Figure 18. The most compatible glass components are numerically designated in the flow diagram and further identified in Table 8. The similarity of thermal coefficients of expansion is of prime importance for compatibility. Of secondary importance is the compressive stress in the final glass structure. Compressive stress allows some thermal mismatch. Tensile stress is always catastrophic in this and other normal glass structures.

Table 8

GLASS TCE DATA

Glass	Thermal Coefficient of Expansion x 10^{-7}	Component
Corning 1720	42	faceplate
Corning 3320	40	funnel and neck glass
Corning 7720 (Nonex)	36	electron gun stem
Schott 8486	41	funnel candidate
Schott 8487	40	neck glass
Corning 7593	42	frit
Owens-Illinois SG7	42	frit

The sequence of the assembly flow diagram is followed in reviewing each fabrication operation. The difficulties and associated solutions particular to the assemble of this CRT are fully explained in their turn. Figure 19 dimensionally defines the outline of the finished tube. Figure 20 further identifies the CRT with potted leads attached in preparation for shipment. The sources of Corning and Schott glass are noted in Figure 21, and photographs of the finished CRT are shown in Figure 22.

3.1 Faceplate Fabrication

Faceplates were coated at Lockheed Missiles and Space Co, Inc., Palo Alto, California as previously described.

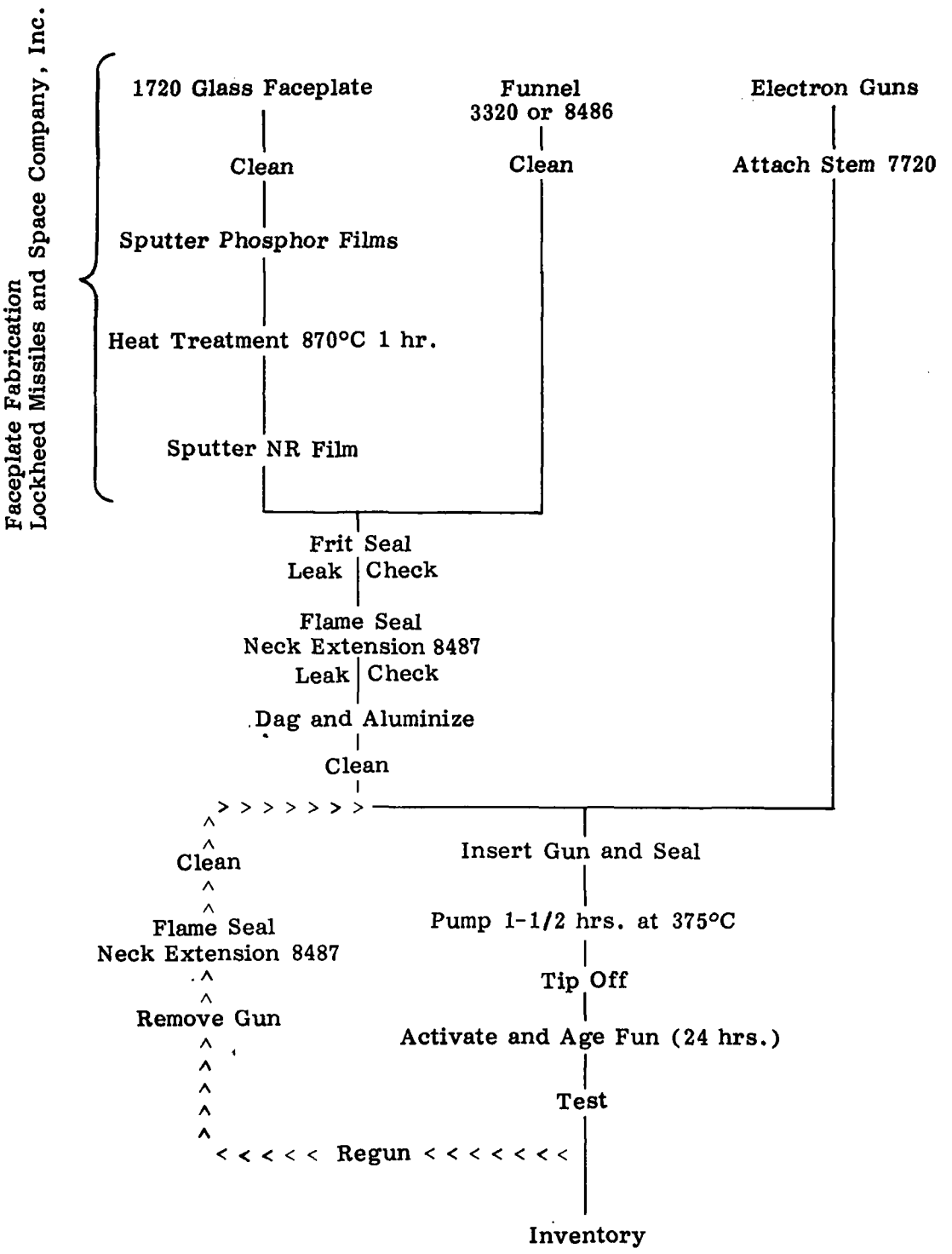

Figure 18. CRT Fabrication Flow Diagram

aa43971

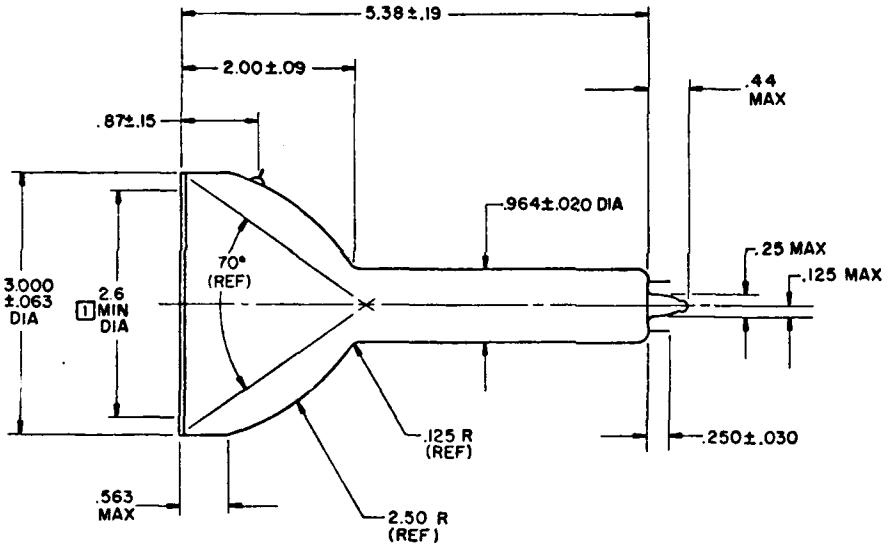

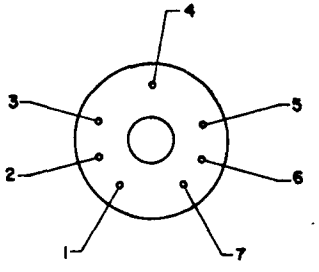

BOTTOM VIEW
PIN DETAIL
SCALE·2/1

SOCKET CONNECTIONS	
PIN	CONNECTION
1	GRID NO. 1
2	HEATER
3	GRID NO. 2
4	CATHODE
5	GRID NO. 2
6	FOCUS
7	HEATER

1. USEFUL SCREEN DIAMETER.

NOTES:

Figure 19. Cathode Ray Tube WJ-3414-11

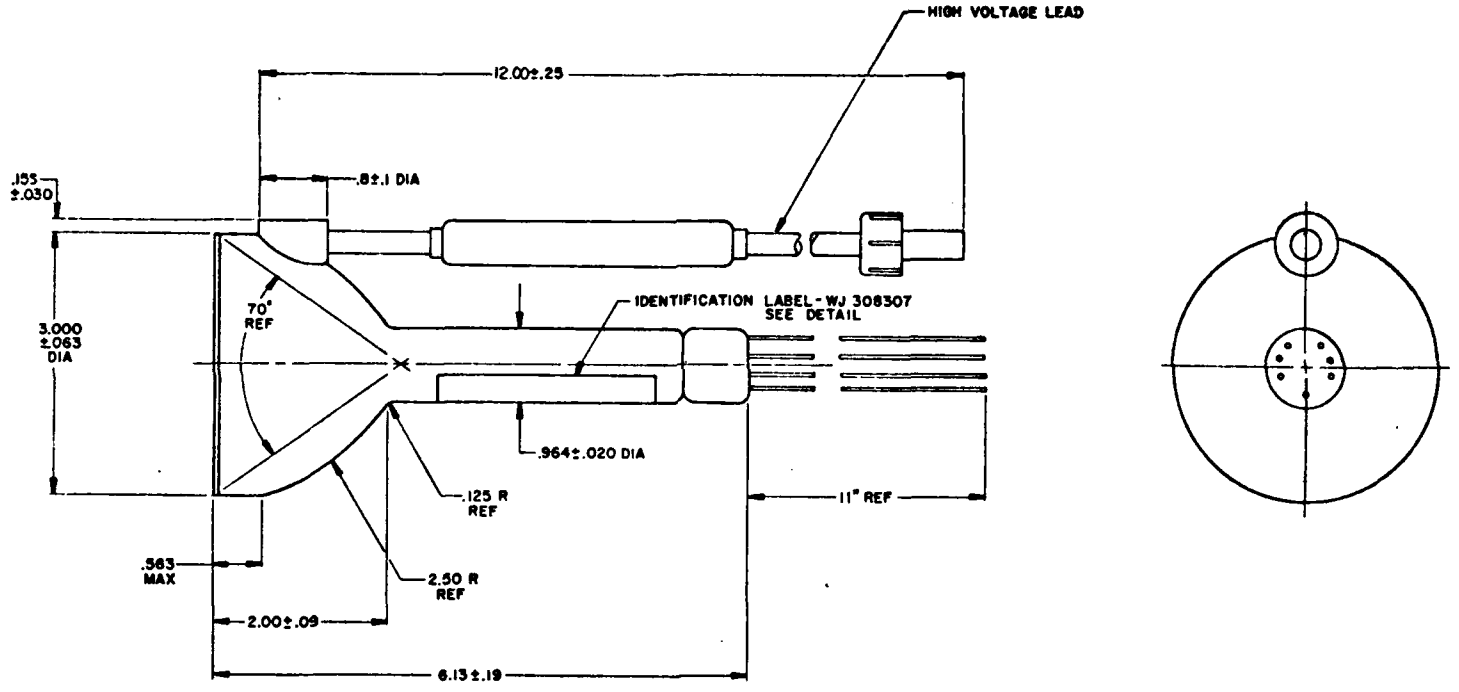

LEAD IDENTITY	
COLOR	CONNECTIONS
WHITE	HEATERS
YELLOW	CATHODE
GREEN	GRID NO. 1
ORANGE	GRID NO. 2
GRAY	FOCUS

Figure 20. Cathode Ray Tube Outline WJ-3414-11

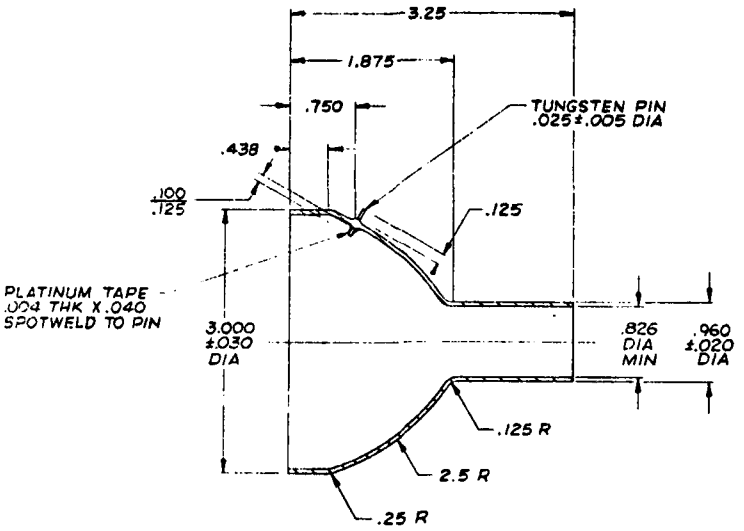

APPROVED SOURCE(S) OF SUPPLY			
DASH NO.	VENDOR	VENDOR'S ITEM IDENT NO.	APPLICATION
	CORNING GLASS WORKS ELECTRONIC MATERIALS DEPT. CODE IDENT 14674		
	SCHOTT JENA GLASWERK INC. 11 EAST 26TH STREET NEW YORK, N.Y. 10010		

NECK GLASS		
.964 ± .02 OD (24.5 ± 0.5 mm OD)	1.4 ± 0.1 mm WALL THICKNESS	0.826 MIN ID (21 mm MIN ID)
SCHOTT 8487 OR CORNING 3320		

Figure 21. Funnel

Figure 22. CRT Photographs

3.2 Frit Seal

Coated faceplates are frit sealed to 3320 glass funnels (Figure 23) to form a subassembly according to the following procedure:

1. Clean faceplate in flowing isopropyl alcohol and blow dry with liquid nitrogen boil off N_2 gas. Repeat if alcohol leaves a film after blow drying.

2. Ultrasonic clean funnel in 10% ammonium biflouride solution, 15 seconds and rinse in copious water.

3. Using 120 mesh SiC paper, grind funnel edge to form a minimum 0.15 inch wide flat edge. Using 240 mesh SiC grit, grind faceplate against funnel to remove high spots and to form a flush faceplate-funnel contact.

4. Mix frit with an organic binder (Figure 24).

5. Apply frit slurry to form 3/16 inch thick uniform ridge on edge of funnel.

6. Firmly press funnel on faceplate.

7. Dry subassembly in air at approximately 50°C for an hour (this may be changed to 200°C for 2 hours).

8. Add excess frit at faceplate-funnel contact to form a fillet of 1/8 inch radius.

9. Repeat Step 7 if Step 8 was necessary.

10. Assemble as per frit sealing fixture assembly sketch (Figure 23).

11. Heat in an inert atmosphere at 35°C/minute to the flowing temperature of the frit, soak at temperature the prescribed time for the frit. Cool to room temperature at 15°C/minute or less.

The frit sealing fixture assembly is shown assembled and disassembled in Figures 25 and 26. The grinding Step 3) is necessary to create a sufficient volume of frit of constant thickness to insure repeatability in this sealing operation. Moreover, grinding eliminates any effect of the faceplate bulk warpage (2.5.2).

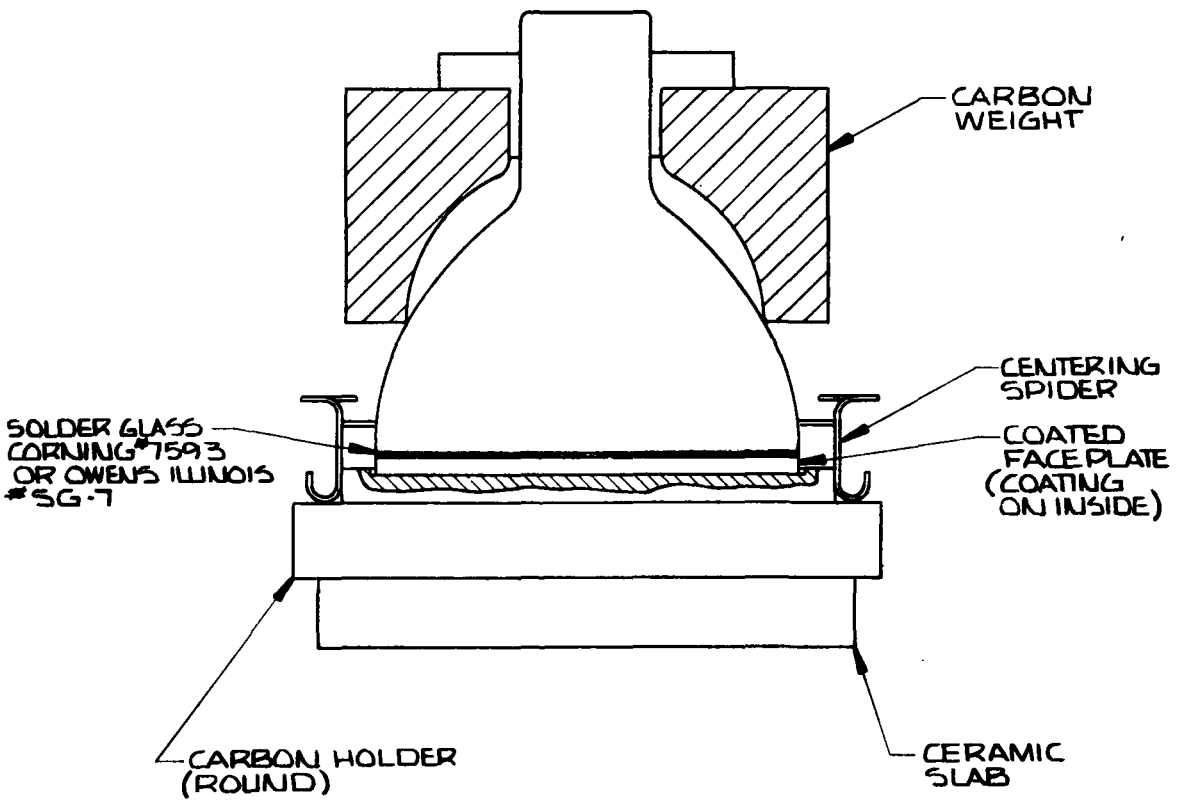

Figure 23. Frit Sealing Fixture Assembly

Organic Binder compounded by Pierce-Stevens Chemical Corp.
710 Ohio Street
Buffalo, N. Y.

(5 gallons minimum quantity)

Material is nitrocellulose in amyl acetate

Item No.	Pierce-Stevens No.	Solid Content	Viscosity at 25°C (centipoises) (Brookfield Viscosimeter Type L F with #1 spindle @ 60 RPM)
1	F1016A	1.00-1.40%	40-50
2	F1016E	1.15-1.35%	40-50

Item 2 is repackaged by Corning as "Suspension Vehicle" and is supplied with their frit at no charge - when requested. (It can not be shipped by air. They will not sell it separately).

Figure 24. Organic Binder

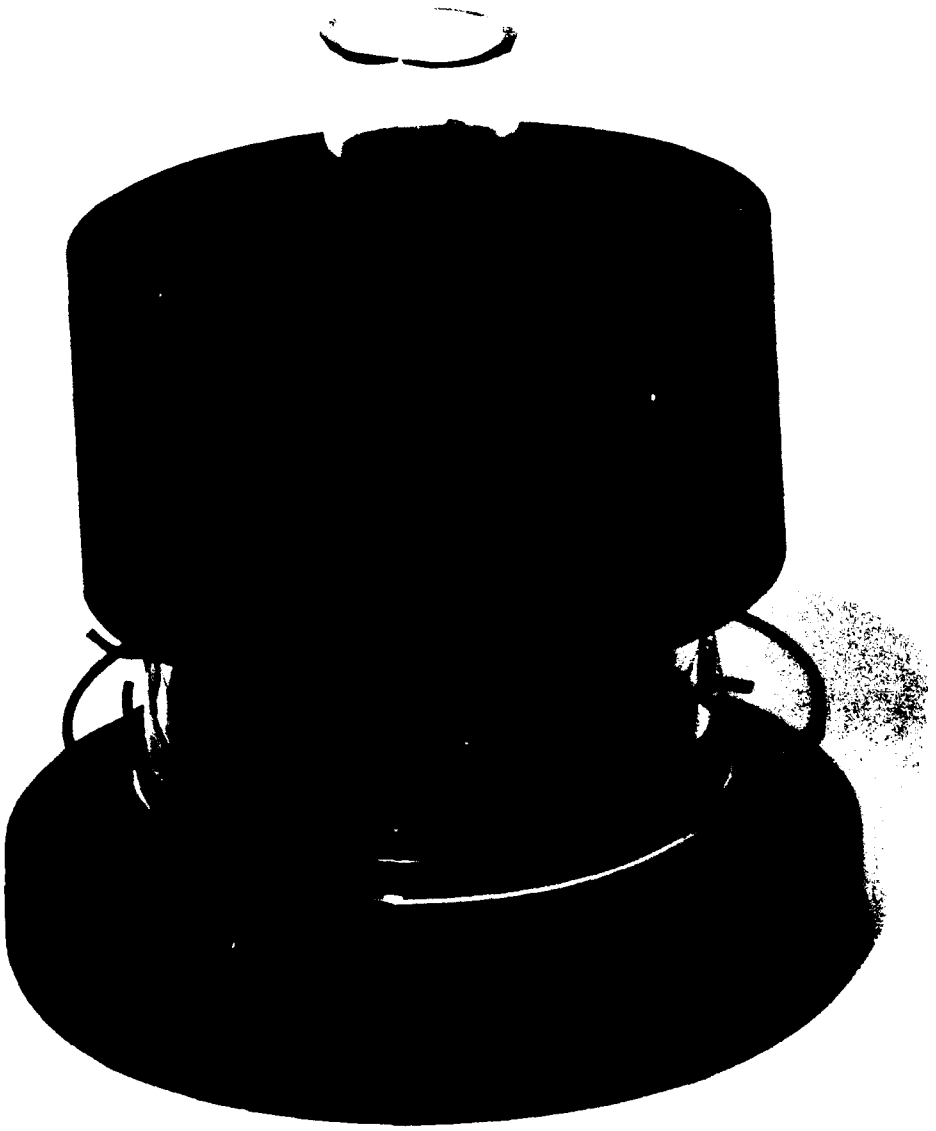

Figure 25. Frit Sealing Fixture Assembly

p43957

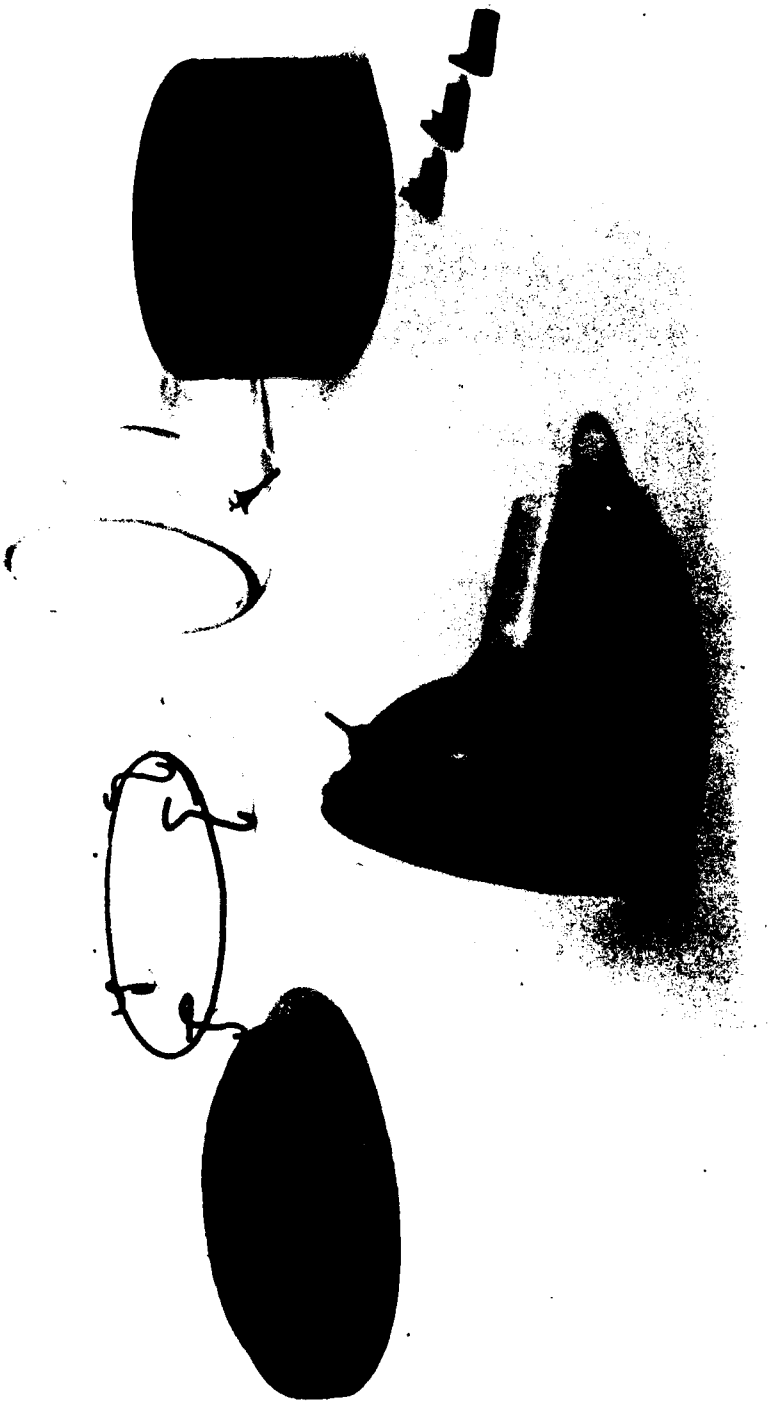

Figure 26. Frit Sealing Fixture Disassembly

3.2.1 SG-7 Frit Versus 7593 Frit

The salient differences are the following:

Owens-Illinois SG-7	Corning 7593
Flow Temperature is 600°C under load	Flow Temperature is 640°C under load
Amorphous (does not crystallize)	Devitrifies (crystallizes)
Discolors in inert atmosphere firing	Does not discolor in inert atmosphere firing

The identifiying glass modifier in Corning 7593 frit is titanium dioxide. The identifying glass modifier in Owens-Illinois SG-7 is copper oxide. After firing in an inert atmosphere the SG-7 changed color from the original greenish to a reddish color. This indicates some reduction of the copper or some other component to a lower valence state. Most important, the expansion coefficient was not sufficiently changed to degrade the integrity of the seal.

Corning 7593 frit always survived the inert atmosphere firing without color change.

3.2.2 Problems – Engineering Design

Two problems, frit seal thickness and frit porosity were serious impediments in this program. The first caused fracture of the funnel glass in processing shortly after the frit seal operation. The lethal failure was immediately recognized as it prevented further processing. The second was more subtle. The porous frit has a much lower electrical breakdown strength than dense frit. However, the completed tube will still operate properly unless a ground strap (or the like) happens to touch the external frit surface (either frit). At that instant an arc discharge is heard as leakage current will avalanche and burn a hole through the frit and the tube goes to air. The mechanism is further described below. The point being made is the lack of clear correlation between cause and effect. In each of these problems the proper application of the frit is the solution, not the use of a different frit.

3.2.3 Frit Seal Thickness

The first problem was a result of the following incorrect logic and/or information: the difference in thermal expansion coefficients of 1720 and 3320 glass is sufficiently small (2×10^{-7} $\Delta L/L°C$); therefore, the frit

should be as thin a film as possible adhering to both faceplate and funnel and not introducing the bulk properties of a third glass. This is, in fact, good tube practice and logic, but the proof is in the result. The 3320 funnel consistently fractured parallel to the frit seal 1/32 of an inch or less from the frit seal. When the thickness of the frit was increased greater than 0.100 inches there was sufficient frit glass to take up the stress between the 3320 and 1720 glass components. An excellent, repeatable frit seal resulted.

3.2.4 Frit Porosity

The second problem can be addressed by considering the source of pores and the electrical conduction in/on the porous glass. The pores result from gas entrapped in the molten frit. Fining is impossible at the low frit sealing temperature as the glass is much too viscous for the bubbles to rise. The gas entrapped stays entrapped. The two sources are residual organics from the organic binder and absorbed water vapor. Heating to 50°C for one hour will drive off all the amylacetate but it will not breakdown the nitrocellulose. Of greater importance is the absorbed water vapor. The powdered glass frit has a very large surface to volume ratio. Very large amounts of water can be and are absorbed on the surface. This water is desorbed during the frit sealing firing cycle. Some part of it is entrapped in the molten glass. There is sufficient gas volume to leave only thin walls of glass between pores.

Upon cooling, the water vapor is readsorbed on the internal pore surface. This chemisorbtion creates ion sites on the surface allowing an electrically conductive surface. These sites can store charge, even if conduction is not possible. Allow the surface of one pore to be charged to 15 kV. Also recall there are several variable valence cation species in these frits. There now exists a very strong electric field across the thin wall separating the charged pore from the neutral pore. This field facilities valence changes of variable valence cations. Electron hopping occurs from cation to cation and finally to the surface of the adjacent pore. This pore eventually becomes charged. Continue this process to the next pore and the next. Now, if at this point, you ground the last pore, this stored charge as electron current will avalanche through the thin walls as each pore discharges its stored charge all at once. Holes will be burned through all the thin walls separating the pores, an arc discharge will be heard and the CRT will go to air.

The absorbed water can be driven out of the unmelted fritted subassembly by heating to 200 to 300°C for a minimum of one hour. Then fire normally to melt the frit. We do not know if the pores are completely eliminated, but this technique is reportedly used in industry to eliminate this electrical breakdown problem. It is clear this technique will increase the thickness of the pore walls, thereby reducing the electric field and reducing leakage current through the glass.

3.2.5 Subassembly Thermal Shock Resistance and Frit Patching

Coating 1720 glass faceplates with La_2O_2S changes the coefficient of expansion from 42 x 10^{-7}/°C to a complex function of the geometry, the temperature and thermal history of the structure. Considering the thermal history, upon cooling from 667°C the coated glass surface is subjected to a compressive stress. The faceplate warps or bows (Figure 26) as one surface is constrained to a smaller dimension than the other. Below 667°C the glass becomes rigid. At room temperature the location of the maximum strain gradient in the faceplate-funnel subassembly is evident after an inspection of the subassembly structure (Figure 27). The fritted funnel constrains the periphery of the faceplate to 40 x 10^{-7} $\Delta L/L°C$; a fraction of an inch away, the lanthanum oxysulfide constrains the faceplate to 60 x 10^{-7} $\Delta L/L°C$. The resultant stress across that fraction of an inch reduces the fritted subassembly thermal shock resistance significantly. The normal heating rate in the frit sealing temperature cycle is 35°C per minute. This heating rate was used to heat a subassembly to patch the frit seal with frit to seal a leak. The massive fractures of the faceplate appeared to initiate at the maximum stress location and were confined to this area. 15°C/minute allowed successful frit patching. Soak time at flow temperature for the frit was 20 minutes.

Patching a high voltage feedthru is accomplished by first preheating the glass at the feedthru gently with a torch. Then heat the pin to red heat for one second. Repeat this if a good oxide coating is not formed on the pin. After cooling, apply a small amount of frit-water slurry to the pin at the glass-pin junction. Heat in an inert atmosphere at 15°C/minute to the flow temperature of the frit. Hold at temperature 5 minutes. Cool to room temperature at 15°C/minute or less.

An additional problem presents itself when patching an aluminized subassembly. The NR film at the aluminum interface is metallic vanadium. Heating to 640°C to patch the frit seal allows considerable aluminum-vanadium alloying. Aluminum can then reach the vanadium oxide and reduce it to the metal.

$$3V_2O_5 + 10Al = 6V + 5Al_2O_3$$

$$\Delta F° \ 600°K = -692 \pm 30 \text{ kcal}$$

The combined result is very rapid degradation of the NR film properties. Two patch attempts visibly discolor the Al film as shown in Figure 28. Four patch attempts have the effect shown in Figure 29 (again viewing the Al covered surface). It is highly suggested from these results that patching an aluminized subassembly should be attempted once or not at all.

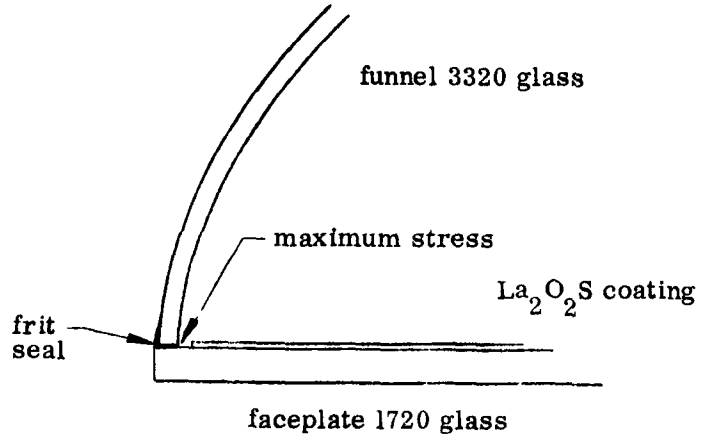

material	TCE
1720 glass	$42 \times 10^{-7}/^{o}C$
3320 glass	$40 \times 10^{-7}/^{o}C$
SG-7 frit	$42 \times 10^{-7}/^{o}C$
7593 frit	$42 \times 10^{-7}/^{o}C$
La_2O_2S	$60 \times 10^{-7}/^{o}C$

Figure 27. Maximum Stress Location in Cross Section View of Faceplate

Figure 28. Al-V Alloying After Two Frit Patch Attempts

Figure 29. Al-V Alloying After Four Frit Patch Attempts

3.2.6 Controlled Atmosphere Frit Firing

The NR film is very sensitive to further oxidation during the frit sealing thermal cycle. This was explained in 2.4. It was observed that dry nitrogen and argon were equally effective inert gases for frit sealing as long as all traces of water and oxygen are absent. Argon 99.999% and boil off nitrogen from the liquid nitrogen tank were the gases used with success. The muffel furnace utilized had been used consistantly for only dry hygrogen or dry nitrogen firing for months previous to its use in this program.

3.3 Neck Extension

The monochorme tube to be replaced has a neck outside diameter of 0.840 + 0.06 - 0.03 inches. This size Corning 3320 tubing was used initially in this program until our supply was depleted. To reorder from Corning necessitated waiting until the once a year down draft furnace 3320 melt (July 1, June 4 order deadline). Minimum order is 100 pounds. Tubing of this diameter and type (Corning 3320) was unavailable elsewhere. Schott Glass (West Germany) 8687 tubing was a very good TCE match. Their closest metric size tubing was 24.5 ±0.5 mm (0.964 ±0.02 inches). Such an oversize neck will not fit in the yoke for the monochrome tube that is to be replaced. However, it was judged good for these development tubes.

3.4 Electron Gun Stem

The thermal coefficient of expansion mismatch between the nonex glass stem (Corning 7720) and the Schott 8786 neck glass is 5×10^{-7} $\Delta L/L°C$. This is quite large. However, the flame seal area in the final glass structure is under compression. This reduces the risk of the large mismatch considerably. There was no reoccurring problem with this flame seal.

3.5 Electron Gun

A laminar flow electron gun was utilized in this CRT to gain an advantage in resolution and brightness over that capable utilizing a crossover electron gun. Two laminar flow gun configurations were used: a bipotential gun, and an Einzel lens gun. The most austere problem encountered in this program was cathode poisoning. This occurred in completed CRT's, using faceplates No. 22 through 37. The solution is thought to be within our grasp.

The advantageous characteristics of the laminar flow gun results from the relatively uniform electric field intensity immediately above the cathode surface. The resulting emission density from the cathode surface, hence in the beam, is relatively uniform. A crossover gun has an electric field

intensity that is a strong function of the radial distance from the cathode center. The electron density emitted from the cathode surface, hence in the beam, is strongly dependent upon the radial distance from the beam center. Well, by the time all is said and done (Ref. 2) the more uniform electron density beam (laminar flow gun) yields improved resolution and higher brightness as opposed to the crossover gun electron beam.

3.5.1 Bipotential Versus Einzel

The Einzel gun configuration has electrical requirements most closely approximating those of the monochromic CRT to be replaced (Table 9). An Einzel gun CRT would fulfill the goal of replaceability. The bipotential gun configuration yields line widths and brightness slightly superior to the Einzel gun configuration. Bipotential gun CRT data would necessarily identify the present upper limits of a production tube. The exerciser (3.6) is adjusted to operate the bipotential gun configuration.

3.5.2 Cathode Poisoning

During the initial aging of some CRT's, unknown contaminates were evolved and the electron emitting barium metal on the cathode surface reacted irreversibly. The rate of electron emission decreased as a result. This phenomena is commonly known as cathode poisoning. The poisoning problem was severe on faceplates 25, 28 and 30. The contamination evolution only occurred during CRT operation, during electron bombardment of the faceplate.

It was discovered that elemental sulfur was found on the cooler (less than 870°C) parts of the faceplate heat treatment furnace (at LMSC). Recall the atmosphere is H_2S, SO_2, H_2O at temperature. There is a strong possibility that elemental sulfur may have condensed on the faceplate during cool down. Subsequent deposition of the vanadium oxide NR film would secure the sulfur quite well at the La_2O_2S-NR film interface.

It is believed that this sulfur is the contaminant. The location of the sulfur would explain the reason for contaminant evolution only during electron bombardment of the screen. Moreover, it explains the inability to eliminate the contaminant by vacuum heat treatments of the completed faceplates. The sulfur can be removed from the La_2O_2S surface by a vacuum heat treatment to 350°C for one hour before the NR film is deposited.

It is not known how to remove it after NR film deposition without destroying the NR film.

Table 9

WJ-3414-11 ELECTRICAL REQUIREMENTS

	WJ-3414-11 Einzel Gun	WJ-3414-11 Bipotential Gun	Existing Monochrome Tube
Heater Voltage	6.3	6.3	6.3
Heater Current	450 mA	450 mA	330 mA
G2 Voltage	500	400 or 500	100
G1 Cut-Off Voltage	-50 ±20%	-50 ±20%	-11 to -19
Focus Voltage	500 ±100 volts one voltage for all colors is possible	2.7 kV green 2.1 kV yellow 1.5 kV red	100
Anode Potential	18 kV green 15 kV yellow 10 kV red	18 kV 15 kV 10 kV	7 kV
Capacitance	Typical	--	
Grid 1	20 pf	--	
Cathode	20 pf	--	
Focus	10 pg	--	
Screen	30 pf	20 ±10 pf	

3.6 Exerciser

The exerciser is an electronic system that can drive these high contrast tubes in TV modes of operation. The exerciser demonstrates full screen raster operation at 10, 15 and 18 kV screen potential. These accelerating potentials correspond to red, yellow and green color displays respectively.

The vertical deflection is driven by a raster circuit for full screen illumination or a dc power supply to allow deflection of the horizontal line to any desired location on the screen. Variable intensity control is provided by potentiometers on the front panel. The exerciser was completed and delivered to ERADCOM personnel January 24, 1979.

3.7 CRT Data

The operating and test parameters ar shown below in Tables 10 and 11.

Table 10

OPERATING PARAMETERS

Heater:	6.3 volts at 0.45 ±10% amps
Grid 2:	500 volts
Anode Potentials:	10 to 20 kilovolt
Focus Voltage:	
Bipotential Gun:	1.4 to 3 kilovolts
Einzel Gun:	500 ±100 volts to attain optimum spot size for anode potential range
Cut-Off:	50 ±10 volts

Table 11

TESTING PARAMETERS

2 in. x 2 in. Raster, 11 Lines	
Writing Speed:	5000 inches/second
Refresh Rate:	60 hertz
Duty Cycle (11 Line Display):	26.4% (electron beam on time)
Duty Cycle of Single Line Being Measured:	2.4% (brightness data)

Test Parameters:

The peak line brightness and line width are measured on one line of the eleven line raster at different anode potentials and grid drives after minimizing the line width by a focusing voltage adjustment. The line width is measured at the 50% amplitude points as determined with a slit analyzer and photometer. The grid drive versus brightness data is displayed in Figure 30, 31, 32, and 33 for anode voltages of 10, 15, 18 and 20 kilovolts respectively. This data is listed in Tables 12 and 13. Also included in the tables is line width information for selected values.

Figure 34 reiterates by displaying the brightness versus grid drive data for each anode potential for CRT (faceplate 19).

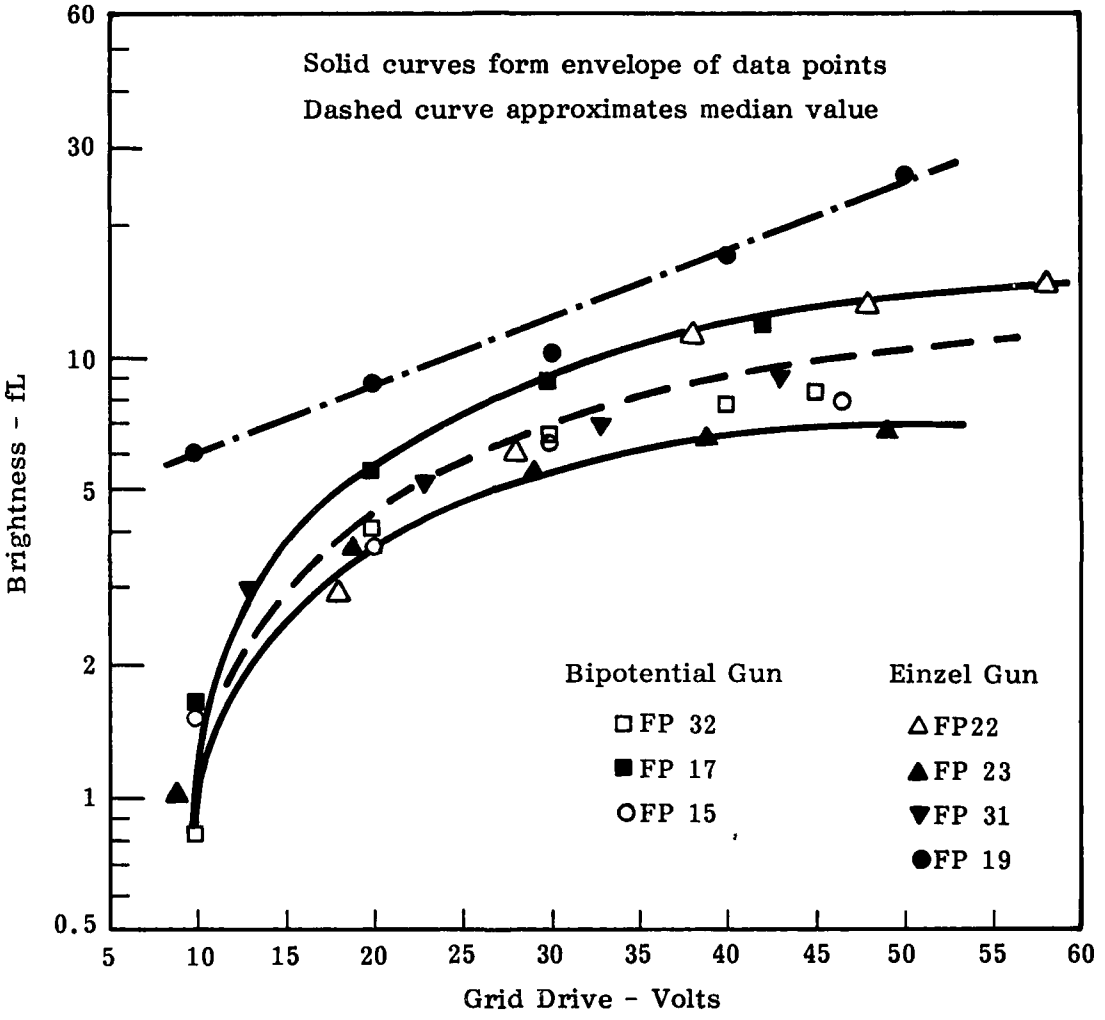

Figure 30. CRT Brightness Versus Grid Drive Data
10 kV Anode Potential

aa43961

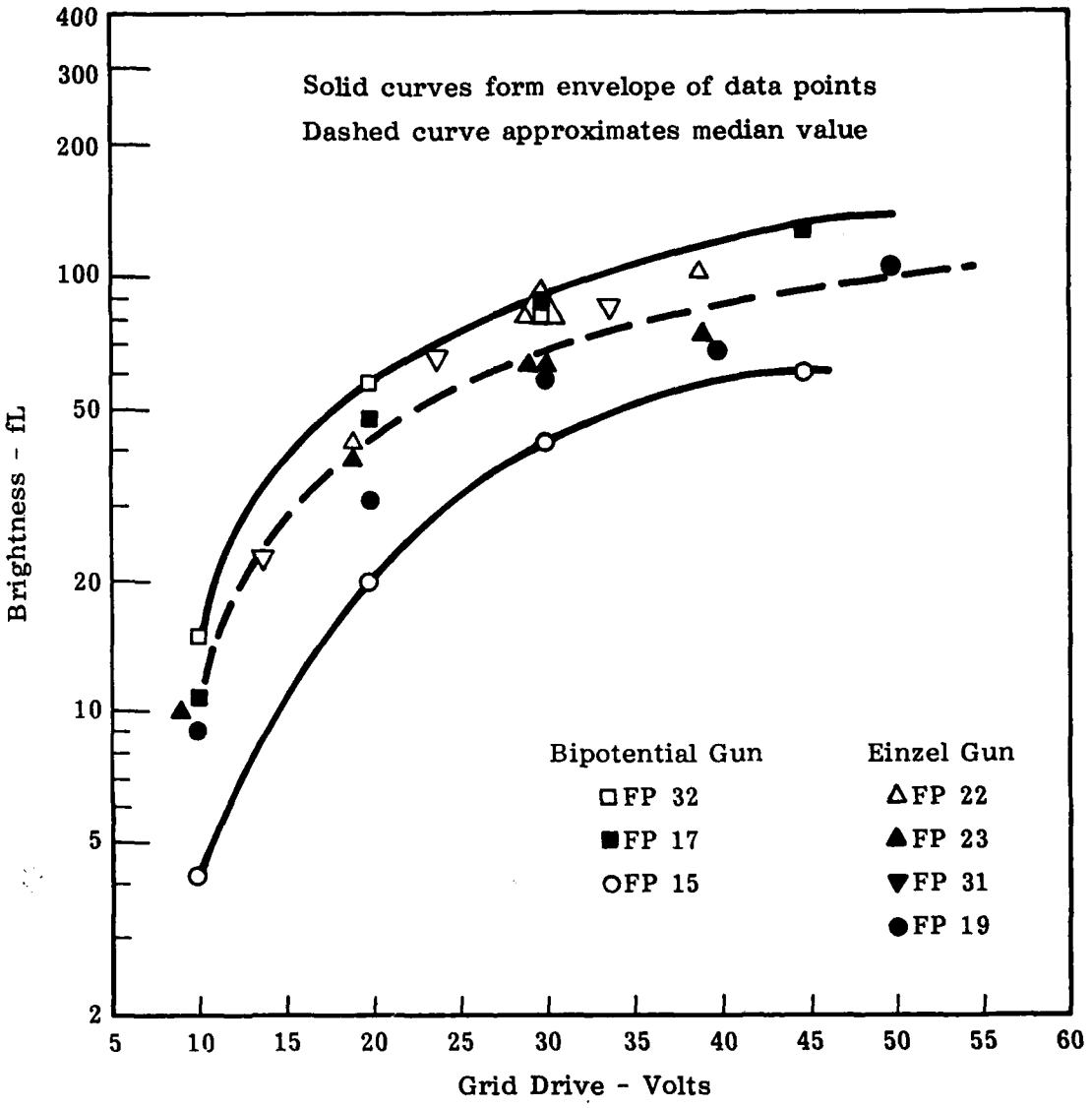

Figure 31. CRT Brightness Versus Grid Drive Data
15 kV Anode Potential

aa43962

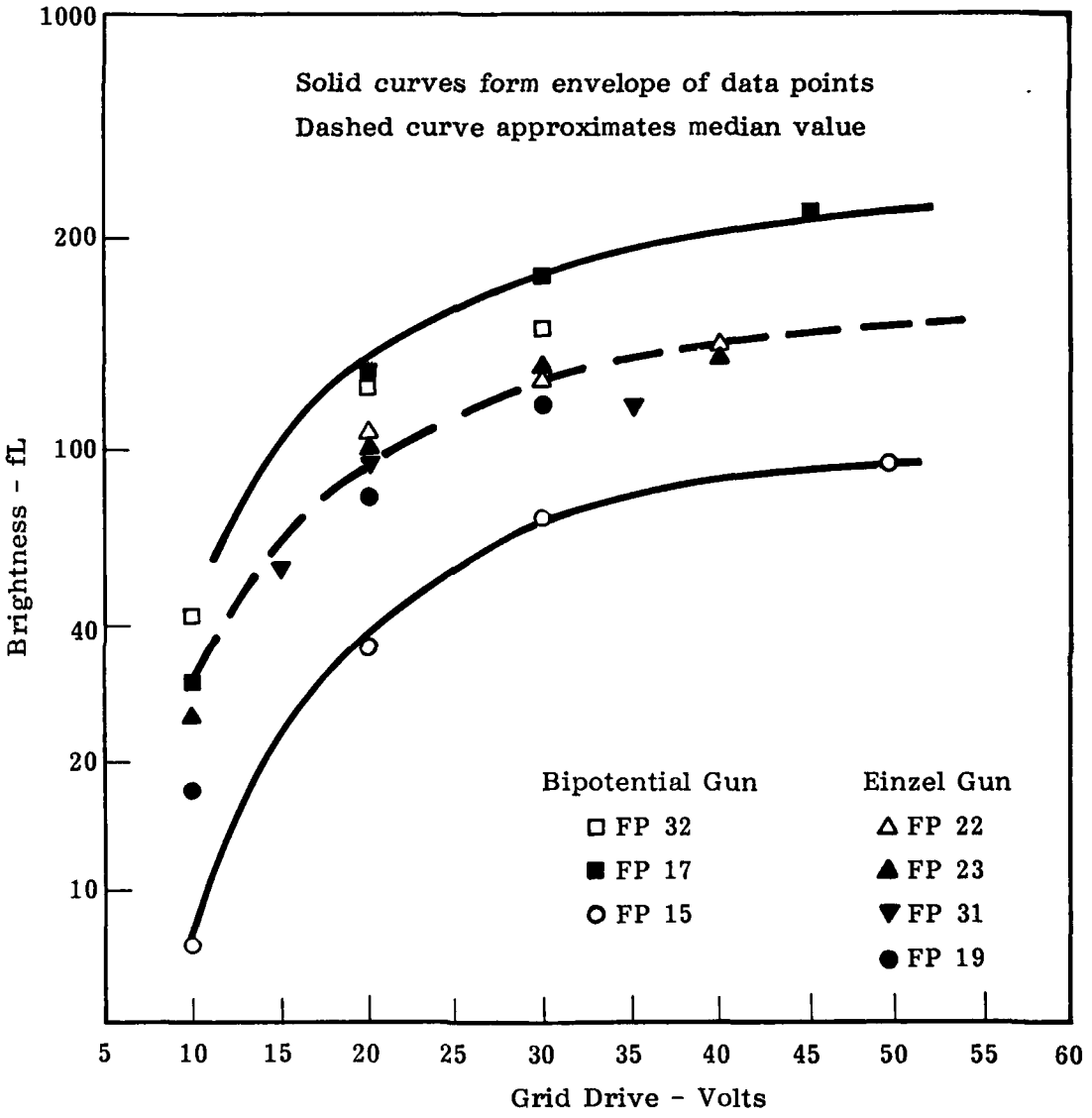

Figure 32. CRT Brightness Versus Grid Drive Data
18 kV Anode Potential

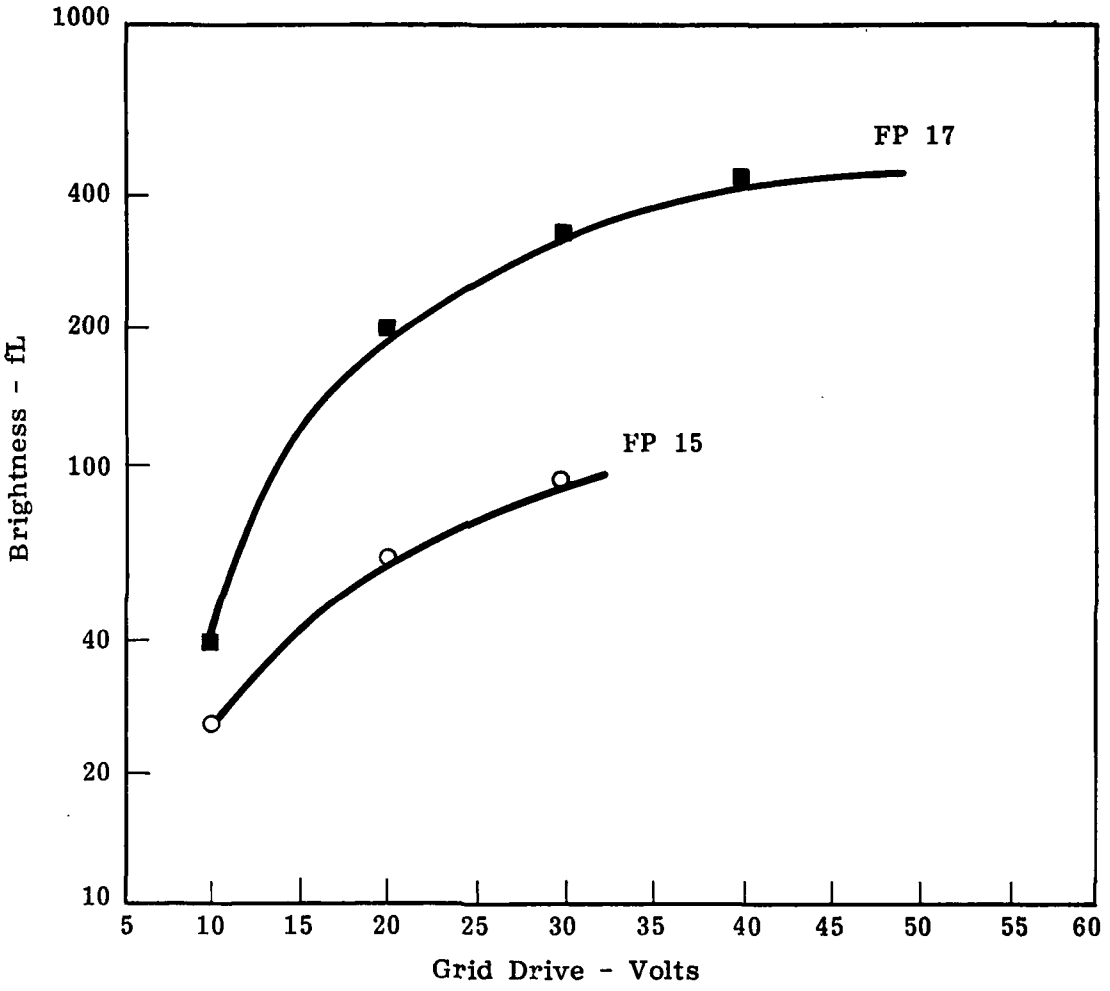

Figure 33. CRT Brightness Versus Grid Drive Data
20 kV Anode Potential

aa43964

Table 12

EINZEL GUN CONFIGURATION CRT DATA

Anode Potential (kilovolts)	Grid Drive (volts)				Brightness-Peak Line (fL)				Line Width (inches)		
	s/n 4 fp22	s/n 5 fp23	fp31*	s/n 3 fp19	s/n 4 fp22 △	s/n 5 fp23 ▲	fp31* ▼	s/n 3 fp19 ●	s/n 4 fp22	s/n 5 fp23	fp31
10	18	9	13	3	3	1	3	6			
	28	19	23	20	6	3.7	5	8.5			
	38	29	33	30	11	5.4	7	10			
	48	39	43	40	13	6.4	9	17			
	58	49		50	15	6.9		26			
14				10				9			
				20				31			
				30				59			
				40				68			
				50				105			
15		9	14			10	26				0.0041
	19	19	24		41	37	65				0.0048
	29	29	34		80	64	84				0.0057
18		10	15	10		25	57	17		0.0035	0.0036
	20	20	20	20	105	102	94	81	0.0042	0.0040	0.0045
	30	30	35	30	153	160	134	130	0.0055	0.0060	0.0070
	40	40			169	160			0.0077	0.0070	

* Faceplate 31 was tested, then rejected for high cutoff, then regunned.

Note: Graph Symbols are for Figures 30 through 33.

Table 13

BIPOTENTIAL GUN CONFIGURATION CRT DATA

Anode Potential (kilovolts)	Grid Drive (volts)			Brightness-Peak Line (fL)			Line Width (inches)
	s/n 1	s/n 2	s/n 7	s/n 1	s/n 2	s/n 7	
	fp15	fp17	fp32	fp15	fp17	fp32	fp32
				○	■	□	
10	10	10	10	1.5	1.6	0.8	
	20	20	20	3.7	5.3	4	
	30	30	30	6.4	8.8	6.5	
			40			7.9	
	46.5	42.1	45	7.9	11.8	8.2	
15	10	10	10	4.3	10.7	15	0.0020
	20	20	20	20	47.5	58	0.0028
	30	30	30	43	88.5	80	0.0042
	44	45		60	125		
18	10	10	10	7.7	31.4	44	0.0015
	20	20	20	37	153	148	0.0027
	30	30	30	73	260	182	0.0041
	49.5	45.2		95	345		
20	10	10		26	40		
	20	20		62	202		
	30	30		94	340		
		45.6			445		

Note: Graph symbols for Figures 30 through 33.

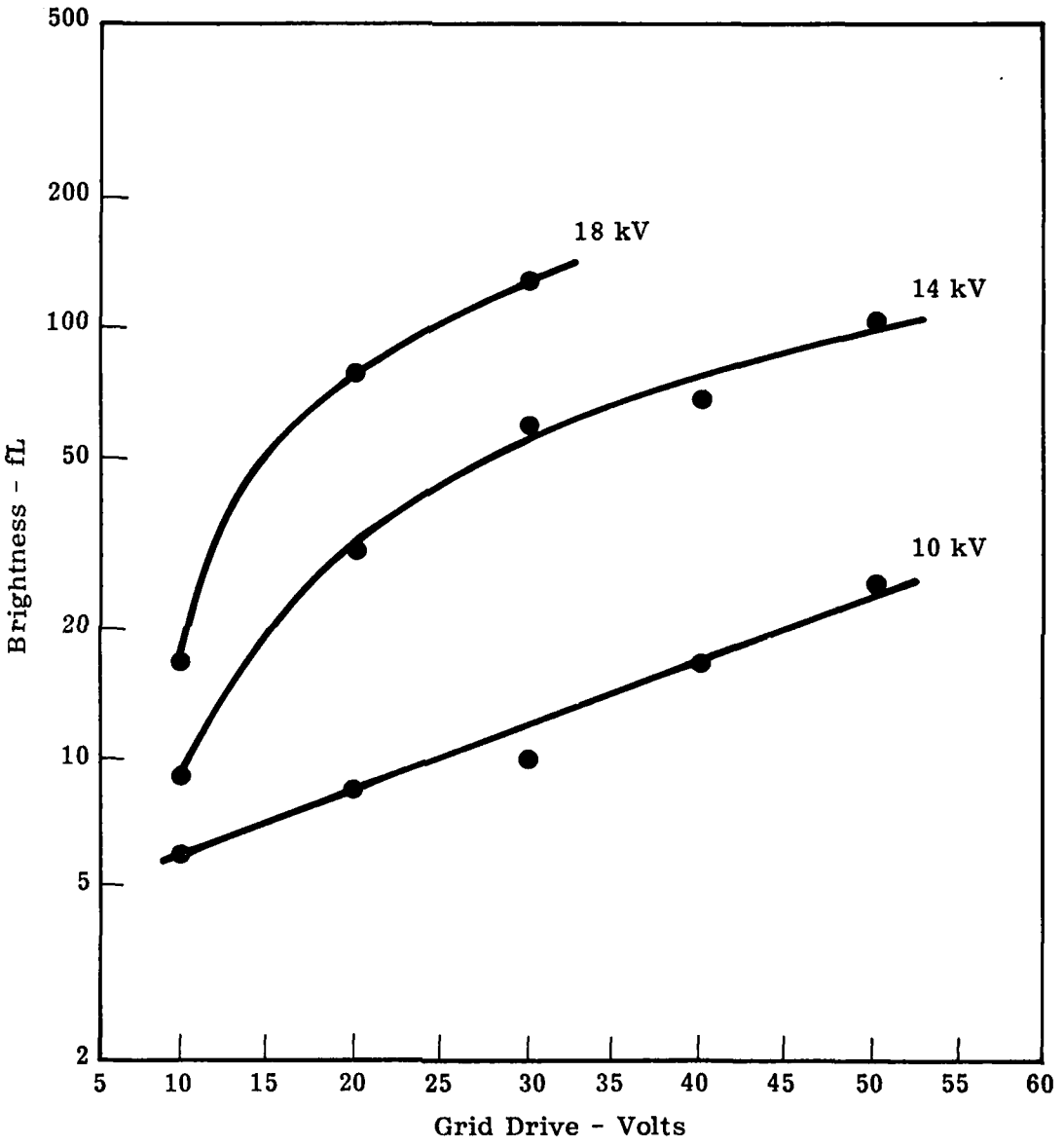

Figure 34. CRT (FP 19) Brightness Versus Grid Drive Data

3.7.1 Discussion - Line Width

The line width data is very conforting. Typical line widths are below 0.005 inch for the bipotential gun configuration and below 0.008 inch for the Einzel gun configuration (see Tables 12 and 13 for complete data).

3.7.2 Discussion - Brightness

The CRT data is revealed quite well in the brightness versus grid drive curves. To present the data more concisely, Table 14 was made by recording the median and maximum values of brightness at 20 volts grid drive and extrapolating the median (and maximum) to 50 volts grid drive. With the cut-off voltage greater than 50 volts, to volt grid drive can be achieved (the specification is 40 to 60 volts).

3.7.3 50,000 Inches/Second Data

CRT (faceplate 32) was tested at a writing speed of 50,000 inches per second. The data is presented in Table 15 and Figures 35 and 36.

Table 14

BRIGHTNESS (fL)

Anode Potential (kV)	Brightness (fL)	
	Grid Drive	
	20 V median/maximum	50 V median/maximum
10	4.5/5.5	10/14
15	45/58	100/135
18	100/160	200/360
20	130/200	290/450

Table 15

50,000 INCHES/SECOND DATA

Grid Drive (volts)	Cathode Current (microamps)	Brightness (fL)	Line Width (inches)
10	2	5.9	0.0019
20	10	30	0.0024
30	26	64	0.0035
40	58	89	0.0060

Notes:

1) Bipotential faceplate 32 CRT data at 50,000 inches/second writing speed, 60 hertz refresh rate.
2) Focus voltage is constant at 3270 volts.
3) Anode potential is constant at 18 kV.
4) Plotted in Figures 35 and 36.

3.7.4 Einzel Gun Versus Bipotential Gun

The brightness data indicates an advantage only at higher anode potentials. The line width data shows the bipotential gun configuration to be decidedly advantageous. The brightness data for CRT (faceplate 19) is open to question as the CRT experienced an anode feedthru leak shortly following data compilation. The bipotential gun should have yielded slightly superior gun performance over the Einzel gun tubes. The brightness at 10 kV was best of all but that data will be discussed in 3.7.7. At 15, 18 and 20 kV the brightness is the worst.

3.7.5 Line Width - Focus Voltage Dependence

The normal test procedure is to minimize line width (adjust focus) before each brightness-line width measurement. As a result the functional dependence of line width on focus voltage is not obvious. For replacement tube considerations the result of the extent of this functional dependence must be insignificant. To show this an Einzel lens CRT was tested at constant focus voltage (900 volts) and constant cathode current (75 microamps) at three anode voltages (10, 15, and 18 kV). The observed line width fluctuation was within the proposed maximum of 0.012 inches (Table 16).

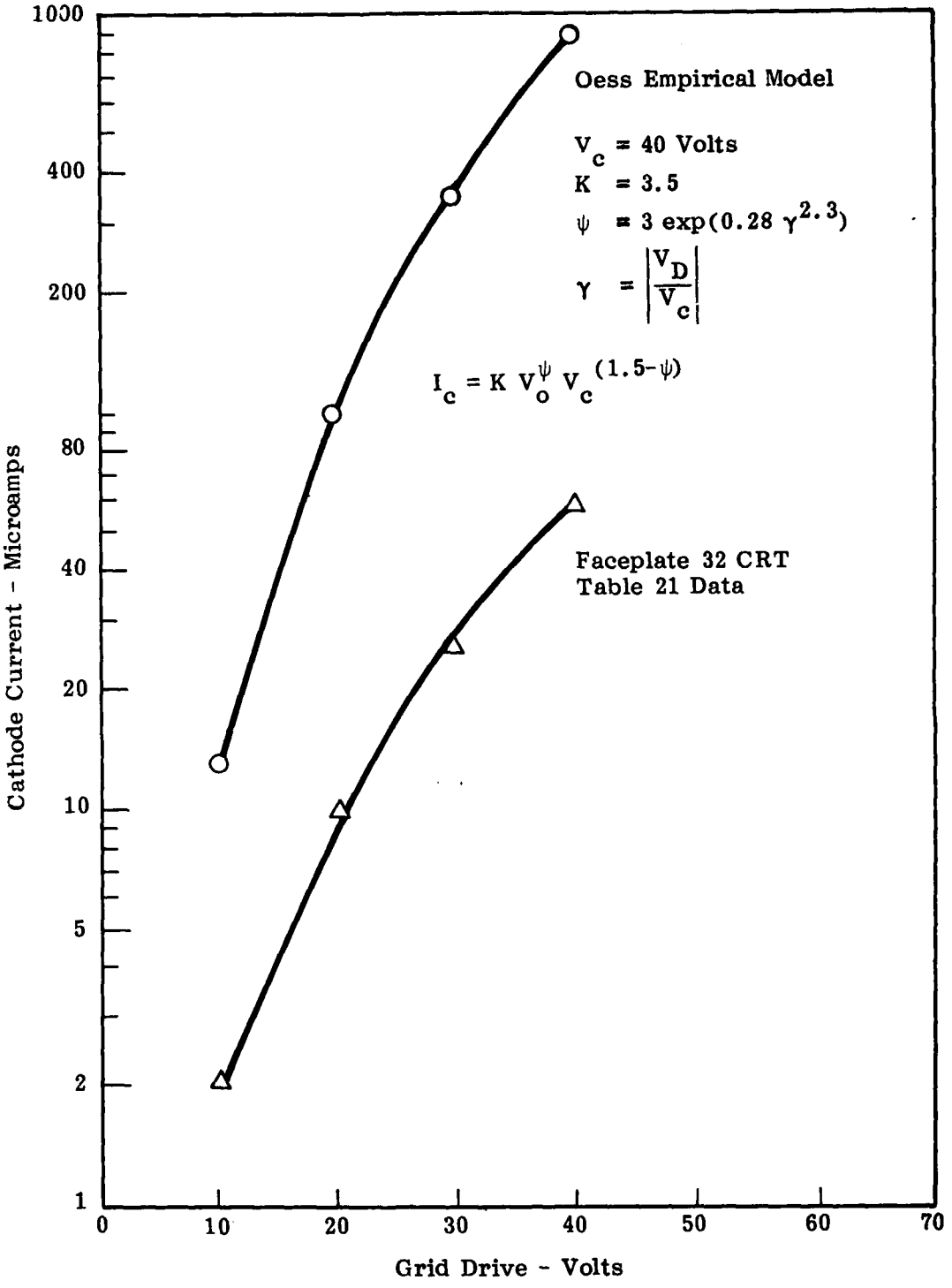

Figure 35. Cathode Current As a Function of Grid Drive

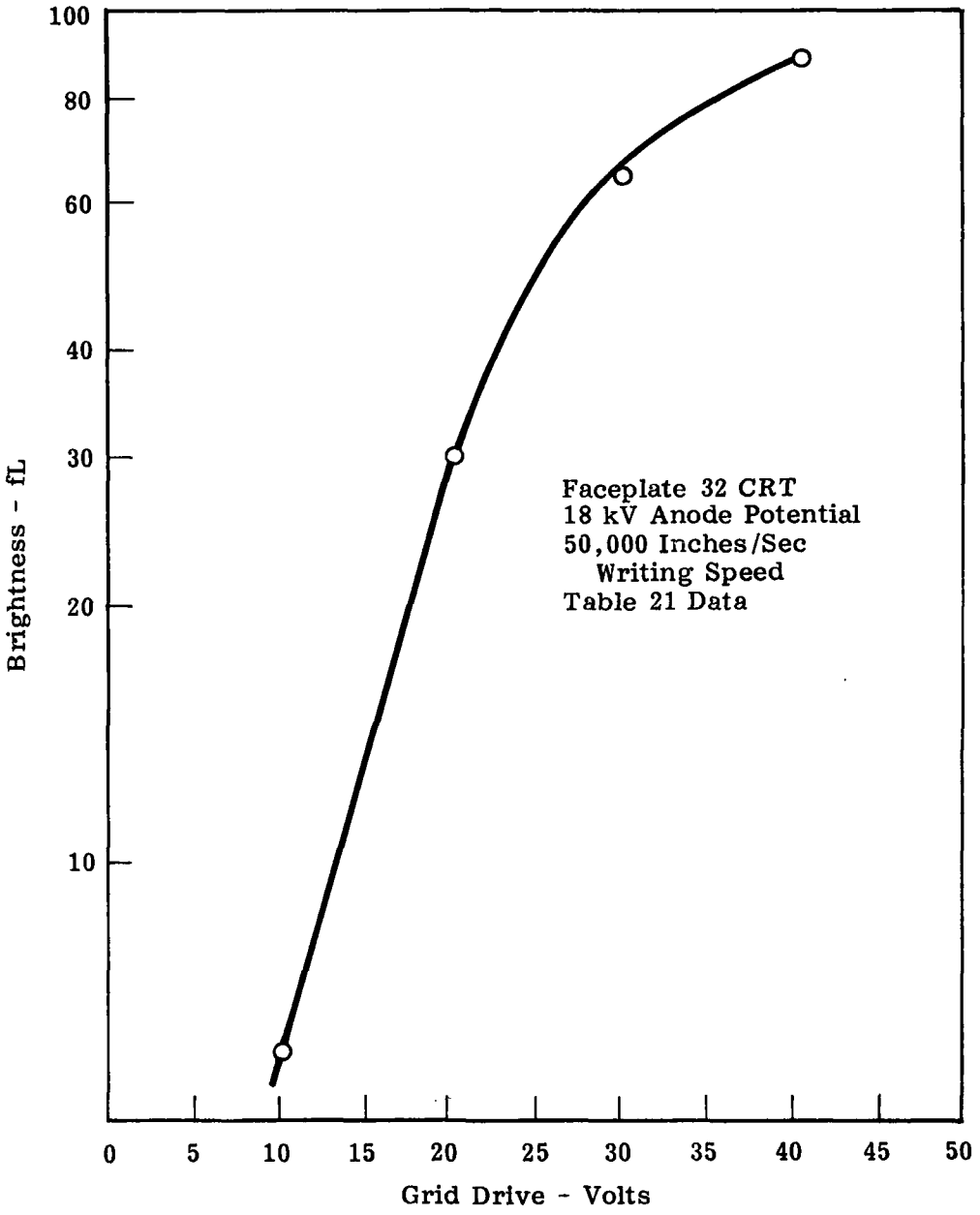

Figure 36. Brightness Versus Grid Drive, FP 32 at 50,000 Inch/Sec Writing Speed

Table 16

EINZEL GUN CRT DATA AT
CONSTANT FOCUS VOLTAGE

Anode Voltage (kV)	Line Width (inches)	Brightness (fL)
10	0.0115	6
15	0.0057	80
18	0.0077	127

3.7.6 Discussion - Saturation

The shape of the brightness versus grid drive semilog plot indicates a saturation effect. Note the decrease in the rate of increase of brightness for increasing grid drives near maximum grid drive. At 10 kV the asymptotic approach to a constant brightness is clearly a limitation.

No saturation effect was clearly evident in the brightness versus electron energy (anode potential) data, only brightness versus grid drive. The grid drive determines the electron beam density (current or charge per unit time) activating the phosphor, not electron energy. Note that the saturation occurs at cathode currents in excess of 30 microamps; the demountable system operates at a constant 5 microamps. The CRT data indicates more serious saturation at lower anode potentials. The source of saturation is either a deficiency in the electron gun operation or a material property of the two layer phosphor thin film structure. Lacking anode current versus brightness data, it is difficult to precisely determine whether the gun or phosphor is the problem.

The cathod current versus frid drive data for the faceplate 32 CRT (Table 15) can be compared to an emperically determined model by F. G. Oess (Ref. 3). The relationship of cathode current as a function of grid drive was determined to be:

$$I_c = KV_d^{\psi} V_c^{(1.5-\psi)} \quad (1)$$

$$\psi = 3 \exp(0.2\gamma^{2.3}) \quad (2)$$

$$\gamma = \frac{V_d}{V_c} \qquad (3)$$

where:

I_c is the cathode current

K is the modulation constant

V_c is the cut-off voltage

V_d is the grid drive

ψ is the defined exponential function of V_d and V_c

γ is the grid drive fraction.

Arbitrarily choosing $K = 3.5$ and realistically $V_c = 40$ volts, the cathode current for 10, 20, 30 and 40 volt grid drives is 13, 103, 345, and 885 units respectively. Figure 35 shows the shape of this semilog plot. Oess assumed a Gaussian emission distribution to determine this emperical functional relationship. Also plotted is the cathode current versus brightness data for the faceplate 32 CRT. The shape of the plot is similar; the absolute values are different. The similar shape or slope of the plots indicates normal gun operation *if it can be assumed* the anode current is proportional to the cathode current. The lack of anode current data does not allow 100% justification of this assumption. After years of experience building CRTs of this size, shape and gun design, we feel this assumption is valid.

To a first approximation, a conventional CRT will demonstrate brightness in proportion to anode current. With the conclusion of the preceding paragraph, brightness is in proportion to the cathode current. The difference in shape or slope of the faceplate 32 CRT cathode current (Figure 35) and the brightness data (Figure 36) approaching maximum grid drive suggests the phosphor is the cause of saturation. It is essential to experimentally confirm the source of this saturation problem.

3.7.7 Discussion - CRT (Faceplate 19)

The data for faceplate 19 at 10 kV anode potential exhibits a straight line on the semilog plot. The faceplate 19 curves for all three anode potentials are shown on Figure 34. The curves for 14 and 18 kV anode potentials exhibit the characteristic multiple exponential shape. In like manner, every other curve for all other CRTs at all anode potentials exhibit this. This CRT was not exceptional in its fabrication. The validity of the measurement data is questionable.

3.8 Individual CRT Fabrication History

The disposition of CRT attempts, identified by faceplate number is shown in Table 16. The individual failures have been reported at length in monthly and interim reports. This final report is intended to be an overall examination of the development of a high contrast color CRT. The information in this table is incomplete. However, the knowledge gained from these failures comprises this entire report. Therefore, to expand on this table would be redundant.

Table 17

CRT FABRICATION HISTORY

Group	Faceplate Number	Date 1979
II	17	Second Delivered CRT ship S/N 002
	18	NR film became transparent due to oxygen in frit seal furnace atmosphere
	19	Went down to air while soldering HV lead - repaired
	20	Frit seal furnace too hot, the glass deformed
	21	Faceplate aluminizing test S/N 003
III	22	4-2 frit seal 5-15 patch frit seal 5-18 patch HV feedthrough 5-31 ship S/N 004
	23	4-11 frit seal 4-12 patch CRT made 5-15 down to air 5-18 frit seal patch 6-15 ship S/N 005
	24	5-24 frit seal 6-14 patch frit seal 6-15 patch frit seal CRT made 6-29 Down to air at test 7-? frit seal patch 7-19 reject at pump, example of Al-V_2O_5 reaction
	25 (CP)	5-20 frit seal 6-19 cathode poisoning (CP) and high cut-off - regun 7-11 tube arced and went down to air 7-19 new funnel frit sealed - cracked faceplate
	26	Ft. Monmouth polished faceplate made good seal to funnel but no HV feedthru in funnel
	27	NR film lost during faceplate salvage attempt

Table 17 (Continued)

Group	Faceplate Number	Date 1979
III (cont)	28 (CP)	Ft. Monmouth frit seal 7-17 cold cathode - regun 8-20 poison cathode - regun Shipped S/N 006
	29	5-26 frit seal 5-31 patch frit seal 6-27 arc through frit seal refunnel good subassembly might poison cathodes
	30 (CP) (CP) (CP)	5-29 poison cathode - regun 6-13 cathode - heater short - regun 7-12 poison cathode - regun 9-4 poison cathode - regun Shipped as RGA analysis tube S/N 008
	31	5-25 broken at potting - regun 6-19 high cut-off - tested for brightness data then regunned 6-29 down to air hold in fear of cathode poison
	32	7-19 down to air 8-21 down to air - frit broke refunnel 9-4 Ship S/N 007
	33	patch - fracture faceplate
	34	patch - crack faceplate
	35	lost in salvage attempt
	36	patch - crack faceplate
	37	patch - fracture faceplate

4.0 SUMMARY OF RESULTS

Emphasized Detailed Program Objectives

Objective 1.1.1.1-1

The transparent phosphors used are sputtered thin films of lanthanum oxysulfide (La_2O_2S) doped with europium and terbium to yield red and green luminescence, respectively. The resulting CRT's indicated cathodoluminescent efficiencies sufficient for replacing the Dumont KC3055 CRT used in the AN/A PR-39.

Objective 1.1.1.1-4

The phosphor films are backed with a uniform nonreflecting coating. The specular reflection from this coating, on the phosphor side, is measured to be less than 6.5% (objective: less than 1%). The diffuse reflectance is measured to be less than 1.0% (objective: less than 0.25%). Heating cycles for CRT fabrication were judged to have little effect on the optical properties of the coating. However, these time-temperature treatments must be held to a minimum.

Objective 1.1.1.2

Table 9 compares the electrical requirements of the high contrast color CRT to those of the monochrome tube to be replaced. The similarity has been maximized. The focus voltage and anode potential differ as anticipated. The second grid potential could be supplied by the new focus voltage power supply as it exceeds the present G-2 voltage.

The phisical similarity is successful. The neck glass diameter can be duplicated exactly given enough lead time to order the glass.

The contrast capabilities must be examined to determine if this CRT can optically replace the existing monochromatic tube. The calculations in Section 2.8 reveal the abilities of this high contrast color CRT in the worst case conditions, bright direct sunlight (1.24×10^4 fc). Under these conditions the reflectance is 932.4 fL. Of this amount 557.3 is the result of reflectance at the front surface. By coating the front surface with an antireflective coating the reflected ambient light could be reduced to 375 fL, which is the result of the refractive index mismatch at the glass-phosphor interface. This is the minimum for this tube design (faceplate material choice). The contrast ratio in these worst case conditions is determined from the maximum luminance at 20 kV and 50 volt drive (450 fL) and the equations noted below (Tables B1 and B2 in Appendix B). Without an antireflective coating the contrast ratio is 1.44. With such a coating the contrast ratio is 2.06 under brightest direct sunlight.

A contrast ratio of 1.41 will allow one shade of gray discernible to the eye; a contrast ratio of 2 corresponds to two shades of gray (contrast ratio = $(\sqrt{2})^n$ where n is the number of shades of gray. In bright direct sunlight this CRT, without enhancement devices will allow human eye resolution of illuminated, non-illuminated areas and one shade of gray. Using the green display for day viewing and the red display for night viewing, this CRT will fulfill the contrast needs of the AN/APR-39 radar system. The resolution (line width) of an Einzel lens configuration replacement tube is well within the proposed limites (0.016 inches) with the focus voltage held constant. It is concluded: a high contrast color CRT for replacement in the AN/APR-39 is a reality.

Objectives 1.1.1.2.1 and 1.1.1.2.5

Table B1 provides quantitative criteria to determine the contrast ratio for a given CRT luminance (fL) under the worst case conditions - direct bright sunlight. Table B2 provides similar criteria when a simple anti-reflective coating is used. To determine these tables and the contrast at lower ambients for this CRT the formula developed in 2.8 is used.

$$\text{Contrast} = 12.5199 \frac{L}{A} + 1$$

where:

L = CRT luminance (fL)

A = ambient luminance (fL)

With an antireflective coating on the front surface of the CRT;

$$\text{Contrast} = 29.993 \frac{L}{A} + 1$$

L and A as above.

These equations enable the back calculation of the necessary luminance required for any contrast ratio and a specific ambient.

5.0 CONCLUSIONS

This program developed a viable CRT fabrication technolgy utilizing thin film phosphors deposited on the CRT faceplate. The thin film deposition technique was optimized to yield a faceplate with specular reflection less than 6.5% and diffuse reflection less than 1%. A frit sealing technique was developed to seal the 1720 glass faceplate to the 3320 glass funnel using a (Corning 7593) or an amorphous (Owens-Illinois 5G-7) frit. Upon incorporation of the faceplate into a cathode ray tube, the line width (at 50% amplitude) was well below the proposed maximum of 16 mils. Specifically, the line width measured less than 6 mils for the bipotential gun configuration CRT's at all anode potentials adjusting the focus voltage for minimum line width at each measurement. The line width measured less than 12 mils for the Einzel lens gun configuration at one constant focus voltage for all anode potentials.

5.1 Further Development

Further development in four specific areas is necessary to optimize this CRT. The first and second are improvements in the fabrication process; development in two other areas will increase the CRT brightness, hence the contrast of the display.

The dielectric breakdown strength of the frit can be improved by reducing its porosity. This can be accomplished by drying the frit more completely (200°C in air for 2 hours) before firing.

The source of the cathode poisoning is thought to be the elemental sulfur identified on the La_2O_2S film after heat treatment (1/3 of a monolayer). An additional vacuum firing (350°C for 1 hour) before NR film deposition would remove this sulfur.

The faceplate heat treatment (H_2S atmosphere) is limited to a maximum of 870°C by the 1720 flass softening point (915°C). The maximum increase in cathodoluminescent efficiency, hence brightness, is attained at 1050°C. The use of sapphire as the faceplate substrate with 1050°C heat treatment would increase the brightness approximately 15%.

The brightness can also be improved by solving the saturation problem. At this time the problem has not been identified with sufficient accuracy to propose a solution. This is the only problem area that necessitates basic investigations to understand the nature of the problem.

AD-A084 687 WATKINS-JOHNSON CO SCOTTS VALLEY CA F/G 9/1
HIGH CONTRAST CRT.(U)
FEB 80 N H LEHRER, G A HOLMQUIST DAAB07-77-C-2639
UNCLASSIFIED DELET-TR-77-2639-F NL

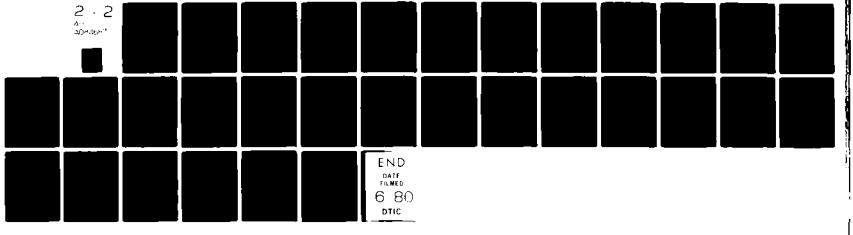

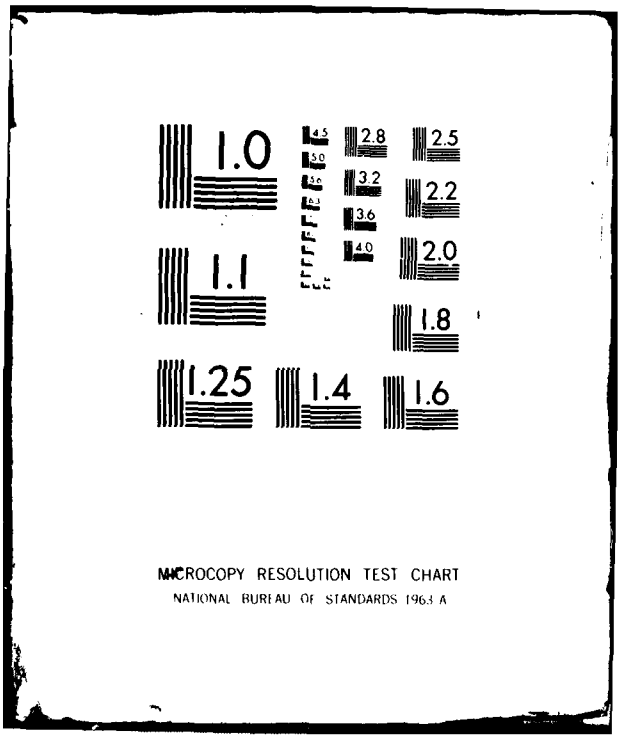
1.0
1.1
1.25
1.4
1.6
1.8
2.0
2.2
2.5
2.8
3.2
3.6
4.0
4.5
5.0
5.6
MICROCOPY RESOLUTION TEST CHART
NATIONAL BUREAU OF STANDARDS 1963 A

REFERENCE

1. P. Pascal, Nouveau Traite de Chimil Minerale, 12, 96.

2. N. H. Lehrer, "Application of the Laminarflo Gun to Cathode Ray Tubes," SID Journal, March/April 1974, p. 7-11.

3. F. G. Oess, "CRT Considerations for Raster Dot Alphanumeric Presentations," April 1979.

TEPAC Engineering Bulletin #21
Electronic Industries Association
2001 Eye Street, N.W., Washington, D.C. 20006

APPENDIX A

U.S. PATENT 4,132,919

United States Patent [19]

Maple

[11] **4,132,919**

[45] **Jan. 2, 1979**

[54] **ABSORBING INHOMOGENEOUS FILM FOR HIGH CONTRAST DISPLAY DEVICES**

[75] Inventor: **T. Grant Maple**, Sunnyvale, Calif.

[73] Assignee: **Lockheed Missiles & Space Company, Inc.**, Sunnyvale, Calif.

[21] Appl. No.: **859,724**

[22] Filed: **Dec. 12, 1977**

[51] **Int. Cl.**[2] **H01J 29/20**; H01J 1/62

[52] **U.S. Cl.** ..... **313/466**; 96/82; 96/84 M; 250/487; 313/112; 313/474; 350/164; 350/166; 358/252; 427/66; 427/68; 427/70; 428/472; 428/539; 428/913

[58] **Field of Search** ..... 313/466, 474, 415, 461, 313/463, 110, 112; 358/252; 250/487; 350/164, 166; 351/163; 96/84 M, 82; 427/64, 66, 107, 68-70, 109; 428/913, 472, 539

[56] **References Cited**

U.S. PATENT DOCUMENTS

2,312,206	2/1943	Calbick	313/474
2,331,716	10/1943	Nadeau et al.	350/164 X
2,616,057	10/1952	Coltman	427/106 X
3,042,542	7/1962	Anders	428/428
3,560,784	2/1971	Steele et al.	313/441
3,825,436	7/1974	Buchanan et al.	313/468
3,936,136	2/1976	Ikeda et al.	350/164 X
3,946,267	3/1976	Lustig et al.	313/474 X
3,960,441	6/1976	Kamiya et al.	350/164
4,042,390	8/1977	Steele	427/64
4,069,355	1/1978	Lubowski et al.	427/69 X
4,071,640	1/1978	Ignasiak	427/68 X

Primary Examiner—Harold Ansher

Attorney, Agent, or Firm—Richard H. Bryer; Billy G. Corber

[57] **ABSTRACT**

This invention relates to light absorbing inhomogeneous films and their use in luminescent display devices such as cathode ray tubes and electroluminescent panels to achieve high contrast ratio and minimal halation effect, and more particularly to an inhomogeneous film having a composition varying continuously from metal oxide to metal, and the method of making same. The metal is selected from the group consisting of tantalum and vanadium.

15 Claims, 2 Drawing Figures

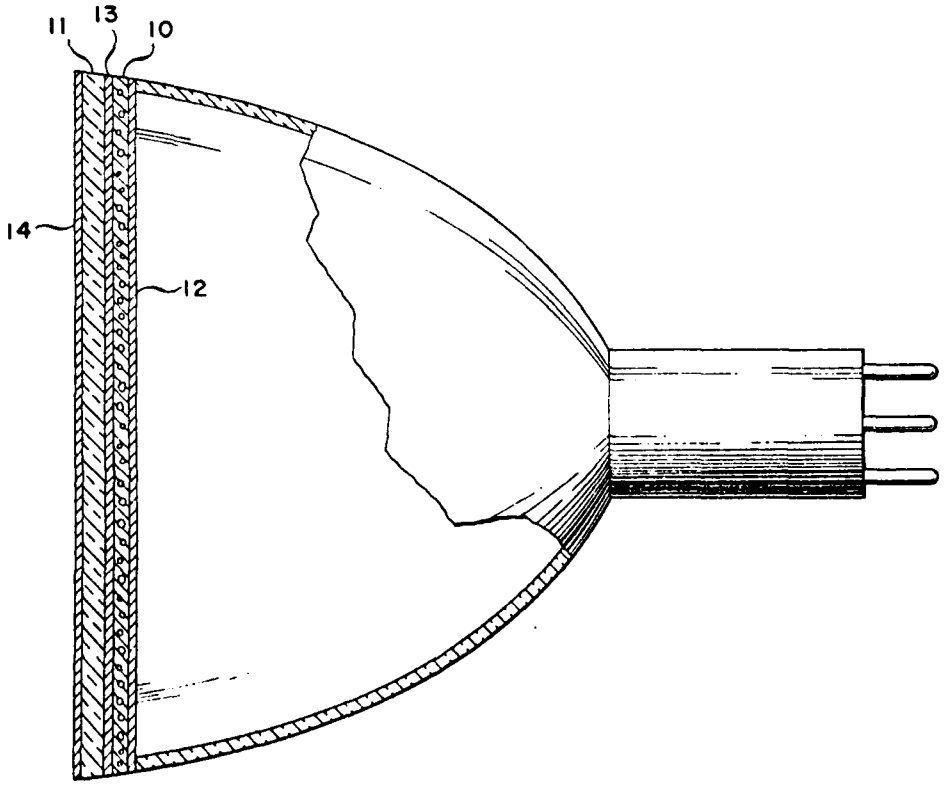

FIG. 1

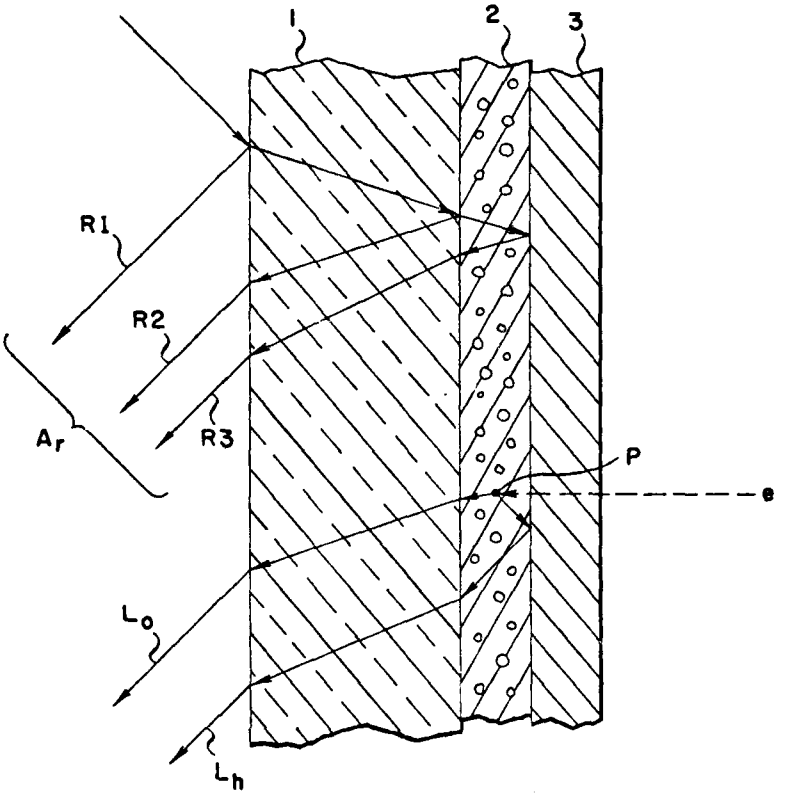

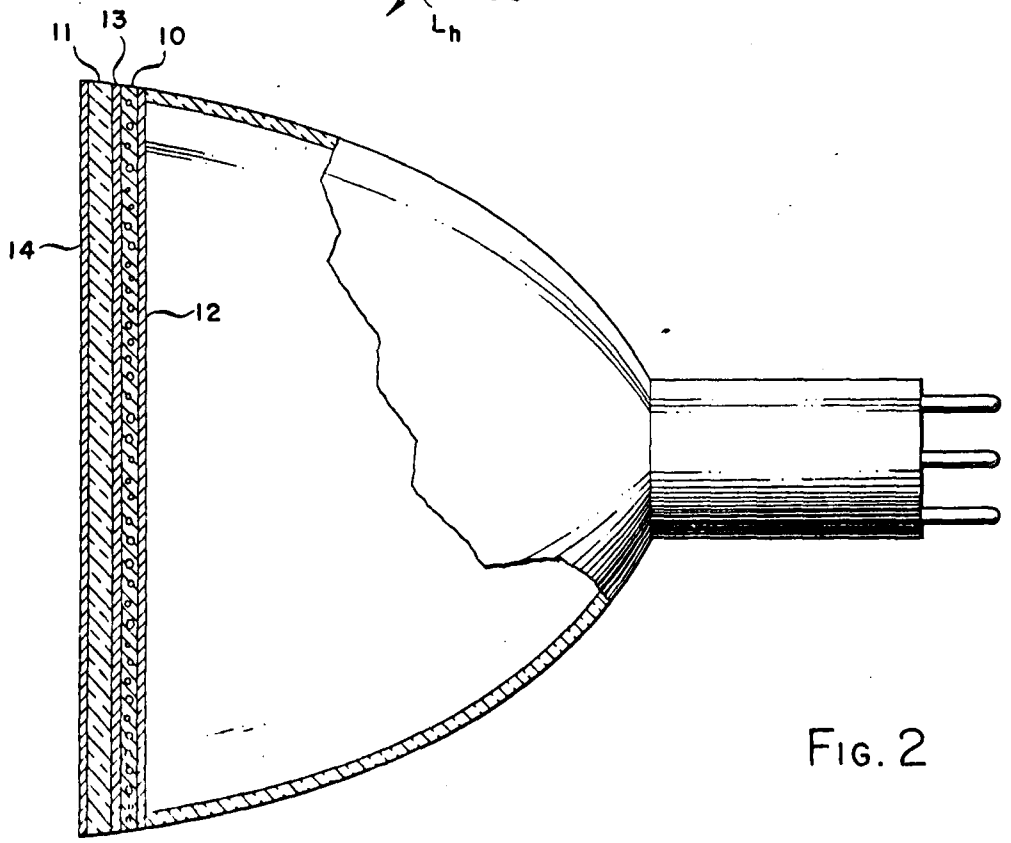

FIG. 2

ABSORBING INHOMOGENEOUS FILM FOR HIGH CONTRAST DISPLAY DEVICES

BACKGROUND OF THE INVENTION

It is well known that ambient illumination, that is light originating from sources external to the display device, is reflected to the observer from various optical interfaces of the device and thus reduces the image contrast by increasing the apparent brightness of the dark image areas. Under conditions of high ambient illumination, the image contrast is severly degraded. In addition, a part of the light emitted by the luminescent material of the device also undergoes undesired reflections, producing a further degradation of contrast and of resolution. When the luminescent material consists of a layer of phosphor material in the form of small powder particles, scattering of the emitted light also occurs, further degrading resolution.

Various means for overcoming these problems have been proposed. These include the use of various filters including polarizing, neutral density and restricted angle or multi-apertured opaque filters. Other methods include the incorporation of a dark material into the glass of the tube face, or a black dye in the phosphor dielectric layer of the display device. All of the methods have the common disadvantage that the emitted light as well as the reflected ambient light intensity is reduced, with the result that the improvement is contrast ratio is less than desired because the emitted light intensity is a factor upon which the contrast ratio depends.

The remarkable reflection-reducing properties of inhomogeneous films were recognized as early as 1880 by Lord Rayleigh (Proc. Lond. Math. Soc. 11, 51, 1880); the properties of such films have been extensively reviewed in a recent series of articles by Jacobsson (Progr. in Optics 5, 247, 1965; Arkiv Fysik 31, 191, 1966; Physics of Thin Films 8, 51, 1975). According to Jacobsson, experimental studies to date have been mainly devoted to transparent inhomogeneous films composed of graded mixtures of two nonabsorbing materials such as ZnS—Na_3AlF_6, ZnS—CeF_3, CeO_2—CeF_3, and CeO_2—MgF_2. These films were found to be durable and of good optical quality. A high index mixture of Ge—ZnS has been produced for application in the infrared wavelength region but were found to be relatively soft and sensitive to moisture and inferior to Ge—MgF_2 films. KBr—Au films were found to have a very low absorption index, with $k = 0.01$ even at a concentration of gold of 0.16 parts by volume of gold. By contrast, an absorption index of 1.0 was found for a Ge—Au mixture containing 0.1 parts by volume of gold. Ge—In films were also found to have relatively high absorption. Due to the low solubility of In in Ge, the In was expected to remain a separate phase in the form of more or less spherical inclusions.

An inhomogeneous Ge—Si_xO_y film was shown by Jacobsson (1965) and also Olsen and Brown (Res./Develop. 16, 52, 1965) to lower the reflectance of a Ge surface to that of a surface of Si_xO_y (refractive index 1.62). Even lower reflectance was obtained with Ge—MgF_2 films, although the transmittance was higher than expected (Jacobsson and Martensson, App. Optics, 5, 29, 1966). One of the first applications of inhomogeneous films as an antireflection coating was described by Nadeau and Hilburn in Canadian Pat. No. 418,289 (1944), and U.S. Pat. No. 2,331,716 (Oct. 12, 1944), in which a plastic layer of polystyrene or urea-formaldehyde resin having a high refractive index is diffused into the surface of an article and overcoated with a second plastic of low refractive index such as cellulose caproate or ethylcellulose. An important commercial application of inhomogeneous films as a low reflectance, absorbing coating on sunglasses was described by Anders in U.S. Pat. No. 3,042,542 (German Pat. No. 1,075,808; 1960). The inhomogeneous films described by Anders consisted of a mixture of low refractive index material, CeF_4, ThF_4, MgF_2, or SiO_2, and a metal, Ni, Fe, Mn, or Cr, or lower oxide of Nb, Ta, or Ti.

Recently, Steele has proposed in U.S. Pat. No. 3,560,784 the use of a dark dielectric layer consisting of SiO_2 with a tapered concentration of codeposited aluminum applied to the rear side of a light transmissive phosphor layer to serve as a light absorbing layer. The tapered concentration of aluminum results in a continuous variation of the index of refraction through the layer, and such layer comprises an optically inhomogeneous film. Steele claimed novelty for a high contrast cathode ray tube utilizing this construction in which the refractive index of the silicon oxide was substantially equal to that of the phosphor. Phospors suitable for use with the inhomogeneous film of Steele were not otherwise identified. The same objective was the object of an earlier patent of Coltman (U.S. Pat. No. 2,616,057) in which the light absorbing layer was described as lampblack or the black deposits produced by evaporating metals such as aluminum or antimony under poor vacuum conditions.

Up to the present, the deposition of tapered inhomogeneous films such as in the Steele patent has required the evaporation of two different materials, with the rate of evaporation of each varied as a function of time. Also, it is usually desired that the initial portion of the deposit consist of one component only with the end portion consisting of the second different material only. Steele shows the initial and end materials to be SiO_2 and aluminum, respectively. These requirements pose severe technical difficulties and to achieve reproducible results, elaborate monitoring and control equipment is required so that despite the superior performance offered by inhomogeneous films as compared to homogeneous films, very limited commerical application has been made of inhomogeneous films.

Osterberg (J. Opt. Soc. Am. 48, 513, 1958) has shown that transmitted waves cannot suffer loss of energy by reflection as they traverse nonabsorbing, inhomogeneous media in which the optical properites have no discontinuities. This result is strictly true only when the medium is infinite in extent. For practical applications, film thicknesses used are of the order of the wavelength of light so that interference due to reflection at the boundaries occurs. The width of the reflectance minimum has been found, however, to be greater than can be achieved with homogeneous films. It also has been shown by Osterberg that inhomogeneous absorbing media similarly cannot exhibit reflectance when the optical properties are continuous. In this case, the medium need not be infinite in extent. Anders (Dunne Schichten fur die Optik, Wissenschafftliche Verlagsgesellschaft mbH, Stuttgart, 1965, English translation as Thin Films in Optics, The Focal Press, London, 1967) has observed that a film thickness of only one wavelength is sufficient for essentially complete absorption in an absorbing inhomogeneous film. This property is basic to the dark dielectric layer described by Steele in

U.S. Pat. No. 3,560,784 (1971) since the tapered concentration of aluminum results in an absorbing inhomogeneous film. The deposition of such film entails, however, the technical difficulties previously described, including the deposition of two different materials from two sources.

SUMMARY OF THE INVENTION

Briefly, in accordance with the invention, it has been discovered that an inhomogeneous film of a novel tapered composition varying from metal oxide to metal has superior light absorption properties. The metal is selected from the group consisting of tantalum and vanadium. The film is to be prepared by a new method of deposition which has attractive features of simplicity as contrasted with previously known methods for preparing inhomogeneous films, requires only a single source of material, and results in highly reproducible light absorping properties.

More particularly, the films may be prepared by means of RF or DC reactive sputtering wherein the target is vanadium or tantalum metal and the sputtering atmosphere consists of a mixture of argon and oxygen, with the partial pressure of the oxygen continually varied during deposition of the film in such a manner as to provide the desired inhomogeneity. In one embodiment of the invention, the initial partial pressure of oxygen is selected such that the initial portion of the deposited film consists of transparent, nonabsorbing tantalum oxide. Once deposition has been initiated, the oxygen partial pressure is thereafter gradually reduced until it becomes zero. The effect of gradually reducing the oxygen pressure is to cause the deposited film to become increasingly deficient in oxygen. At sufficiently low or zero pressure the material being deposited is metallic, highly absorbing tantalum or vanadium. A gradient of refractive index is associated with the gradient of oxygen deficiency, or excess metal, in the film. The nature of the gradient is dependent on the rate of decrease of oxygen partial pressure and may be varied continuously to achieve any desired gradient of refractive index. The light absorbing properties of the resulting inhomogeneous films have been found to be not critically dependent upon the rate of decrease of oxygen pressure, equally good results being obtained with either a linear or exponential decrease of pressure as a function of time.

Gerstenberg and Colbick (J. Appl. Phys. 35, 402, 1964) have shown that the x-ray diffraction pattern of films produced by DC reactive sputtering of tantalum in oxygen-argon mixtures at oxygen partial pressures of 9×10^{-5} Torr and greater is the same as that of anodic Ta_2O_5. A subsequent study by Sneed and Krikorian (J. Appl. Phys. 37, 3674, 1966) showed that the critical oxygen partial pressure for deposition of Ta_2O_5 varied between 5×10^{-5} and 2×10^{-4} Torr depending upon several system and deposition parameters. For the RF sputtering system used to deposit the films of this invention, a critical oxygen partial pressure of 3×10^{-4} Torr was observed.

For the purposes of this invention it is not essential that the composition of the initial deposit be stoichiometric Ta_2O_5, but rather that it be highly transparent and have a refractive index substantially equal to that of the phosphor layer. The nonreflective film will have its maximum effectiveness when R_3 of FIG. 1 is zero. This occurs when the index of refraction of the nonreflective film is equal to the index of refraction of the luminescent film. In the present invention, the metal oxide of the nonreflective film has an index of refraction very close to that of the La_2O_2S luminescent film described in U.S. Pat. No. 3,825,436. Consequently, the reflectivity R_3 is very low and the incident light becomes absorbed in the nonreflective film.

Owing to the excess metal incorporated into the films, the films of the invention have appreciable electrical conductivity. This property is particularly desirable where the films are to be used in place of the usual aluminum thin film electrode of typical cathode ray screens since the conductivity of the films prevents charge accumulation associated with incidence of the electron beam on the screen, which would otherwise distort the information to be presented.

It has been found that tantalum and vanadium are uniquely suited as target materials for preparing an inhomogeneous film having the desired properties for use as a nonreflecting layer in light emitting phosphor display devices such as cathode ray tubes. For such devices, it is desirable that the film absorb both the incident ambient light and the light emitted from the back side of the phosphor layer, and in addition prevent light originating at the filament of the electron beam gun from reaching the observer. The film must, therefore, be opaque to all light. Other target materials which have been tried in accordance with the method of the invention include tin, niobium, aluminum, titanium, and molybdenum. The inhomogeneous films thus obtained corresponded to a complete transition between the limits of a clear, transparent oxide film and an opaque metallic film and, with the exception of the aluminum films, were dark when viewed from the oxide side of the film. However, distinct interference colors were noted which can be attributed to internal reflections occurring within the films. According to the Osterberg article, such internal reflection can arise in absorbing inhomogeneous films only at discontinuities of the optical properties within the films. Such discontinuities could arise if there were abrupt changes in the type of oxide being deposited, in contrast with the gradual incorporation of oxygen vacancies and excess metal into a single type of oxide as appears to occur with the tantalum and vanadium systems. Oxides which differ in crystal structure or in valency of the metal component may be expected to have distinctly different indices of refraction. More than one oxide is known to exist in the metal-oxygen systems of tin, niobium, aluminum, titanium, and molybdenum. Although there is evidence for at least one oxide other than Ta_2O_5 in the tantalum-oxygen system, diffraction studies by Hollands and Campbell (J. Mater. Sci. 3, 544, 1968) on homogeneous films produced by reactive sputtering of tantalum in argon-oxygen atmospheres at various oxygen content between 0 and 100 percent oxygen indicated that the deposited oxide has the Ta_2O_5 structure. Similar studies of the sputtered vanadium oxide structure have not yet been made, but, analagous to the Ta oxide case, the vanadium oxide is probably V_2O_5.

Control of the oxygen partial pressure may be conveniently accomplished by means of a micrometer valve placed in the line supplying oxygen to the sputtering system. Variation of the rate of decrease of oxygen pressure may, furthermore, be automated by connecting a variable speed electric motor through a gear chain to the micrometer valve and the voltage actuating the motor programmed in time. Other means of providing a predetermined automatic variation of the oxygen partial

pressure are known and may be used. By measurements of the oxygen partial pressure in the system as a function of micrometer setting and measurements of deposition rates at various fixed oxygen pressures, information required for producing a desired gradient of composition is readily obtainable. Such automation will ensure a very high degree of reproducibility of film properties but is not essential as it has been found that very satisfactory nonreflecting films can be produced by a skilled operator through manual operation of the micrometer valve.

BRIEF DESCRIPTION OF THE DRAWING

The invention may be more easily understood from the following description and accompanying drawing in which:

FIG. 1 is a cross-sectional view of a faceplate of a conventional cathode ray tube in which the passage of incident ambient light and light emitted by the phosphor of the cathode ray tube is schematically represented; and

FIG. 2 is a cross-sectional view of the faceplate of a cathode ray tube constructed in accordance with the invention.

DESCRIPTION OF THE PREFERRED EMBODIMENTS

Referring more particularly to FIG. 1, there is shown the cross-section of a faceplate of a conventional cathode ray tube in which the passage of incident ambient light and light emitted by the phosphor is schematically represented. Ambient light incident from the left upon the glass face 1 of the cathode ray tube is partially reflected, ray Rl, at the air-glass interface; typically, the intensity of Rl is about 4 percent of the incident ambient intensity for a glass having a refractive index of 1.5. Additional reflections R2 and R3 occur at the interfaces between the glass and the phosphor film 2 and between the phosphor film 2 and the aluminum thin film electrode 3, the magnitude of the reflections depending upon the difference in refractive indices of the materials on each side of the interfaces in accordance with the well-known Fresnel equations (see Jenkins and White, Fundamentals of Optics, Third Ed., 1957, p. 510; Born and Wolf, Principles of Optics, Fifth Ed., 1975, p. 40; or Heavens, Optical Properties of Thin Solid Films, 1955, pp. 51–54). For normal incidence, the reflectivity at a boundary between isotropic dielectric media is

$$R = \left(\frac{n_o - n_1}{n_o + n_1}\right)^2$$

and at a boundary between a dielectric and a metal

$$R = \frac{(n_o - n_1)^2 + k_1^2}{(n_o + n_1)^2 + k_1^2}$$

where $n_1 - ik_1$ is the complex index of refraction of the metal.

The index of refraction of lanthanum oxysulfide is 2.22 at 5440 A° (La_2O_2S:Tb green emission; see Sobon et al., J. Appl. Phys. 42, 3049, 1971), and for an aluminum film $n = 0.82$ and $k = 5.99$ (Drummeter and Haas, Physics of Thin Film 2, 339, [1964]). The reflectivity at an La_2O_2S — Al boundary is thus 83.8 percent. By contrast, the reflectivity for an La_2O_2S — Ta_2O_5 boundary is calculated as 0.29 percent, using a value of 2.12 for the index of tantalum oxide films deposited by electron beam bombardment as determined by Yeh et al. (J. Appl. Phys. 47, 4107, 1976). A portion of the reflected rays R2 and R_3 may undergo additional reflections, not depicted in the drawing, at the air-glass and glass-phosphor interfaces. Also depicted in FIG. 1 is the emission of light at a point P in the phosphor 2 produced by absorption of electrons projected from an electron gun, not shown, situated to the right of the drawing. A portion of the light, L_o, is emitted toward the observer at the left and a portion toward the aluminum electrode 3; the latter portion of emitted light undergoes reflection at the phosphor-aluminum interface. A portion of the light emitted toward the observer may be reflected at the phosphor-glass interface and a further portion reflected at the glass-air interface. That light which is emitted oblique to the plane of the phosphor is displaced laterally with respect to the normal axis through point P during transit through the faceplate, in accordance with Snell's law, $n_0 \sin \theta_0 = n_1 \sin \theta_1$, where θ_0 and θ_1 are the angles of incidence and refraction, respectively (Jenkins and White, loc. cit. p. 5). Reflections result in the halation, L_h, depicted in the figure.

As the result of successive reflections, a large proportion of the ambient light A_r may be reflected toward the observer and will affect the degree to which the emitted light is visible to the observer. The visibility is expressed as the contrast ratio C, where

$$C = \frac{A_r + L_o}{A_r},$$

A_r is the intensity of reflected ambient light and L_0 is the emitted light viewed by the observer. Since under high ambient illumination intensity A_r may greatly exceed L_0, it is evident that a very low contrast ratio can occur. It is clear that the contrast ratio can be increased only by reducing the intensity of reflected ambient light A_r.

For the interface between glass of index 1.5 and a lanthanum oxysulfide phosphor of index 2.22, the reflectivity is 3.75 percent. Both this value and that for the air-glass interface are very small compared to that of the phosphor-aluminum interface. The intensity of ambient light reflected to the observer is therefore predominantly due to reflection at the phosphor-aluminum interface, and thus the most effective means of improving the contrast ratio is to reduce the reflectivity at this interface. As will be evident from the examples of this invention, this objective is attained by replacing the aluminum with the inhomogeneous film of the invention.

Calculations according to the Fresnel equations indicate that when the refractive index of that part of the inhomogeneous film at the interface with lanthanum oxysulfide has a value between 1.82 and 2.71, the interfacial reflectivity will be less than 1 percent; and, for a value between 1.93 and 2.55, less than 0.5 percent. For a phosphor of index n_p, the inhomogeneous film index n_i corresponding to 1 percent reflectivity is $n_i = 0.82\ n_p$ to $1.22\ n_p$, and for 0.5 percent reflectivity, $0.87\ n_p$ to $1.15\ n_p$.

It is thus evident that the interfacial reflectivity can be reduced to a negligible amount, with a most substantial improvement of contrast, without the necessity of the exact match of refractive indices corresponding to

zero reflectivity; such exact match is difficult to attain in practice.

Using the value 2.10 for the index of the tantalum oxide component of the inhomogeneous film of the invention, it can be calculated that the interfacial reflectivity is less than 1 percent for a phosphor having an index between 1.72 and 2.56, or less than 0.5 percent for an index between 1.82 and 2.29, thus indicating that the films of the invention are also suitable for use with phosphors other than lanthanum oxysulfide.

In FIG. 2, there is shown a cross-section of the faceplate of a cathode ray tube construced according to the present invention. A cathodoluminescent phosphor material **10** is deposited on the glass faceplate **11**. A metal oxide-metal absorbing inhomogeneous film **12**, where the metal is tantalum or vanadium, is deposited on the back side of the phosphor material **10** by the method of the present invention, described more fully hereinafter. A preferred phosphor material for the luminescent display devices of the invention is described in U.S. Pat. No. 3,825,436. This phosphor has the formula Ln_2O_2S:RE, where *Ln* is at least one trivalent rare earth host ion selected from the group consisting of lanthanum, gadolinium, yttrium and lutetium and RE is at least one trivalent activator ion selected from the group consisting of rare earth ions having atomic numbers 59 through 70 and in which from about 0.001 percent to 20 percent of the trivalent host ions have been replaced by at least one said activator ion. However, other continuous crystalline phosphor films deposited by conventional vacuum deposition methods, such as described in U.S. Pat. No. 3,347,693, or deposited by the method of U.S. Pat. No. 3,108,904 are suitable. Irrespective of the phosphor material employed, it is important that it be deposited as an essentially smooth and continuous transparent film without significant surface texture, thereby avoiding the scattering of light inherent to the use of a powder phosphor layer. Rather than a single phosphor film, the phosphor material **10** may consist of multiple films, each film capable of emitting a different color; see U.S. Pat. No. 3,825,436.

In order to avoid unwanted reflections at the interface between the glass **11** and the phosphor **10** which may arise by reason of a mismatch of the respective refractive indices, a quarter-wave homogeneous film **13** of a suitable material, having refractive index n_b satisfying the Strong relation $n_b = \sqrt{n_a n_c}$, where n_a is the refractive index of the glass and n_c is the refractive index of the phosphor, is optionally deposited on the glass plate **11** prior to deposition of the phosphor film **10**. The interface reflectivity will thereby be reduced to zero at the given wavelength, but appreciable reflectivity may occur at other wavelengths. A broader minimum with respect to wavelength can be achieved by alternatively depositing a nonabsorbing inhomogeneous film in place of the homogeneous film. Additionally, an antireflection coating **14** of conventional type may also be optionally applied to the exterior of the glass plate **11** to eliminate reflection that would otherwise occur at the air-glass interface.

It will be understood that the optional antireflection coating **14** and optional homogeneous film **13** or the alternative optional nonabsorbing inhomogeneous film **13** are not essential for obtaining good contrast in most applications for which the ambient illumination is moderate, but may be desirable under extremely high ambient illumination intensity, such as that provided in direct sunlight.

The absorbing inhomogeneous films of the invention comprise at the phosphor-film interface a metal oxide having a refractive index closely matching that of the phosphor and at the opposite metal side an index approximately that of the bulk metal. Illustratively, an absorbing inhomogeneous tantalum oxide-tantalum film is readily made according to the invention with a refractive index of approximately 2.1 at its interface with the phosphor, thus providing a close match to the refractive index of lanthanum oxysulfide which has been determined to have an index of approximately 2.2, and is therefore particularly suited for use with the inhomogeneous film of this invention and is also one of the brightest of known phosphors. The refractive index at the tantalum side of the inhomogeneous film has a refractive index approximating that of a bulk tantalum which is known to have the complex index 2.53–2.76i.

An absorbing inhomogeneous vanadium oxdide-vanadium film is also readily made according to the invention and as will be evident from the example, provides nearly as close match to the refractive index of lanthanum oxysulfide as is obtained with the tantalum oxide-tantalum film. As it is known that an inverse relationship exists between electron range and the periodic number and density of the components of a film (see Feldman, Phys. Rev. 117, 455, 1960), the vanadium-based film of the invention has particular advantages when it is desired to operate a cathode ray tube or luminescent display device at lower anode voltages.

In another embodiment of this invention, the tantalum oxide-tantalum absorbing inhomogeneous film disclosed herein may be advantageously substituted for the special dark dielectric layer of the luminescent panels described in U.S. Pat. No. 3,560,784. The relative simplicity of the method of preparing the films described herein and greater reproducibility of properties of the films prepared by the method of this invention are made evident in Example 1 hereof and the films of this invention may be more economically prepared by reason of the less technically complex equipment required to produce the films than those of U.S. Pat. No. 3,560,784.

It will be readily understood that thin films of inert materials such as silicon oxide may be deposited on the phosphor film prior to deposition of the absorbing inhomogeneous film to serve as a barrier against any possible reaction between the phosphor and the inhomogeneous film that may, for example, be promoted by localized heating due to electron bombardment at high electron beam densities. Where appropriate for matching refractive indices of the adjoining materials, the barrier film may advantageously consist of a mixture, such as silicon oxide and aluminum oxide.

In the examples which follow, a detailed description of the novel method of preparing the absorbing inhomogeneous films of the invention is provided. A conventional RF sputtering system was used for preparing the films of the examples. Equally satisfactory results may also, however, be obtained by use of DC sputtering. As is well known to those skilled in the art of sputtering, the sputtering atmosphere pressure employed for RF sputtering, typically 1 to 5 microns, differs appreciably from that employed for DC sputtering, typically 50 to 100 microns. It is, therefore, to be expected that somewhat different oxygen pressures may be required when DC sputtering to attain results equivalent to those of RF sputtering. It is also known that deposition rates may vary between sputtering systems of different manufacture. RF systems which employ added DC bias or

crossed electrical and magnetic fields have characteristically high deposition rates. Appropriate allowance must therefore be made for the particular system used. A preliminary calibration of the desired system for deposition rates and film characteristics at various fixed oxygen partial pressures, at a given input power level, will readily establish the conditions for preparing an inhomogeneous film having the desired refractive index gradient and thickness.

The absorbing, inhomogeneous films of the invention may also be prepared by the conventional two-source evaporation method, utilizing a metal oxide as one source and the metal component of the oxide as the second source. The preferred method, by reason of greater convenience and the high reproducibility attainable, is, however, the use of RF sputtering.

EXAMPLE 1

The sputtering system used was a conventional RF system with liquid nitrogen trap and water-cooled substrate support; DC bias or magnetic field were not utilized. The target was a 5-inch diameter tantalum metal disc and the source to substrate distance was 5 cm. A shutter was interposed between target and substrate during the presputter clean-up period. The system was initially evacuated by a diffusion pump to a pressure of less than 1×10^{-6} Torr, following which the high vacuum valve was partially closed to act as throttle between the sputtering chamber and the diffusion pump. This permitted the diffusion pump to operate within an efficient low pressure range while the higher pressure required for sputtering could be maintained within the sputtering chamber through the continuous admission of the sputtering gases. Th sputtering atmosphere consisted of a mixture of argon and oxygen, with argon being the dominant component. After partially closing the high vacuum valve, a flow of oxygen was established, the flow being regulated by a micrometer valve to obtain the desired pressure in the sputtering chamber as determined by means of an ionization gauge. The flow of argon was next established and adjusted with a second micrometer valve to provide a total pressure of 5 microns. As the sputtering atmosphere consisted predominantly of argon at all times, no further adjustment of the argon micrometer valve was necessary. The sputtering discharge was then initiated at 400 watts input RF power, and the reflected RF power reduced to a negligible amount by tuning of an impedance matching network. Sputtering was continued for 45 minutes with the shutter in place to prevent deposit on the substrate. This insured removal of undesired possible contaminants absorbed on the target or chamber walls. At the end of this presputtering period, the shutter was opened to allow deposition on the substrate. Deposition was terminated at the desired time by switching off the RF supply.

A preliminary series of depositions using microscope slides as substrates was made at various fixed oxygen pressures. The films obtained were accordingly homogeneous films. Deposition times were 15 minutes; film thicknesses were measured by multiple-beam interferometry. The results are summarized in Table I.

Table I

Films Prepared at Fixed Oxygen Pressures				
Sample	O_2 Pressure Torr	Thickness A°	Deposition Rate A°/min.	Appearance
1	5.0×10^{-4}	1112	74	Clear, pale red
2	4.0×10^{-4}	1432	96	Clear, pale red
3	3.0×10^{-4}	1538	104	Clear, pale pink
4	2.0×10^{-4}	1818	121	Clear, pale green
5	1.75×10^{-4}	2354	157	Light Brown
6	1.6×10^{-4}	2629	175	Dark Brown
7	1.5×10^{-4}	2641	176	Very Dark
8	1.5×10^{-4}	2652	177	Black
9	1.4×10^{-4}	2487	166	Black, metallic
10	1.25×10^{-4}	2318	155	Black, metallic
11	1.0×10^{-4}	1939	129	Metallic, dark
12	5.0×10^{-5}	1449	97	Metallic, dark
13	0	1567	105	Metallic, dark

Target - Tantalum

This shows that by changing the oxygen pressure in the sputtering chamber the deposited film is changed from the clear metal-oxide form to the opaque metal form.

The absorbing inhomogeneous films of the example were prepared in the same manner, except that sapphire substrates provided with a La_2O_2S:Tb or La_2O_2S:Eu phosphor film of 1 micron thickness previously deposited by the RF sputtering method of U.S. Pat. No. 3,825,436 were used an the oxygen partial pressure was gradually reduced during the deposition period by adjustment of a micrometer valve according to the schedule of Table II, chosen to produce an approximately exponential rate of pressure decrease and a reasonably linear rate of film thickness increase.

Table II

Inhomogeneous Film Schedule	
Time min.	O_2 Pressure Torr
0	3.4×10^{-4}
1	2.6×10^{-4}
2	1.75×10^{-4}
3	1.8×10^{-4}
4	1.7×10^{-4}
5	1.6×10^{-4}
6	1.5×10^{-4}
7	1.3×10^{-4}
8	1.13×10^{-4}
9	1.0×10^{-4}
10	9.3×10^{-5}
11	8.6×10^{-5}
12	6.6×10^{-5}
13	5.0×10^{-5}
14	0
15	End of Run

The reflectivity of several absorbing inhomogeneous tantalum oxide-tantalum films prepared according to the method of the method of the example were measured with a Spectra Spot Brightness Meter, Model UB-1/2, using a diffuse white light source to illuminate the samples. The reflectivity of an uncoated sapphire substrate was also measured. From these measurements and the known refractive indices of sapphire and La_2O_2S, 1.76 and 2.14, respectively, the reflectivity of the phosphor-absorbing film interface was determined by calculation using Snell's laws as referenced above.

The results are presented in Table III, together with results for similarly prepared substrates having a commercially deposited silicon monoxide-tapered aluminum coating.

The exceptionally low reflectivity and high reproducibility of the Ta_2O_5-Ta films of the invention as compared with commercial SiO—Al films is clearly evident from Table III.

It is to be emphasized that the particular schedule of the example was chosen for convenience only and is not essential for preparing light absorbing films for use in cathode ray tubes and luminescent panels. Tantalum oxide-tantalum films with similarly low reflectivities have been prepared according to other oxygen partial pressure schedules. It is only essential that the variation of refractive index be reasonably continuous and the films have sufficient thickness to be essentially opaque.

Table III

Reflection at Phosphor-Absorbing Film Interface		
Sample		Reflectivity %
Commercial SiO-Al No.	1	6.5
"	2	5.1
"	3	4.5
"	4	2.8
"	5	1.8
"	6	13.6
"	7	9.2
"	8	15.0
"	9	2.2
"	10	7.9
Experimental Ta_2O_5-Ta No.	1	0.0
"	2	0.4
"	3	0.0

EXAMPLE 2

Films were prepared as in Example 1, but substituting a vanadium metal target for the tantalum target.

A preliminary series of 15-minute depositions of homogeneous films gave the results summarized in Table IV.

Table IV

Films Prepared at Fixed Oxygen Pressures				
Sample	O_2 Pressure Torr	Thickness A°	Deposition Rate A°/min.	Appearance
1	5.0×10^{-4}	696	45	Clear, pale yellow
2	4.0×10^{-4}	998	67	Clear, yellow
3	3.0×10^{-4}	772	52	Clear, yellow
4	2.0×10^{-4}	1111	74	Clear, yellow-green
5	1.8×10^{-4}	1788	119	Brown
6	1.7×10^{-4}	4462	297	Metallic, dark
7	1.5×10^{-4}	5224	348	Metallic, dark
8	1.0×10^{-4}	2551	170	Metallic
9	0	2946	190	Metallic

The inhomogeneous films of the example were also prepared as in the preceding example but following the schedule of Table V.

Table V

Inhomogeneous Film Schedule	
Time min.	O_2 Pressure Torr
0	3.15×10^{-4}
1	1.45×10^{-4}
3	9.3×10^{-5}
4	8.0×10^{-5}
5	7.4×10^{-5}
6	6.4×10^{-5}
7	5.95×10^{-5}
8	5.55×10^{-5}
9	5.2×10^{-5}
10	5.0×10^{-5}
11	4.76×10^{-5}
12	4.6×10^{-5}
13	0
14	0
15	0
16	End of Run

The reflectivity of several absorbing inhomogeneous films prepared according to the method of the example were measured in Example 1, and the reflectivity of the phosphor-absorbing film interface determined using Snell's laws. The results are presented in Table VI.

Table VI

Reflection at Phosphor-Absorbing Film Interface		
Sample		Reflectivity %
Experimental V_2O_5-V No.	1	1.5
"	2	0.4
"	3	0.1

What is claimed is:

1. A viewing screen for a luminescent display device comprising a transparent viewing portion, a luminescent phosphor layer on the interior surface of said viewing portion and a light absorbing inhomogeneous film covering and adherent to said phosphor layer, said film having a tapered composition varying continuously from a metal oxide at a point remote from said interface at the phosphor-film interface to the metal constituent of said oxide such that said film exhibits a continuous gradient of refractive index from an index approximating the index of said phosphor at the phosphor-film interface to an index approximating the index of said metal at said remote point, and said metal oxide being selected from the group of oxides consisting of tantalum oxide and vanadium oxide.

2. A viewing screen in accordance with claim 1 wherein said phosphor has the formula Ln_2O_2S:RE, where Ln is at least one trivalent rare earth host ion selected from the group consisting of lanthanum, gadolinium, yttrium and lutetium and RE is at least one trivalent activator ion selected from the group consisting of rare earth ions having atomic numbers 59 through 70 and in which from about 0.001 percent to 20 percent of the trivalent host ions have been replaced by at least one said activator ion.

3. A viewing screen in accordance with claim 2 wherein Ln is lanthanum.

4. A viewing screen in accordance with claim 1 wherein said display device is a cathode ray tube.

5. A viewing screen in accordance with claim 1 wherein said phosphor layer consists of multiple phosphor films, each film capable of luminescing at a different color.

6. A luminescent display device comprising a transparent viewing portion, a phosphor layer on the interior surface of said viewing portion, a light absorbing inhomogeneous film covering and adherent to said phosphor layer and excitation means for causing said phosphor layer to luminesce, said inhomogeneous film having a tapered composition varying continuously from a metal oxide at the phosphor-film interface to the metal constituent of said oxide facing said excitation means such that said film exhibits a continuous gradient of refractive index from an index approximating the index of said phosphor at the phosphor-film interface to an index approximating the index of said metal, and said metal oxide being selected from the group of oxides consisting of tantalum oxide and vanadium oxide.

7. A display device in accordance with claim 6 wherein said device is a cathode ray tube.

8. A display device in accordance with claim 6 said phosphor has the formula Ln_2O_2S:RE, where Ln is at least one trivalent rare earth host ion selected from the group consisting of lanthanum, gadolinium, yttrium and lutetium and RE is at least one trivalent activator ion selected from the group consisting of rare earth ions having atomic numbers 59 through 70 and in which

from about 0.001 percent to 20 percent of the trivalent host ions have been replaced by at least one said activator ion.

9. A display device in accordance with claim 8 wherein Ln is lanthanum.

10. A display device in accordance with claim 6 wherein said phosphor layer consists of multiple phosphor films, each film capable of luminescing at a different color.

11. A method for making a viewing screen for luminescent display devices consisting essentially of the steps of:

forming a luminescent phosphor layer on a transparent substrate, and

forming a light absorbing inhomogeneous film on said phosphor substrate, said film having a tapered composition varying continuously from a metal oxide at the phosphor-film interface to the metal constituent of said oxide at a point remote from said interface such that said film exhibits a continuous gradient of refractive index from an index approximating the index of said phosphor at the phosphor-film interface to an index approximating the index of said metal at said remote point and said metal oxide being selected from the group of oxides consisting of tantalum oxide and vanadium oxide.

12. A method in accordance with claim 11 wherein said phosphor has the formula Ln_2O_2S:RE, where Ln is at least one trivalent rare earth host ion selected from the group consisting of lanthanum, gadolinium, yttrium and lutetium and RE is at least one trivalent activator ion selected from the group consisting of rare earth ions having atomic numbers 59 through 70 and in which from about 0.001 percent to 20 percent of the trivalent host ions have been replaced by at least one said activator ion.

13. A method in accordance with claim 12 wherein Ln is lanthanum.

14. A method in accordance with claim 11 wherein said display device is a cathode ray tube.

15. A method in accordance with claim 11 wherein said phosphor layer consists of multiple phosphor films, each film capable of luminescing at a different color.

* * * * *

APPENDIX B

CRT OPTICS CALCULATIONS

B1.0 CRT CONTRAST STUDY

We present here a more precise analysis than that previously reported. The contrast ratio C is defined as:

$$C = \frac{\text{light emitted and reflected from an excited area}}{\text{light reflectcted from an unexcited area}} = \frac{L_{obs} + A_{refl}}{A_{refl}}$$

Our first task is to develop a rigorous expression for the reflection of ambient light from the CRT faceplate. The interfaces for reflection of ambient light are depicted in Figure B1.

The refractive indices for air, glass, the phosphor film, the non-reflective (NR) film and the aluminum electrode are represented by n_0, n_1, n_2, n_3, n_3 and n_4, respectively. The amplitude reflectances are r_1 for the air-glass, r_2 for the glass-phosphor, r_3 for the phosphor-NR film, and r_4 for the NR film-aluminum interfaces, respectively.

For convenience, we restrict the analysis to the normal incidence case. This should be adequate for most purposes because the observer will usually view the CRT from a position directly in front of the CRT, and it is known that the non-normal incidence case is satisfactorily represented by the normal incidence treatment for angles of incidence differing from the normal up to about 30 degrees.

The absorption in the phosphor film is negligible for thicknesses of the order of 1 micrometer, so we shall regard the phosphor as a nonabsorbing (or dielectric) medium.

The following treatment is based on the superposition of solutions obtained by resolving the model of Figure B1 into simpler systems.

B1.1 Glass Plate with Single Nonabsorbing Film on Back

In the first case, we consider a glass plate with a single non-absorbing film on the back furface (surface furthest from observer) as illustrated in the accompanying sketch.

The reflectivity of a nonabsorbing film of thickness d_f sandwiched between semi-infinite media having refractive indices m_1 and m_3 for the glass and NR film respectively is:

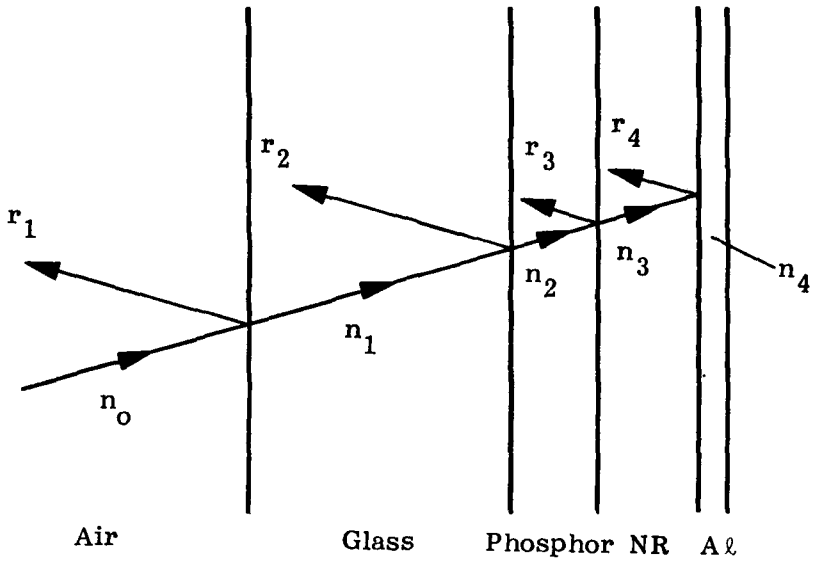

Figure B1. Cross-Section of CRT Faceplate Showing Interfaces for Reflection of Ambient Light

$$R_f = \frac{r_2^2 + r_3^2 + 2 r_2 r_3 \cos \phi_f}{1 + r_2^2 r_3^2 + 2 r_2 r_3 \cos \phi_f} \quad (1)$$

where the phase shift ϕ_f is:

$$\phi_f = \frac{4\pi n_2 d_f}{\lambda} \quad (2)$$

and

$$r_2 = \frac{m_1 - m_2}{m_1 + m_2} \quad (3)$$

$$r_3 = \frac{m_2 - m_3}{m_2 + m_3} \quad (4)$$

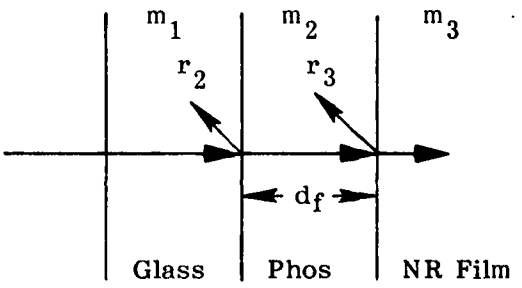

Case 1 Sketch

In a second case, we treat the glass plate as sandwiched between semi-infinite media of air and film material. Thickness of the plate is large compared to the wavelength of visible light, so interference effects do not occur. For infinitely many internal reflections, the reflectivity is:

$$R_{p_A} = \frac{p_1 + p_2 - 2p_1 p_2}{1 - p_1 p_2} \quad (5)$$

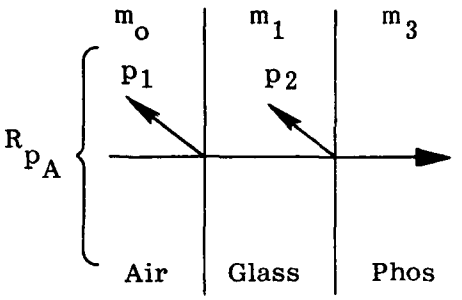

Case 2 Sketch

where p_1 is the reflectivity at the air-glass interface and p_2 is the reflectivity at the glass-film interface. Clearly, $p_2 = R_f$ while p_1 is given by:

$$p_1 = \left(\frac{n_1 - n_o}{n_1 + n_o}\right)^2 \tag{6}$$

so that

$$R_{p_A} = \frac{p_1 + R_f - 2p_1 R_f}{1 - p_1 R_f} \tag{7}$$

Thus, if the film thickness and refractive indices are known, a value for R_{p_A} and be calculated.

B1.2 Glass Plate with Phosphor Film and Ideal NR Film - $r_3 = 0$

Now, if the NR film of Figure B1 is a perfect absorber, this implies that the refractive index of the NR material at the phosphor film-NR film interface is identical to that for the phosphor film. In this ideal case, the reflectivity at the phosphor film-NR film is zero. The reflectivity at the glass-phosphor film interface will then be the same as if the phosphor-NR film combination were replaced with a semi-infinite media of phosphor material. The reflectivity is now given by Equation (5) with p_1 and p_2 simply:

$$p_1 = \left(\frac{n_1 - n_o}{n_1 + n_o}\right)^2 \qquad (8)$$

$$p_2 = \left(\frac{n_2 - n_1}{n_1 + n_o}\right)^2 \qquad (9)$$

B1.2.1 Glass Plate with Phosphor Film and Non-Ideal NR Film - Case 3, $r_3 \neq 0$

If the NR film is not ideal, there may be (a) reflectance at the phosphor film-RN film interface due to mismatch of refractive indices, or also (b) reflection from the NR film - aluminum interface if the NR film is not a perfect absorber. We shall not attempt a solution for case (b) because the NR films to be employed are inhomogeneous films for which the refractive index is variable through the film and exact solutions are possible only for certain unique index gradients. Also, ambient light must traverse the film twice in order to contribute appreciable reflectance at the phosphor film-NR film interface, and since only films having considerable absorption are of interest for CRT applications, the intensity of ambient light reflected from the NR film-aluminum interface will be negligibily small on arriving again at the phosphor film-NR film interface.

Even were such reflected ambient to make an appreciable contribution, the effect would be nearly the same as though there were an additional degree of mismatch between the interface indices for the phosphor and NR films.

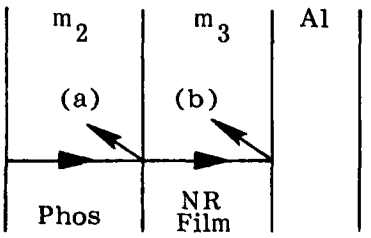

Case 3 Sketch

B1.2.2 Mismatch of Indices for Phosphor and NR Films

Here it is assumed that the NR film is a perfect absorber, but a mismatch of refractive indices occurs at the phosphor film-NR film interface. In this case, r_3 is not zero. The reflectivity is given by Equation (5) with R_f of Equation (1) substituted for p_2, as in Case 1. Thethickness of the phosphor film must be known in order to calculate the reflectivity. The next case is to calculate the intensity of light emitted by the phosphor which reaches the observer.

To simplify the treatment, we shall consider the NR film to be ideal, so that no emitted light is reflected at the phosphor-NR film interface. The problem then reduces to obtaining an equation for the transmittance of light emitted from a point in the phosphor, through the glass plate. Since no light is reflected at the phosphor-NR film interface, the problem is simply that of transmission for aplate sandwiched between semi-infinite media of phosphor film and air. For nonabsorbing materials, the transmittance T is:

$$T = 1 - R \tag{10}$$

where R is the reflectivity for the same system. The reflectivity is:

$$R = R_{p_o} = \frac{p_2 + p_1 - 2p_1 p_2}{1 - p_1 p_2} \tag{11}$$

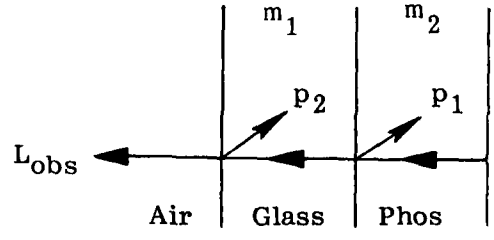

where p_1 is the reflectivity at the phosphor-glass interface and p_2 is the reflectivity at the glass-air interface. Thus,

$$p_1 = \left(\frac{n_2 - n_1}{n_2 + n_1}\right)^2 \tag{12}$$

$$p_2 = \left(\frac{n_1 - n_o}{n_1 + n_o}\right)^2 . \tag{13}$$

Thus, if L is the luminance of the phosphor,

$$L_{obs} \approx T_p L = \left(1 - R_{p_o}\right) L . \tag{14}$$

For ambient light of incident intensity A, the light reflected to the observer when the NR film is ideal is:

$$A_{refl} = AR_{p_A} \tag{15}$$

where P_p is given by Equation (7) with

$$p_1 = \left(\frac{n_1 - n_o}{n_1 + n_o}\right)^2 \tag{16}$$

$$p_2 = \left(\frac{n_2 - n_1}{n_2 + n_1}\right)^2 \tag{17}$$

Here p_1 and p_2 are interchanged with the p_1 and p_2 of the emitted light equations.

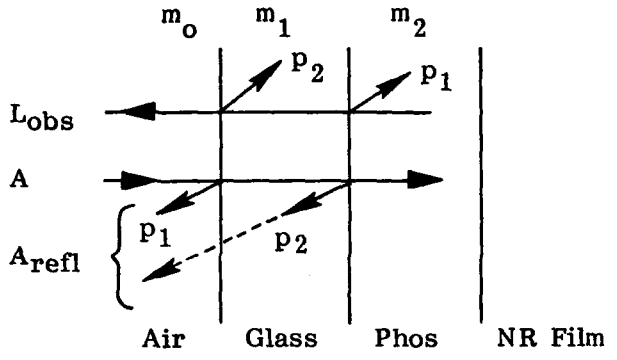

The value of R_p is independent of direction:

$$R_p = \frac{p_2 + p_1 - 2p_1 p_2}{1 - p_1 p_2} \tag{18}$$

therefore with no light emitted from the enexcited area, the contrast ratio is:

$$C = \frac{L_{obs} + A_{refl}}{A_{refl}} \tag{19}$$

$$= \frac{(1 - R_p) L + R_p A}{R_p A} \tag{20}$$

Taking the solar illuminance constant as 13.67 lumens/cm^2, the ambient illumination of a CRT faceplate in direct sunlight is 1.27×10^4 fc.

For a faceplate of Corning #1720 aluminosilicate glass and La_2O_2S phosphor film, $n_o = 1$, $n_1 = 1.53$, $n_2 = 2.20$. Then, $p_1 = 0.043884$ and $p_2 = 0.032265$. Hence, $R_p = 0.073422$, so that the ambient light reflected to the observer is $A_{refl} = 032.4$ fL. Of this amount, 557.3 fL is the result of reflection at the front surface.

By coating the front surface with an antireflection coating, the reflected ambient light could be reduced to 375 fL, which is the result of the mismatch between the glass and the phosphor film.

Substituting the above values of R_p, the contrast equation becomes:

$$C = \frac{(1 - 0.073422)L + (0.073422)A}{0.073422A}$$

$$= 12.61990 \frac{L}{A} + 1 \quad . \tag{21}$$

For direct sunlight, $A = 1.27 \times 10^4$ fL, so we have

$$C = 0.004 \times 10^{-3} L + 1 \quad . \tag{22}$$

Table B1 presents the contrast ratio for various values of L, when no front surface AR coating is used.

With an AR coating on the front surface, sufficient to make R_p the reflectivity of the glass-phosphor interface, then

$$R_p = 0.032265 \quad . \tag{23}$$

and

$$C = \frac{(1 - 0.032265)L + 0.032265A}{0.032265A}$$

$$= 29.993 \frac{L}{A} + 1 \quad . \tag{24}$$

For direct sunlight:

$$C = 2.362 \times 10^{-3} L + 1 \quad . \tag{25}$$

Table B2 presents the contrast ratio for various values of L attainable with use of a front surface AR coating.

Figure B2 provides a graphical comparison of the two cases.

If the mismatch between the glass and the phosphor could be eliminated by using a phosphor having an index the same as the glass, the effect on contrast would be as follows:

Assuming no AR coating and an ideal NR film, the reflectivity becomes simply that of the front surface. That is, $p_2 = 0$, then

Table B1

No. AR-1720-La_2O_2S - IDEAL NR

L	C
100	1.099
200	1.199
300	1.298
400	1.398
500	1.497
600	1.596
700	1.696
800	1.795
900	1.894
1000	1.994

Table B2

$C = 2.362 \times 10^{-3} L + 1$

AR-1720-La_2O_2S - IDEAL NR

L fL	C
100	1.236
200	1.472
300	1.709
400	1.945
500	2.181
600	2.417
700	2.653
800	2.889
900	3.126
1000	3.362
2000	5.723
3000	8.056
4000	10.446
5000	12.808

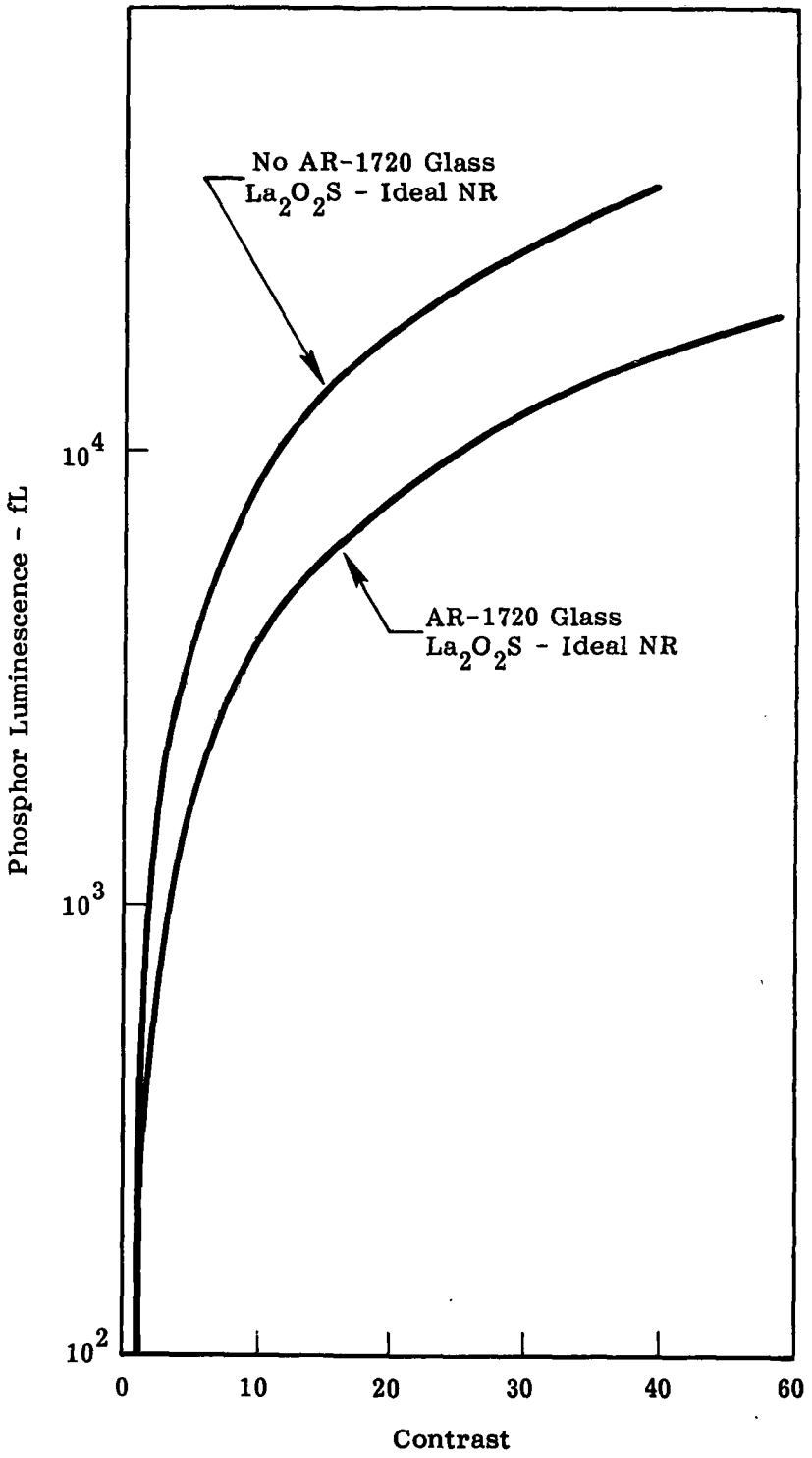

Figure B2. Contrast Ratio for Various Values of L

$$R_p = 0.043884 \tag{26}$$

and

$$C = \frac{(1 - 0.043884)L}{0.043884A}$$

$$= 21.787 \frac{L}{A} + 1 \quad . \tag{27}$$

For direct sunlight

$$C = 1.716 \times 10^{-3} L + 1 \tag{28}$$

The curve is intermediate between the two previous curves.

If the NR film is not ideal, the reflectivity must be calculated using Equations (1) and (7). In addition to the refractive indices, the thickness of the phosphor film and the reflectivity at the phosphor-NR film interface must be known.

For a 1720 glass - La_2O_2S - Non-ideal NR film CRT, we have $n_o = 1$, $n_1 = 1.53$ and $n_2 = 2.20$.

Assuming a La_2O_2S thickness of 12,000 Å and a reflectivity at the La_2O_2S - NR interface of 0.5%, then at a wavelength of 5400 Å

$$r_3 = \sqrt{R_3}$$

$$r_3 = (0.005)^{1/2} = 0.0707107 \tag{29}$$

$$r_2 = \frac{1.53 - 2.20}{1.53 + 2.20} = -0.17962 \tag{30}$$

$$p_1 = \left(\frac{1.53 - 1}{1.53 + 1}\right) = 0.043884 \tag{31}$$

$$p_2 = \left(\frac{m_2 - m_1}{m_2 + m_1}\right)^2 = 0.032265 = R_f \tag{32}$$

$$R_p = \frac{p_2 + p_1 - 2p_1 p_2}{1 - p_1 p_2} = 0.073421 \tag{33}$$

$$C = \frac{(1 - R_p)L}{R_p A} + 1 \tag{34}$$

The ambient illumination of the CRT faceplate in direct sunlight is 1.27×10^4 fc.

$$C = 9.937 \times 10^{-4} L + 1 \tag{35}$$

which differs little from our first curve.

B2.0 REFLECTIVITY CALCULATIONS

In Section 2.8, the results of calculating the reflectivity of normally incident light (i.e., perpendicular to the plane of the faceplate, were presented for: (1) a glass plate with a nonabsorbing film on its surface, (2) a glass plate with a phosphor film and an ideal NR film, and (3) a glass plate with phosphor film and non-ideal NR film. The results of calculating the reflectivity for oblique incidence are presented in this section.

The reflectivity of a nonabsorbing film between semi-infinite media for oblique incidence, is given as before, by the equation:

$$R_f = \frac{r_{1f}^2 + r_{2f}^2 + 2r_{1f} r_{2f} \cos \phi_f}{1 + r_{1f}^2 r_{2f}^2 + 2r_{1f} r_{2f} \cos \phi_f} \tag{36}$$

Here, however, ϕ_f is given as

$$\phi_f = \frac{4\pi n_f d_f \cos \theta_f}{\lambda} \tag{37}$$

where θ_f is the angle at which light is refracted in the film. If θ_f is the angle at which light is incident upon the film, by Snells's law

$$n_o \sin \theta_o = n_f \sin \theta_f \tag{38}$$

Also, for oblique incidence, it is necessary to distinguish between the parallel and perpendicular polarization components of light, for which the Fresnel coefficients are:

$$r_{1p} = \frac{n_f \cos \theta_a - n_a \cos \theta_f}{n_f \cos \theta_a + n_a \cos \theta_f} \tag{39}$$

$$r_{2p} = \frac{n_2 \cos \theta_f - n_f \cos \theta_2}{n_2 \cos \theta_f + n_f \cos \theta_2} \tag{40}$$

and

$$r_{1s} = \frac{n_a \cos \theta_a - n_f \cos \theta_f}{n_a \cos \theta_a + n_f \cos \theta_f} \tag{41}$$

$$r_{2s} = \frac{n_f \cos \theta_f - n_b \cos \theta_b}{n_f \cos \theta_f + n_b \cos \theta_b} \tag{42}$$

Denoting the reflectance intensity for the p-component by I_p^r and for s-component by I_s^r, the overall reflectivity is:

$$R_f = \frac{I_p^s + I_s^r}{2} \tag{43}$$

The calculated reflectivities of this section are the specular reflectivities. The models for the calculations have been selected to represent ambient light incident on the external surface of a cathode ray tube. It is assumed that the light is incoherent, so that interference does not occur between light reflected from the front surface and rear surface of the glass although infinitely many reflections occur between the glass surfaces. The phosphor film, of the order of 1 micron thickness is, however, a thin film so that interference does occur for reflections from the two surfaces of the film.

Thin film optical calculations for oblique incidence are relatively tedious, and particularly so in the case of absorbing materials. Extensive thin film calculations are ordinarily performed with the aid of a computer. For many purposes, however, a limited number of points, say 20 or so, permit construction of a reflectivity curve with satisfactory definition. It has been found that a programmable calculator, such as the TI-59, is well suited for such calculations, and several programs have been written for the purpose.

The calculated results are presented in Tables B3, B4, B5 and B6, for a glass plate, a glass plate with an La_2O_2S film of 12,889 Å thickness, a glass plate with an La_2O_2S film of 12,273 Å thickness, and a glass plate with an La_2O_2S film and idean NR film, respectively.

Calculations were made for these two La_2O_2S film thicknesses because minimum reflectivity at normal incidence occurs for an La_2O_2S film thickness of 12,886 Å, and maximum reflectivity for 12,273 Å. When an ideal NR film is present, the thickness of the La_2O_2S film is immaterial.

In the tables I_D^r represents the reflected intensity for the p-component and I_D^s the reflected intensity for the s-component. R si the overall reflectivity for unpolarized light.

The calculated overall reflectivities are shown graphically in Figure B3. The curve labeled "Plate + La_2O_2S Film" is for a 12,272 Å thickness. The hump in this curve peaking at 45° is the result of interference in the film.

It is seen from Figure B3 that the reflectivity is nearly constant from 0° to 40°, the reflectivities increase rapidly. It is also seen from the figure that the reflectivity for the plate + La_2O_2S + NR film, for angles greater than 40°, the reflectvity increases rapidly. It is also seen from the figure that the reflectivity for the plate + La_2O_2S + NR film is less than for the plate alone. This is because the plate has two glass-air-interfaces, each having a reflectivity of 0.04388, while the plate + La_2O_2S + NR combination has one glass-air interface (reflectivity = 0.04388) and one glass-phosphor interface (reflectivity = 0.03227). The overall reflectivity is given by the equation:

$$R = \frac{r_1 + r_2 - 2r_1 r_2}{1 - r_1 r_2} \qquad (44)$$

Table B3

GLASS PLATE

Oblique Incidence

Media	Index	θ_o, Deg	I_p^r	I_s^r	R
Air n_o	1	0	0.08408	0.08408	0.08408
1720 Glass n_1	1.53	5	0.08328	0.08488	0.08406
Air n_2	1	10	0.08086	0.08735	0.08410
		15	0.07680	0.09161	0.08421
		20	0.07106	0.09793	0.08449
		25	0.06362	0.10667	0.08515
		30	0.05449	0.11840	0.08645
		35	0.04379	0.13385	0.08882
		40	0.03185	0.15405	0.09295
		45	0.01945	0.18031	0.09988
		50	0.00809	0.21438	0.11123
		55	0.00073	0.25838	0.12956
		60	0.00279	0.31484	0.15881
		65	0.02371	0.38643	0.20407
		70	0.07884	0.47555	0.27720
		75	0.18997	0.58356	0.38676
		80	0.38036	0.70978	0.54507
		85	0.65914	0.85073	0.75493
		90	1.00000	1.00000	1.00000

Table B4

GLASS PLATE OVER La_2O_2S FILM

Oblique Incidence

Media	Index	θ_o, Deg	I_p^r	I_s^r	R
Air n_o	1	0	0.29367	0.29367	0.29367
1720 Plate n_1	1.53	5	0.29195	0.29518	0.29357
La_2O_2S n_2	2.20	10	0.28550	0.29843	0.29197
Air n_3	1	15	0.27074	0.29979	0.28527
		20	0.24289	0.29367	0.26828
Film Thickness	12886.4 Å	25	0.19819	0.27393	0.23611
(Max for $\theta_o = 0$)		30	0.13887	0.23702	0.18794
Wavelength	5400 Å	35	0.07729	0.18967	0.13348
		40	0.03489	0.16026	0.09757
		45	0.02421	0.19247	0.10834
		50	0.03421	0.29656	0.16538
		55	0.04264	0.42818	0.23541
		60	0.03786	0.54392	0.29089
		65	0.02814	0.63301	0.33057
		70	0.04149	0.70365	0.37257
		75	0.11981	0.76829	0.44405
		80	0.30417	0.83713	0.57065
		85	0.60971	0.91504	0.76238
		90	1.00000	1.00000	1.00000

Table B5

GLASS PLATE OVER La_2O_2S FILM
Oblique Incidence

Media	Index	θ_o, Deg	I_p^r	I_s^r	R
Air n_o	1	0	0.08404	0.08408	0.08404
1720 Plate n_1	1.53	5	0.08344	0.08505	0.08425
La_2O_2S n_2	2.20	10	0.08340	0.09000	0.08670
Air n_3	1	15	0.08877	0.10476	0.09676
		20	0.10438	0.13713	0.12075
Film Thickness	12272.7 Å	25	0.13035	0.19173	0.16104
(Min for $\theta_o = 0$)		30	0.15916	0.26379	0.21147
Wavelength	5400 Å	35	0.17825	0.33908	0.25867
		40	0.17633	0.40175	0.28904
		45	0.14860	0.44161	0.29510
		50	0.10042	0.45571	0.27807
		55	0.04890	0.44802	0.24846
		60	0.01749	0.43198	0.22474
		65	0.02426	0.43375	0.22900
		70	0.07822	0.48241	0.28032
		75	0.18981	0.58437	0.38709
		80	0.37784	0.71794	0.54789
		85	0.65554	0.85952	0.75752
		90	1.00000	1.00000	1.00000

Table B6

GLASS PLATE OVER La_2O_2S FILM OVER IDEAL NR FILM
Oblique Incidence

Media	Index	θ_o, Deg	I_p^r	I_s^r	R
Air n_o	1	0	0.07342	0.07342	0.07342
1720 Glass n_1	1.53	5	0.07288	0.07397	0.07342
La_2O_2S	2.20	10	0.07124	0.07563	0.07344
		15	0.06851	0.07850	0.07350
		20	0.06468	0.08270	0.07369
		25	0.05976	0.08846	0.07411
		30	0.05376	0.08846	0.07493
		35	0.04685	0.10600	0.07643
		40	0.03919	0.11884	0.07901
		45	0.03121	0.13548	0.08337
		50	0.02373	0.15703	0.09038
		55	0.01822	0.18530	0.10176
		60	0.01734	0.22271	0.12003
		65	0.02593	0.27283	0.14938
		70	0.05280	0.34081	0.19680
		75	0.11424	0.43413	0.27418
		80	0.24112	0.56364	0.40328
		85	0.49421	0.74490	0.61956
		90	1.00000	1.00000	1.00000

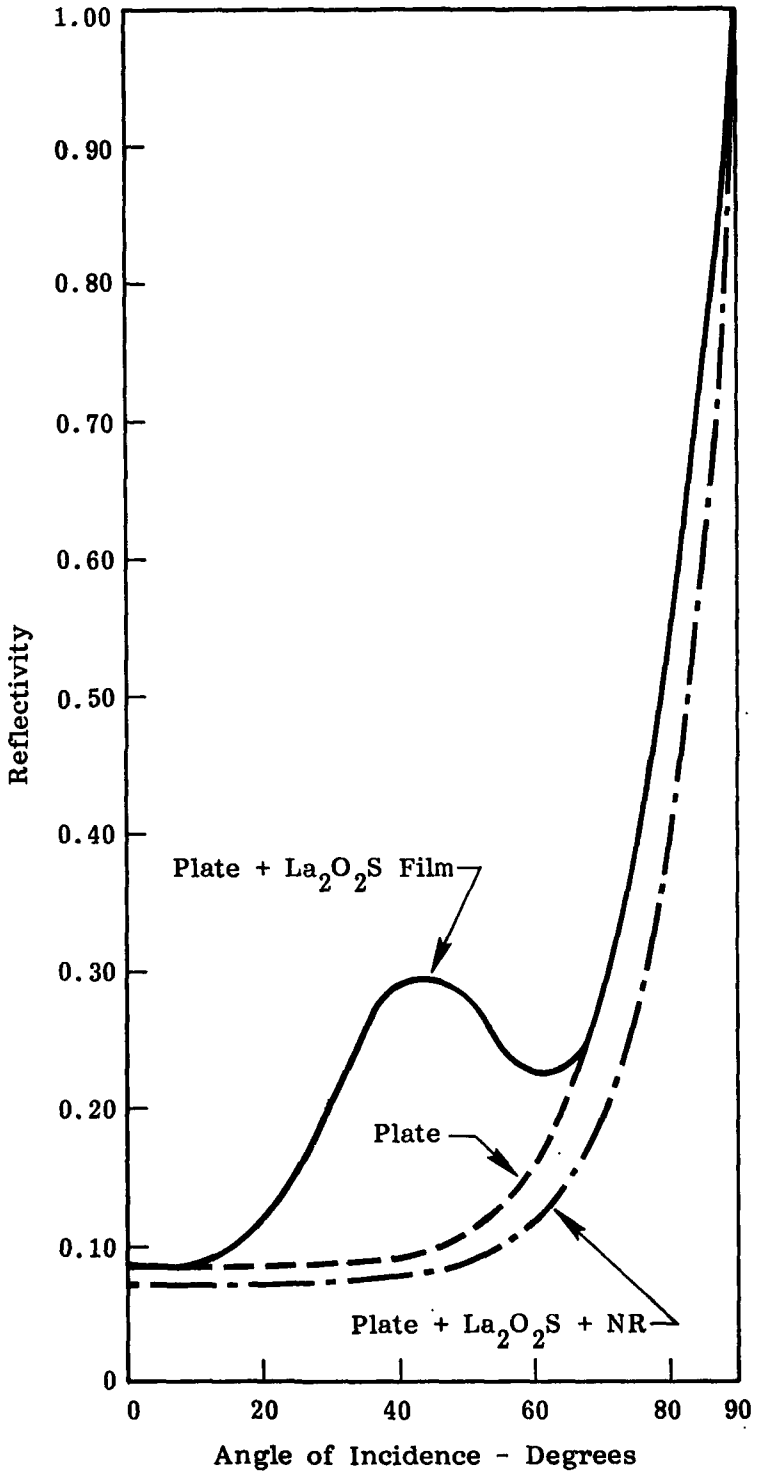

Figure B3. Reflectivity Versus Angle of Incidence

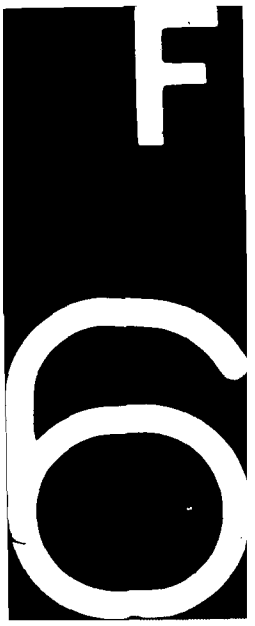
F
6